



UNIVERSITAT  
POLITÈCNICA  
DE VALÈNCIA



## **TRABAJO DE FIN DE MÁSTER**

---

Analysis on the potential of novel hydrogen fuel  
cell vehicle architectures for automotive  
applications

---

Realizado por: Marcos López Juárez  
Dirigido por: Ricardo Novella Rosa

Valencia, septiembre de 2021

---

Máster Universitario en  
Motores de Combustión Interna Alternativos,  
curso 2020-2021

INSTITUTO UNIVERSITARIO CMT-MOTORES TÉRMICOS



## Index

1. Introduction .....	2
2. Objectives .....	3
3. Methodology.....	3
4. Conclusions .....	4
Annex: Publications .....	5

## 1. Introduction

With the rise in cleaner technologies to decarbonize the transportation sector, hydrogen (H<sub>2</sub>) fuel cell vehicles (FCV) are in the spotlight of the industry and scientific community as one of the best options for medium and long-range transport application for their high efficiency, only tank-to-wheel water vapor emissions, fast charging/refueling times, and the logistic advantages and well-to-tank zero emissions that H<sub>2</sub> can offer. Nonetheless, the research focused on the application of fuel cell systems (FCS), consisting of a fuel cell (FC) and a balance of plant (BoP) for automotive application is still limited. Particularly, the FCV architecture in which the FC operates as a range-extender (FCREx) has been previously considered only for heavy-duty, city bus, city logistics vehicles... but its feasibility has not been analyzed for passenger car application yet. Furthermore, despite the use of H<sub>2</sub> in FCV implying zero tank-to-wheel emissions, it does not mean that it implies zero cradle-to-grave emissions, which will depend on the H<sub>2</sub> production pathway, the FCV architecture and its performance.

The main factor affecting the well-to-tank emissions of FCV is the H<sub>2</sub> production pathway. Since H<sub>2</sub> is an alternative fuel that can be produced, instead of extracted, the variability in H<sub>2</sub> production strategies is considerable. Among the main production pathways that stand out nowadays, it is possible to find the production of H<sub>2</sub> through electrolysis with the current electricity mix (black H<sub>2</sub>) or from renewable sources (green H<sub>2</sub>), and from steam methane reforming (SMR – gray H<sub>2</sub>) without or with carbon capture and storage (SMR with CCS - blue H<sub>2</sub>). While green H<sub>2</sub> implies the lowest emissions and is targeted as the main production pathway for future H<sub>2</sub> production in Europe, it is also non-feasible in the short term because of the significant production, storage and distribution infrastructure that requires. In contrast, blue H<sub>2</sub> offers a low-emission solution to massively produce H<sub>2</sub> in the short term, since most of the H<sub>2</sub> nowadays is gray and SMR plant can be adapted with CCS technology.

The information about some of these topics is limited in the literature and has not been explored for FCREx architectures. This MSc thesis intends to fill the aforementioned knowledge gaps in the literature by means of three different studies, each of them focused on a very specific question. The first study, published in the journal *Energy Conversion and Management*, is a life cycle assessment (LCA) that intends to quantify and compare the cradle-to-grave greenhouse gases (GHG-100) and NO<sub>x</sub> emissions of different technologies for the automotive sector, paying special attention to the emissions produced by FCV and hydrogen internal combustion engine vehicles (HICEV) with different H<sub>2</sub> production pathways in the current and EU 2050 scenarios. The second study, published in the journal *Applied Energy*, explores the performance, range, and production costs of FCREx vehicles depending on the sizing of the FC, the battery capacity and the H<sub>2</sub> tank capacity in order to identify the implications of changing any of these three sizing parameters in the aforementioned characteristics. The last study, published in the journal *Applied Energy*, combines the LCA and sizing methodologies of the previous studies to also understand the implications of changing the FC maximum power, battery capacity and H<sub>2</sub> tank capacity on the cradle-to-grave GHG-100 and NO<sub>x</sub> emissions of vehicles with FCREx architecture.



## 2. Objectives

The main objective of these studies is to evaluate and analyze the performance and cradle-to-grave GHG-100 and NO<sub>x</sub> emissions of the novel FCREx architecture applied to passenger cars. The specific objectives that are aimed at in this work are:

- Estimate and compare the GHG-100 and NO<sub>x</sub> produced by H<sub>2</sub> propulsion technologies against those produced by conventional, hybrid and electric powerplants in the whole life cycle with the current and 2050 energy mix EU scenarios.
- Analyze what are the optimum H<sub>2</sub> production pathways to maximize the rate of emissions decrease in Europe and elaborate recommendations in the short, medium, and long term.
- Develop an FCV model consisting of a validated FC model, an adequate BoP whose management is optimized to maximize the FCS efficiency, and an energy management strategy (EMS) optimizer to simulate driving cycles.
- Analyze the variation in performance (total energy and H<sub>2</sub> consumption), range, and production costs of an FCREx vehicle when changing the FC maximum power, the battery capacity and the H<sub>2</sub> tank capacity as sizing parameters.
- Understand the variation in GHG-100 and NO<sub>x</sub> emissions in the vehicle manufacturing cycle, fuel production cycle, and cradle-to-grave process when changing the aforementioned sizing parameters and the H<sub>2</sub> production pathway.
- Elaborate recommendations to minimize the cradle-to-grave emissions of FCREx vehicles.
- Identify the optimum sizing of FCREx architecture components to maximize performance, minimize cost and minimize cradle-to-grave emissions and compared the optimum designs if they do not coincide.

## 3. Methodology

The studies in this document follow two differentiated methodologies that are combined in the last study. The first methodology is the LCA, used for the 1<sup>st</sup> and the 3<sup>rd</sup> papers. The second methodology is the sizing, used for the 2<sup>nd</sup> and the 3<sup>rd</sup> papers.

The LCA was performed mainly using the software GREET<sup>®</sup> v2019 as the life cycle inventory (LCI), although the data extracted from this platform was sometimes corrected with data from the literature. For the first study, the emissions associated to the fuel production cycle were estimated for Diesel, gasoline, compressed natural gas (CNG), electricity, gaseous H<sub>2</sub>, and liquid H<sub>2</sub>. In the case of H<sub>2</sub>, distribution through pipelines and through tube trailers was considered together with production from electrolysis from the EU electricity mix, SMR, and SMR with CCS. Then, the vehicle manufacturing cycle emissions were estimated based on the different systems that compose each vehicle, including their assembly and recycling/disposal when possible. Finally, the emissions associated with the operation cycle were calculated and added to those calculated for the rest of the cycles to calculate the cradle-to-grave total emissions. In the case of H<sub>2</sub> technologies, the effect of H<sub>2</sub>O as a greenhouse gas was also quantified to avoid any possible bias. This process was performed twice with the current EU energy mix and that targeted by the European Union for 2050 and compared to evaluate whether these objectives are enough to produce H<sub>2</sub> through electrolysis with the electricity mix and decrease emissions. The functional unit in this LCA was the total life per vehicle (1 vehicle manufactured and 150000 km of operation), and the impact category gas the GHG-100, although NO<sub>x</sub> were also calculated. The 3<sup>rd</sup> paper was performed using mainly the data of the fuel production cycle generated for the 1<sup>st</sup> paper, while the data from the vehicle manufacturing cycle was adjusted for each specific design.



The performance and range of the FCREx vehicle architecture were analyzed by means of 0D-1D simulations of WLTC 3b driving cycle. To do so, the software GT-Suite v2020 was used with the implemented FC model. First, the FC model was calibrated to experimental data in the literature obtained from a 20 kW PEMFC stack operating under different conditions of temperature and pressure. Secondly, a scalable BoP was designed specifically for the calibrated FC model and its management was optimized to maximize the FCS efficiency with the current density. Then, the resulting FCS model was simplified to a mean values model to decrease the computational cost of each simulation. This last model was then integrated into a FCV virtual environment together with a Li-Ion battery with a variable number of cells and a 120 kW electric motor. The communication between the battery, the FCS and the e-motor was optimized using Pontryagin's Minimum Principle to minimize H<sub>2</sub> consumption through the energy management strategy (EMS). In order to calculate the performance of different FCREx designs, the FC maximum power, the battery capacity and the H<sub>2</sub> tank capacity were varied, and the resulting vehicle weight and components characteristics implemented into the FCV model. Each design was then simulated considering a WLTC 3b cycle, corresponding to the power-to-mass ratio of the FCV (SUV type). The data from these simulations was finally used to estimate the range, H<sub>2</sub> consumption, energy consumption, manufacturing costs, GHG-100 emissions, and NO<sub>x</sub> emissions in each cycle of the cradle-to-grave process. With these, space designs that showed the variation of such parameters as a function of the FC maximum power, the battery capacity and the H<sub>2</sub> tank capacity were generated and analyzed.

## 4. Conclusions

The main conclusions from each study are summarized in this section:

The first paper entitled *Comparative global warming impact and NO<sub>x</sub> emissions of conventional and hydrogen automotive propulsion systems* was an LCA study that allowed the comparison of the cradle-to-grave GHG-100 and NO<sub>x</sub> emissions of Diesel, gasoline, hybrid-gasoline, CNG, electric, HICE and FC vehicles considering the fuel production, vehicle manufacturing, and operation cycles. For the results of this study, it was concluded that FCV with blue H<sub>2</sub> was the best option to minimize GHG-100 in the current scenario, while FCV with gray H<sub>2</sub> minimized the most NO<sub>x</sub> emissions. In the EU 2050 scenario, BEV and FCV with blue H<sub>2</sub> had the minimum and very similar GHG-100 cradle-to-grave emissions. The most optimum distribution strategy and to minimize emissions was central plant production with tube trailer transport of gaseous H<sub>2</sub>. With the current EU mix, FCV and HICEV produced even more emissions than conventional ICEV if H<sub>2</sub> was produced from electrolysis. This production pathway started to become competitive against ICEV only for FCV in the EU 2050 scenario, meaning that the EU objectives are not enough to produce H<sub>2</sub> through electrolysis from the current EU mix and decrease emissions. It was calculated that HICEV would need a fuel consumption of 30 kWh/100 km to match the emissions of BEV with blue H<sub>2</sub>. For that, DI HICE with a range-extender architecture was recommended. Finally, it was suggested that in order to maximize the rate of emissions decrease in the EU, the SMR plant should be converted to include CCS technology and NO<sub>x</sub> catalysts while increasing the renewable share in the electricity mix. In the short term, FCV, and BEV should be promoted and could coexist with other technologies. In the long-term, when the renewable share in the EU mix increases significantly, electrolysis with electricity from the EU mix would be plausible to produce H<sub>2</sub> and decrease emissions, thus allowing the coexistence of HICEV, FCV, and BEV, although it is expected that FCVs dominate the market due to the higher efficiency and range.

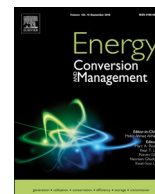


In the second paper *Optimization and sizing of a fuel cell range extender vehicle for passenger car applications in driving cycle conditions*, the range, H<sub>2</sub> consumption, energy consumption and manufacturing costs of FCREx vehicles with different FC maximum power, battery capacity and H<sub>2</sub> tank capacity were analyzed. In this study, it was identified that the maximum range of this architecture for passenger cars with the current state-of-the-art technology was around 700 km with 5 kg of H<sub>2</sub> and a battery of >50 kWh. FCREx designs were compared against equivalent-in-range commercial FCV, showing how this architecture could offer up to 6.8% in energy consumption saving and from 16.8% to 25% in H<sub>2</sub> saving. The optimum design, in terms of performance only, had high battery capacity and high FC maximum power since the increase in efficiency outweighed the increase in vehicle weight. Nonetheless, the suggested FCREx design was with moderate-high FC maximum power, and low-moderate battery capacity to maximize performance while decreasing costs.

The third paper *Impact of Fuel Cell Range Extender Powertrain Design on Global Warming and NO<sub>x</sub> Emissions in Automotive Applications* was performed by using the data from previous studies to convert the design spaces generated for the second paper to show the GHG-100 and NO<sub>x</sub> emissions in the fuel production, vehicle manufacturing, and cradle-to-grave process considering different H<sub>2</sub> production pathways. In this sense, it was showed hoy considering blue H<sub>2</sub> decreased cradle-to-grave GHG-100 and NO<sub>x</sub> emissions by ~60% and ~38% compared to black H<sub>2</sub>. For both emissions, it was concluded that the manufacturing process produced most of the emissions, although the fuel production cycle was more sensitive to the FCREx components sizing, thus dominating how the overall emission changed with FCREx design. The optimum design with blue H<sub>2</sub>, in terms of cradle-to-grave emissions, was found to have low-moderate battery capacity and high-moderate FC maximum power, in line with the selected design in the previous study based on the tradeoff between performance and costs, although it was not the optimum design in terms of consumption alone. From this analysis, it was concluded that, in order to minimize FCREx cradle-to-grave emissions, the decarbonization of the battery manufacturing process, the increase in the renewable share of the EU electricity mix, and the development of infrastructure to massively produce blue H<sub>2</sub> should be prioritized.

## Annex: Publications

- J.M. Desantes, S. Molina, R. Novella and M. Lopez-Juarez. 2020. “Comparative Global Warming Impact and NO<sub>x</sub> Emissions of Conventional and Hydrogen Automotive Propulsion Systems.” *Energy Conversion and Management* 221 (X): <https://doi.org/10.1016/j.enconman.2020.113137>.
- S. Molina, R. Novella, B. Pla, and M. Lopez-Juarez. 2021. “Optimization and Sizing of a Fuel Cell Range Extender Vehicle for Passenger Car Applications in Driving Cycle Conditions.” *Applied Energy* 285 (December 2020): <https://doi.org/10.1016/j.apenergy.2021.116469>.
- J. M. Desantes, R. Novella, B. Pla, and M. Lopez-Juarez. 2021. “Impact of Fuel Cell Range Extender Powertrain Design on Greenhouse Gases and NO<sub>x</sub> Emissions in Automotive Applications.” *Applied Energy* 302: 117526. <https://doi.org/10.1016/j.apenergy.2021.117526>.



# Comparative global warming impact and NO<sub>x</sub> emissions of conventional and hydrogen automotive propulsion systems

J.M. Desantes, S. Molina, R. Novella\*, M. Lopez-Juarez

CMT-Motores Térmicos, Universitat Politècnica de València, Camino de vera s/n, 46190 Valencia, Spain

## ARTICLE INFO

### Keywords:

LCA  
Hydrogen  
Fuel cell  
HICE  
Hybrid vehicles  
Electric vehicles

## ABSTRACT

With the rise of cleaner technologies for transport and the emergence of H<sub>2</sub> as a fuel, most of the emissions in the well-to-wheel process are shifting towards the energy carrier production (fuel or electricity). The objective of this study is to perform a simplified cradle-to-grave Life Cycle Assessment (LCA) that compares the greenhouse gases (GHG) and NO<sub>x</sub> emissions of H<sub>2</sub>, electric and conventional technologies for the automotive sector in Europe and to devise the optimum strategy of vehicle fleet renewal to reduce the emissions. In this study the effect of water as GHG was considered and, unless other studies, the current European energy mix and that meeting the objectives for 2050 were considered (while technology level was kept constant) since H<sub>2</sub> from electrolysis and electric vehicles' well-to-wheel emissions are sensitive to the energy mix. To estimate the emissions, the fuel, vehicle production and operation cycles were considered independently for each technology and then put together. For H<sub>2</sub>, the best production and distribution strategy was steam methane reforming (SMR) with CO<sub>2</sub> sequestration for GHG-100 gases and without capturing CO<sub>2</sub> for NO<sub>x</sub>, both with central plant production and tube trailer transport. Fuel cell vehicles (FCV) with optimum H<sub>2</sub> production always produce the lowest GHG-100 emissions and slightly higher NO<sub>x</sub> than battery electric vehicles (BEV) in the EU 2050 scenario. In contrast, HICEV would need to reach a fuel consumption of around 30 kWh/100 km to be competitive in emissions against BEV, for that, direct injection (DI) combined with a range extender (REx) hybrid architecture is the recommended powerplant concept. Finally, the optimum strategy to reduce emissions that Europe could follow is presented for the short, mid and long term.

## 1. Introduction

Nowadays, there is a major concern about pollution and global warming. Many experts and international organizations claim that it is necessary to decrease greenhouse gases (GHG) in all energy sectors [1,2]. However, CO<sub>2</sub> emissions worldwide are expected to keep growing with population [1,3]. In Europe, 19.4% of GHG come from road transport (792 million tonnes of CO<sub>2</sub> equivalent) [4]. Another focus of major concern is NO<sub>x</sub> emissions, whose effect over human health and ozone formation/depletion is not negligible [5].

To solve this problem, Europe is increasing the share of renewable sources in the energy mix and moving towards the hydrogen economy [2,6]. These two actions must be coupled to produce green hydrogen by using energy from renewable sources and lower GHG emissions in the whole life cycle of hydrogen technologies. Regarding the transport sector, vehicles powered by fuel cells (FC) or hydrogen internal combustion engines (HICE) are viable options to shift towards carbon-free

transport [2,7]. In recent years, the attention of the companies has been focused on FC because of their higher break efficiency compared to HICE. However, HICE are still a good option due to their low manufacturing cost and emissions, so it must not be forgotten.

Life Cycle Assessment (LCA) is a relevant tool to analyze the environmental impact of a given technology considering all aspects along its life. Previous studies show that H<sub>2</sub> PEM fuel cells in Canada and the US could produce less CO<sub>2</sub> emissions if the energy mix is not based primarily on coal combustion [8]. This confirms how H<sub>2</sub> cradle-to-grave emissions depend greatly upon the energy source that is used to produce it. A similar study [9], this time including HICE, demonstrated that H<sub>2</sub> technologies can produce lower emissions than Spark-Ignition (SI) or Compression-Ignition (CI) ICE fueled with gasoline, Diesel and even methanol if only renewable energy is used for the H<sub>2</sub> production. In none of these studies, the energy mix is representative of Europe's current or future situation, the emissions produced by the H<sub>2</sub> tank manufacturing were included nor the technology is representative of

\* Corresponding author.

E-mail address: [rinoro@mot.upv.es](mailto:rinoro@mot.upv.es) (R. Novella).

URL: <http://www.cmt.upv.es> (R. Novella).

<https://doi.org/10.1016/j.enconman.2020.113137>

Received 27 April 2020; Received in revised form 17 June 2020; Accepted 18 June 2020

Available online 17 July 2020

0196-8904/ © 2020 Elsevier Ltd. All rights reserved.

the current state-of-the-art. Other authors have focused their efforts on the analysis of LCA based on modern H<sub>2</sub> technologies and options, but they only analyzed a specific part of the life cycle such as hydrogen production [10,11] and distribution [12], PEMFC manufacturing and recycling [13] and on-board storage [14]. A study similar to the present work was performed by Garcia et al. [15] considering the Spanish electricity mix in Madrid but it was oriented towards public transport and not towards light-duty passenger vehicles. In all the mentioned studies the effect of emitted-on-surface water vapor was not accounted for. Recently, Sherwood et al. [16] estimated the effective global warming potential on a 100-year horizon (GWP-100) of water ranging from  $-10\text{-}3$  to  $5 \cdot 10\text{-}4$  kg eq. CO<sub>2</sub>. These values are low since additional emitted-on-surface water vapor (coming from H<sub>2</sub>-fuelled vehicles) cannot reach the troposphere and therefore, the global warming effect of water vapor is compensated by the increase in the reflectance from low-altitude clouds formed with the additional water vapor (cooling effect).

With the aim of extending the analysis provided by the already available scientific literature and evaluate the EU objectives of increasing the renewable energy share in the electricity mix, this study intends to be a cradle-to-grave cycle assessment that considers state-of-the-art automotive technologies, including SI and CI ICE fueled with gasoline/Diesel/compressed natural gas (CNG), hybrid systems equipping a SI ICE fueled with gasoline (HEV), battery electric systems (BEV), HICEV, and proton exchange membrane FCVs. This study focuses on passenger cars since all this powerplant portfolio potentially fulfills the requirements of this particular application, and it has also the highest impact on NO<sub>x</sub> and CO<sub>2</sub> emissions considering the road transport sector.

The contributions of this paper to the literature are based on estimating the GHG-100 and NO<sub>x</sub> emissions for most of the current automotive and hydrogen technologies for passenger cars considering the EU 2017 and 2050 electricity mixes and the water GHG-100 effect. With this estimation the objectives in the following section were accomplished.

## 2. Objectives

Considering the discussion about the state-of-the-art included in the previous section, the study was divided into a main and general objective and other specific objectives derived from it:

- Estimate and compare the GHG-100 and NO<sub>x</sub> produced by H<sub>2</sub> propulsion technologies against those produced by conventional, hybrid and electric powerplants in the whole life cycle with the current and 2050 energy mix EU scenarios.
  - Understand what are the H<sub>2</sub> production and transport strategies that produce lower emissions with European Union (EU) 2017 and 2050 energy mixes.
  - Assess whether the EU objectives to increase the renewable energy share in the energy mix are enough to produce H<sub>2</sub> uniquely from electrolysis to power the whole vehicle fleet and lower the emissions.
  - Estimate the consumption that should be reached by HICEVs in order to be competitive against BEVs and find out which technology could potentially help to achieve it, if any.
  - Assess the weight of the water vapour effect as a GHG-100 emission in the operation cycle.
  - Establish the most efficient (emissions-wise) strategy to reduce the emissions and reach the H<sub>2</sub> economy in the transport sector.

## 3. Methodology

Cradle-to-grave cycle assessments for a given transport technology should include fuel production, vehicle production, vehicle disposal and operation cycles. The powerplant technologies and their

**Table 1**  
Vehicle technologies and fuels considered in the present study.

Engine	Energy source	Fuel production
BEV	Electricity	Electricity mix
FCV	GH <sub>2</sub> , LH <sub>2</sub>	Electrolysis Steam methane reforming (SMR) SMR with CO <sub>2</sub> sequestration
DI ICE	B10 Diesel	Biodiesel from soybeans + Low sulphur Diesel
PFI ICE	GH <sub>2</sub> , LH <sub>2</sub>	Electrolysis Steam methane reforming (SMR) SMR with CO <sub>2</sub> sequestration
	CNG	Conventional CNG
	E10 Gasoline	Ethanol + Conventional gasoline
	E10 Gasoline (HEV)	Ethanol + Conventional gasoline

corresponding fuels considered in this study are included in Table 1.

### 3.1. System boundaries

The system boundaries for each individual cycles are showed, together with the system inputs and outputs, in Fig. 1. They are those corresponding to a cradle-to-grave LCA, i.e., from the extraction of the raw materials using energy and fuel to the disposal and the recycling of the vehicle. Even though waterborne, solid wastes and other atmospheric emissions such as SO<sub>x</sub> were calculated using GREET®, they were not included in the present study.

### 3.2. Functional units

The functional unit was changed for each cycle to improve the understanding of the analysis. In the fuel production cycle (Figs. 3–5), the functional unit was the MJ of fuel since several fuels with different lower heating values and densities were compared. In the vehicle production cycle, the emissions were calculated per manufactured vehicle. Finally, in the cradle-to-grave cycle, including the previous cycles together with the vehicle operation, the functional unit was the life of the each vehicle considering 150,000 km as the average common life.

### 3.3. Impact category

In this LCA study, Global Warming was the only impact category considered, although NO<sub>x</sub> were also estimated, since they are most concerning emissions in recent years. The GHG were calculated by taking into account CO<sub>2</sub>, CH<sub>4</sub> and N<sub>2</sub>O gaseous emissions. Their GWPs are 1, 28 and 265 kg<sub>CO<sub>2</sub></sub> equivalent respectively [17].

### 3.4. Life cycle inventory

In this study, all the data, unless otherwise specified, were obtained from the GREET® model version 2019 from the Argonne National Laboratory.

The life cycle inventory is explained in detail for each cycle in Sections 3.1–3.3.

### 3.5. Fuel production cycle

In the fuel production cycle, also called well-to-pump, all the processes used to generate the fuel were taken into account. This includes from the extraction of the raw materials (oil or gas) or from the generation of raw fuels (H<sub>2</sub> or electricity) to the distribution to the refueling stations after their conditioning to be used (refinement or compression) as described in Fig. 1. Particularly, alternative fuels differ from conventional ones in the production method. Their main advantage is that they can be generated from renewable energy such as the so-called green hydrogen, so they are virtually unlimited. However, it is not realistic to assume that hydrogen will only be produced from

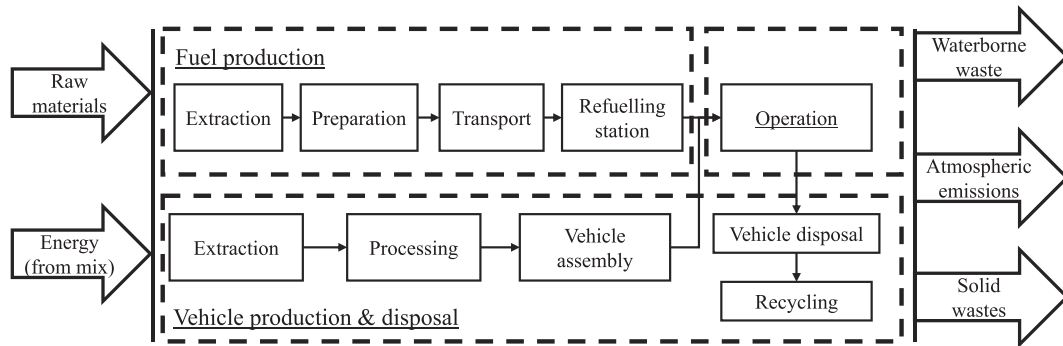


Fig. 1. Cradle-to-grave cycle assessment methodology and boundaries.

renewable energy and, in the case it was accomplished, the overall effect of increasing the renewable energy share to produce hydrogen would most likely coincide with increasing it to be used in the electric grid. Therefore, if alternative fuels are produced from non-renewable energy, the emissions during the whole life cycle might be even larger than those of fossil fuels. In order to quantify this issue in the current EU situation and to assess the adequacy of EU objectives for 2050, the energy mixes at both scenarios are considered in this study as shown in Fig. 2.

For H<sub>2</sub>, different distribution options to the refueling stations were considered: central plant generation with transport via tube trailer or via pipeline and in situ production. The emissions of each distribution strategy were then compared and only that with the lowest emissions was used for the whole LCA. This same methodology is also applied to decide if gaseous or liquid H<sub>2</sub> should be used (GH<sub>2</sub> or LH<sub>2</sub>).

The raw materials considered as inputs in this cycle were mainly crude oil for fuel processing and organic matter such as soybeans to generate biofuels. In this case, the transportation of the immediate products from the raw materials was also considered.

### 3.6. Vehicle production and disposal cycle

The emissions in the vehicle production and disposal cycle were calculated based on the required raw materials for each component. The mechanical components include the vehicle body (conventional material), the powertrain system, the transmission/gearbox, the chassis, the tire replacements, and the electric motor, controller, and generator (HEV, BEV, and FCV). The mechanical components for the HICE vehicle are the same as for a SI ICE car. Li-ion batteries were considered for BEV while Ni-MH batteries were considered for FCV and HEV vehicles. The emissions produced from the recycling of Li-ion batteries were estimated from Ref. [19] considering a pyrometallurgical process. The usage of engine oil, brake, transmission, coolant, windshield and adhesives fluids was included in the production cycle. The

manufacturing of the FC and the H<sub>2</sub> tanks (700 bar of storage pressure, type IV carbon fiber) were also included but their recycling was ignored. This was done because the effect of platinum recycling of the fuel cell stack is negligible in the whole life cycle [20] and there is no data about recycling type IV carbon fiber reinforced polymer tanks.

The raw materials for this cycle were mainly steel, aluminum, magnesium, zinc, copper wires, glass, plastic product, styrene-butadiene rubber, carbon-fiber reinforced plastic and other vehicle materials. The emissions associated with the processing of raw materials and the extraction of elementary materials such as bauxite ore, zinc ore, sand water, etc were included while those generated during the transport to the manufacturing plants neglected [21].

### 3.7. Operation cycle

Emissions in the operation cycle depend mainly on fuel consumption and type of fuel. BEV and FCV CO<sub>2</sub> emissions during operation are zero. In the case of a HICE, 3 g CO<sub>2</sub>/mile (from oil combustion) and 0.3 g NO<sub>x</sub>/mile are emitted based on an FTP 75 cycle [22]. In the case of a CNG ICE, the leakage of CH<sub>4</sub> is also considered due to its high Greenhouse effect. Table 2 shows the fuel consumption for each technology in terms of fuel energy, mass, and volume. A refueling efficiency of 100% was assumed.

The emissions during the operation cycle were estimated based on the GREET® model but scaled with the consumption data from [25,24] because the consumptions given in GREET® were abnormally high.

### 3.8. Cradle-to-grave comparison

Once the emissions per cycle were obtained, they were added to know the total life cycle emissions considering the EU 2017 and EU 2050 energy mixes. The results for each scenario were compared to identify the change in emissions of each technology considering a life of 150,000 km and the compatibility of EU objectives with the

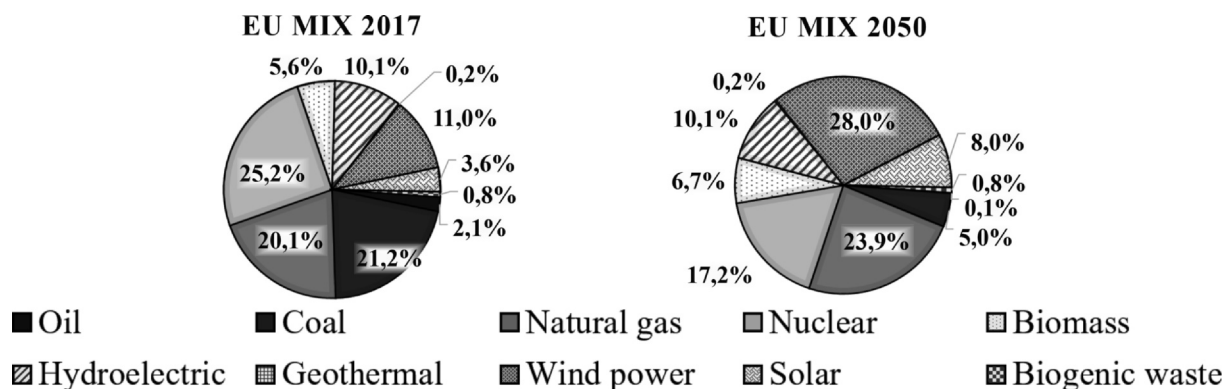


Fig. 2. 2017 [18] and 2050 EU energy mixes [6].

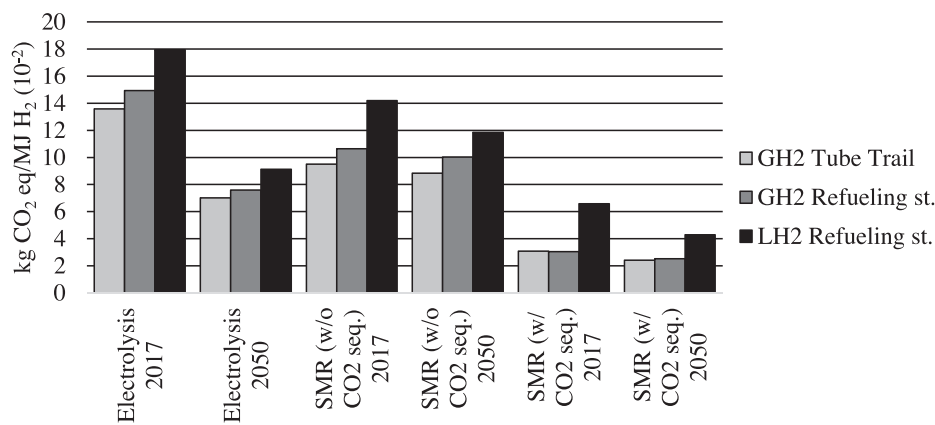


Fig. 3. GHG-100 emissions for gaseous and liquid H<sub>2</sub> fuel cycle.

development of the H<sub>2</sub> economy.

In the case of the emissions produced during the manufacturing and recycling of the vehicle, they are fixed and do not increase with the usage. In contrast, those emitted during the fuel production and operation cycle scale with the life (in km) of the vehicle. Therefore, it is possible that any technology, compared to any other, implies higher emissions during the manufacturing cycle, but they are compensated if the usage is long enough and the ratio emissions/km is lower during this cycle. In order to estimate which technology emits the less as a function of the life (km), the whole life emissions of each technology were plotted against the usage of the vehicle.

#### 4. Limitations

Life cycle assessments are often limited to the amount of information that databases can provide. Therefore, it is necessary to take on certain hypotheses and constraints. This section presents the scope of this LCA study. The limitations of this study are:

- The study is fundamentally based on mid-size passenger vehicles since they compose the majority of the current vehicle fleet.
- Fuel production and engine technologies are assumed to be constant with time. Therefore, the emissions predicted in the EU 2050 scenario associated to these aspects may be under or overestimated.
- Europe and United States technologies for fuel production are assumed to be similar, while the main difference is the energy mix.
- Fuel consumption of HICE and gasoline ICE vehicles were assumed equal. Even though brake efficiency of HICE is higher than that of gasoline ICE, the extra weight of the tanks could compensate for this difference in efficiency.
- The emissions produced to manufacture the machinery needed to

extract or produce the fuel are not quantified. This is negligible in emissions/km basis since fuel production plants would generate fuel for a large vehicle fleet.

- Some results are very similar to each other (Figs. 3–6, even though the tendencies seem correct, an study of uncertainties could provide more value to the analysis. However, not all the data obtained from the literature and from the GREET® model showed the uncertainties in emissions corresponding to each process and pathway. Therefore it was difficult to estimate uncertainties, but the results are expected to be meaningful according to similar literature in the field of study.

#### 5. Results and discussion

##### 5.1. Fuel production cycle

Emissions to produce any fuel may vary largely depending on the production and distribution methods. This fact is highlighted for alternative fuels whose production methodology has not been extensively used and developed in the industry. As such, the recent research was also oriented towards optimizing the hydrogen production and distribution technologies [26,27]. In the case of H<sub>2</sub>, there are mainly two ways of mass-producing it: natural gas steam reforming or steam methane reforming (SMR) and electrolysis. The most extensively used in Europe nowadays is SMR because of the economic and environmental benefits it offers against electrolysis. However, the environmental benefits may no longer be real if the energy mix is mostly composed of renewable energy. In order to understand the sensitivity of these production technologies to the energy mix, the first part of the fuel production cycle analysis was based only on gaseous and liquid H<sub>2</sub> production and distribution strategies. Then, the fuel cycle GHG-100 and NO<sub>x</sub> emissions were compared for the fuels in Table 1.

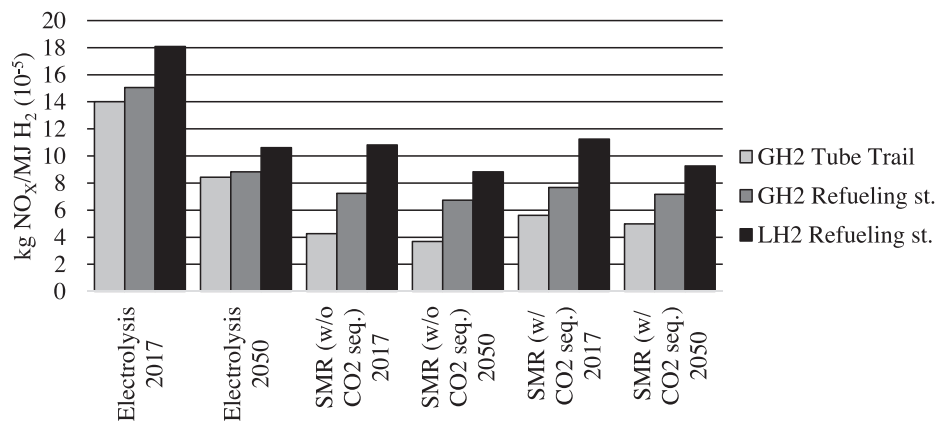


Fig. 4. NO<sub>x</sub> emissions for gaseous and liquid H<sub>2</sub> fuel cycle.

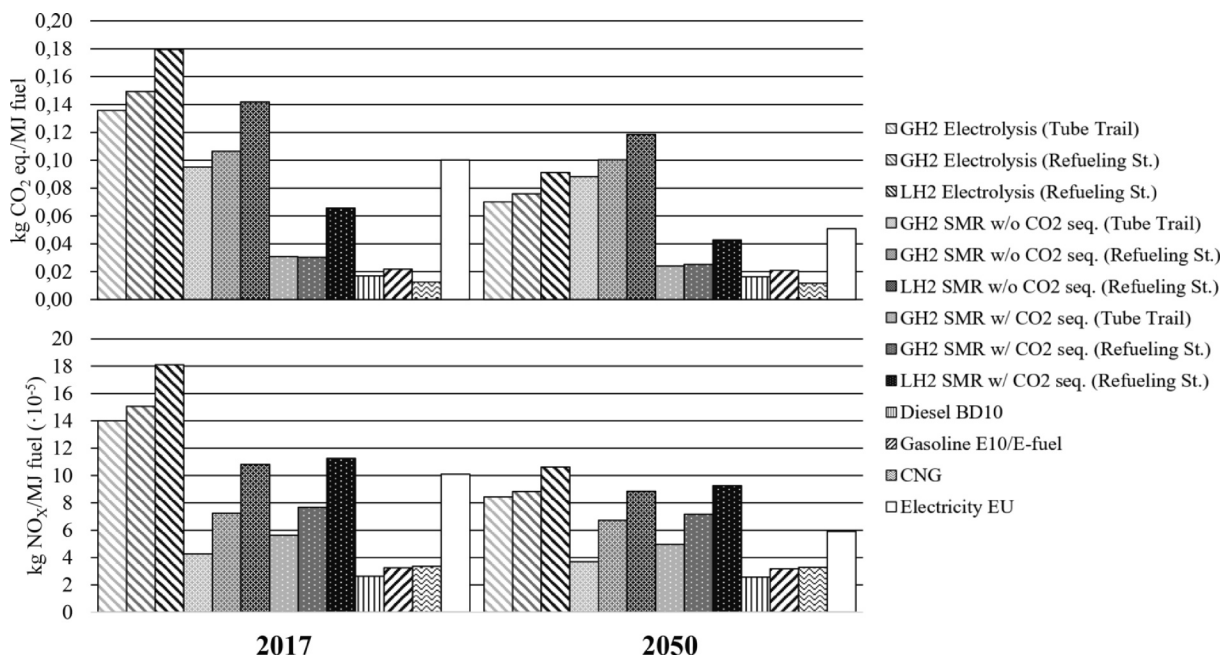


Fig. 5. Fuel cycle comparison for H<sub>2</sub> and conventional fuels in terms of GHG-100 and NO<sub>x</sub>.

Table 2

Fuel consumption of similar passenger vehicles with different engine technology [23,24].

Vehicle	Energy consumption [kWh/100 km]	Fuel consumption [Nm <sup>3</sup> (kg)/100 km]
BEV	14.5	-
H <sub>2</sub> FCV	24.4	8.14 (0.73)
Diesel ICE	45.4	4.54·10 <sup>-3</sup> (3.84)
HICE	58.7	19.6 (1.76)
CNG ICE	67.3	6.62 (5.15)
Gasoline ICE	58.7	6.60·10 <sup>-3</sup> (4.87)
Gasoline HEV	39.5	4.45·10 <sup>-3</sup> (3.28)

5.1.1. H<sub>2</sub> production and distribution strategies

As explained previously in this study, for H<sub>2</sub> it is interesting to consider different production and distribution strategies since Europe is still far from the H<sub>2</sub> economy and thus it is not clear what production methodology will be used in the future.

To produce H<sub>2</sub>, the processes of SMR with and without CO<sub>2</sub> sequestration and electrolysis were considered. For the SMR process with CO<sub>2</sub> sequestration, it was assumed that 90% of this pollutant was not emitted [28]. Regarding the distribution, central plant production with transport to the refueling stations by means of tube trailers and in situ production at the refueling stations was considered. Pipeline H<sub>2</sub>

distribution was not accounted because it is not a short-term solution since a whole distribution network should be developed along Europe. Natural gas current pipeline network can not be used for H<sub>2</sub> because it is not adapted to contain such a highly diffusive gas, although an option could be to distribute H<sub>2</sub> blended with natural gas. From the raw fuel, compressed gaseous H<sub>2</sub> or liquid cryogenic H<sub>2</sub> were considered. Liquid H<sub>2</sub> was not used in the following analyses nor considered for the scenario of central production with distribution because for road transport it is not feasible to keep any fuel at cryogenic conditions for long periods of time. All these scenarios with the EU 2017 and EU 2050 energy mixes are contemplated in Figs. 3 and 4.

Based only on greenhouse emissions, H<sub>2</sub> production via SMR with CO<sub>2</sub> sequestration is indeed the best option (Fig. 3). With the EU 2017 energy mix, fuel production via electrolysis is the worst option regarding GHG emissions. In contrast, with the EU 2050 energy mix electrolysis implies lower emissions than SMR without CO<sub>2</sub> sequestration. This is because most of the energy required to produce H<sub>2</sub> through electrolysis is electrical energy while for SMR most of the energy comes from natural gas combustion the heat up the steam reformer. This makes electrolysis highly sensitive to the energy mix. Unless other studies, H<sub>2</sub> mass production from only renewable energy is not included because it is not realistic to have a solar field near every electrolyzer, so in the future, the most probable approach is to cleanse the energy mix and use the energy directly from the general power line.

Regarding NO<sub>x</sub> emissions (Fig. 4), electrolysis is in both energy mix

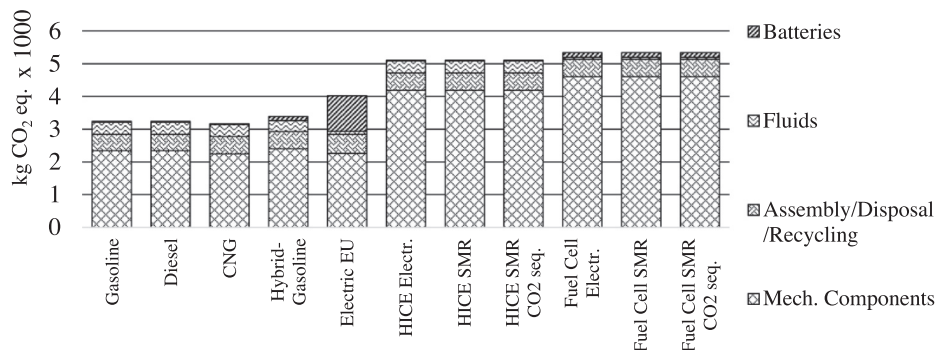


Fig. 6. GHG-100 emissions in the vehicle production cycle.

scenarios the worst option because the share of energy produced from fossil fuels through combustion is still significant. In the case of SMR,  $\text{NO}_x$  emissions are independent of the energy mix because they are mostly produced during the steam reforming where 5–10% of air is needed and is at high temperature during a long time [29].  $\text{NO}_x$  emissions are higher in SMR with  $\text{CO}_2$  sequestration probably because capturing  $\text{CO}_2$  implies higher energy consumption.

According to the results in Figs. 3 and 4, central plant  $\text{H}_2$  production and distribution via tube trailers is a better option than in situ production. Producing  $\text{H}_2$  in each refueling station implies greater water consumption than central production because of economies of scale. This water must be pre-treated, which means higher energy and resource consumption, thus producing higher emissions than central production [25].

Liquid  $\text{H}_2$  could provide a higher vehicle range for the same tank capacity than gaseous  $\text{H}_2$ . However, its liquefaction process requires around 30% of its higher heating value. This high energy demand increases substantially the emissions to produce  $\text{LH}_2$  and makes them more sensitive to the energy mix. If not for the difficulty of storing  $\text{LH}_2$  at cryogenic conditions and the amount of energy required to liquefy it,  $\text{LH}_2$  could be a suitable long-term fuel option.

In sight of the GHG emissions in Fig. 3,  $\text{H}_2$  production via SMR with  $\text{CO}_2$  sequestration and distribution via tube trailer is the best option in the short-term (2017) and mid-term (2050). In contrast, due to the additional energy required to capture  $\text{CO}_2$ , Fig. 4 shows that the best option to minimize  $\text{NO}_x$  emissions is SMR without  $\text{CO}_2$  sequestration instead. In order to address this problem, it is possible to use a  $\text{NO}_x$  trap or catalyst at the exhaust of the SMR process to further reduce  $\text{NO}_x$  emissions. Finally, due to the high sensitivity of electrolysis to the energy mix, this technology has the highest potential for the long-term when a mostly renewable energy mix is expected. In-situ SMR is not considered since it is not feasible to have a  $\text{H}_2$  production plant at each refueling station, but distribution via pipelines could be a good solution for the mid to long-term.

### 5.1.2. Comparative fuel cycle

Once the  $\text{H}_2$  production and distribution strategies were analyzed, they must be compared against the production routes of other conventional fuels. In this section, the aforementioned comparison is presented in Fig. 5. Again, the data is produced for the EU 2017 and EU 2050 energy mixes so that the effect of more-renewable electricity is reflected in the analysis.

According to the results in Fig. 5,  $\text{H}_2$  production generates significantly more GHG-100 and  $\text{NO}_x$  emissions than B10 Diesel, E10 gasoline or CNG fuels. If  $\text{H}_2$  is produced by means of electrolysis, the emissions are the highest while if it is produced through SMR with  $\text{CO}_2$  sequestration, the emissions may be lower than using electricity directly in an electric vehicle.

EU 2050 scenario is characterized by a higher renewable energy share in the energy mix (Fig. 2). As such, all fuel production strategies produce lower emissions. Depending on the grade of dependence on the energy mix, the emissions may change significantly between both scenarios. Electricity directly used as a fuel and  $\text{H}_2$  produced by electrolysis present the highest sensitiveness. However, electrolysis, even in 2050, is expected to generate far more emissions than current fuels. In the case of electricity to power electric vehicles, the emissions during the fuel production cycle will always be lower than  $\text{H}_2$  produced by electrolysis because it avoids an additional energy transformation with its corresponding irreversibilities. The effect of improving the electrolysis or SMR processes with time is not included in this data. Therefore, lower emissions are expected in the actual EU 2050 scenario in an extent that depends on the level of development of these processes. In contrast, conventional hydrocarbon fuels are almost insensitive to this change since electricity is used as an auxiliary resource to power the machinery to extract and refine the fuel but not as the main energy resource to be converted into fuel.

Finally, it is important to remark at this point that emissions during the operation cycle are almost non-existent for  $\text{H}_2$  technologies. Therefore, even though producing conventional fuels may generate lower emissions, the operation cycle must be included to assess the EU objectives and drawing any significant conclusion.

### 5.2. Vehicle production cycle

Differently from the fuel cycle, the emissions generated during the vehicle production are fixed and do not increase with the usage. Even though these emissions may be a minor part of the whole life cycle, they must be included to quantify the effect of the requirement of components such as  $\text{H}_2$  tanks or Li-Ion/Ni-MH batteries. In the case of low emissions technology, such as BEV or  $\text{H}_2$  FCV whose operation cycle is characterized by virtually zero emissions, this cycle can be significant.

In order to make the different vehicle production cycles comparable, a common vehicle body of 740 kg without the powertrain system nor the chassis (where the FC or the batteries can be integrated) was considered. The total weight of the vehicles varies between 1420 kg (gasoline ICEV) and 1640 kg (FCV).

The results of this cycle are only shown for the EU 2017 scenario because the sensitivity to the energy mix is relatively low (Fig. 6). In the EU 2050 scenario, the reduction in emissions ranges from 11% to 13% for all technologies. This effect was included in the cradle-to-grave cycle. Most GHG-100 emissions are produced in the manufacturing process of the mechanical components since they represent most of the mass of the vehicle (body, chassis, powerplant). For HICE and FCV, which generate the most greenhouse gases, the increase in emissions is mainly due to mechanical components. In this case, the need for a carbon fiber reinforced type IV tank to store 700 bar of gaseous  $\text{H}_2$  is the main factor that increases emissions. Among these two technologies, the FCV generates more GHG-100 because of the manufacturing of the fuel cell (102 kW), its corresponding balance of plant and the battery (34 kW) [30].

Emissions coming from batteries manufacturing are greater for the BEV since the Li-Ion batteries are bigger and require higher energy storage capacity than Ni-MH or lead-acid batteries, thus needing more materials. In contrast, ICEV have more emissions coming from fluids since they need engine oil to lubricate the reciprocating mechanism to reduce mechanical losses and increase the durability.

Even though alternative fuels and electricity for transportation may be interesting from the point of view of decentralizing emissions, they produce more pollution during the fuel and vehicle production cycles than conventional fuels. However, this issue is caused by the lack of development of these technologies and may be solved with time.

$\text{NO}_x$  emissions present a similar trend as GHG-100 because they are produced from the electricity usage and high-temperature processes where  $\text{CO}_2$  is also emitted.

### 5.3. Cradle-to-grave cycle

The cradle-to-grave cycle assessment presented in this section includes the fuel production, vehicle production, and operation cycles. In order to get the absolute value of emissions in the fuel production and operation cycles, it is necessary to set a life duration. In this case, life or usage was set to 150,000 km. This value is realistic for current ICEV. However, it may be too high for BEV where batteries degrade over time. This value is used anyway because this issue could be solved by 2050 and not all the ICEV reach 150000 km.

#### 5.3.1. GHG-100 emissions

Once the emissions coming from each cycle are put together, it is possible to realize that each part is significant depending on the technology or scenario considered. For example, in Fig. 7 the GHG-100 emissions in the vehicle production cycle for a FCV are higher than the operation and fuel production cycle if  $\text{H}_2$  is produced from methane

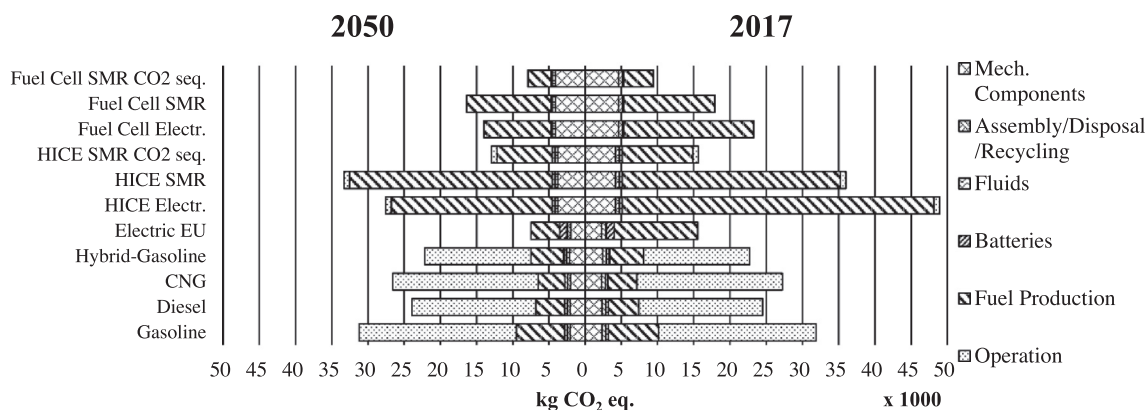


Fig. 7. Cradle-to-grave cycle, GHG-100 emissions.

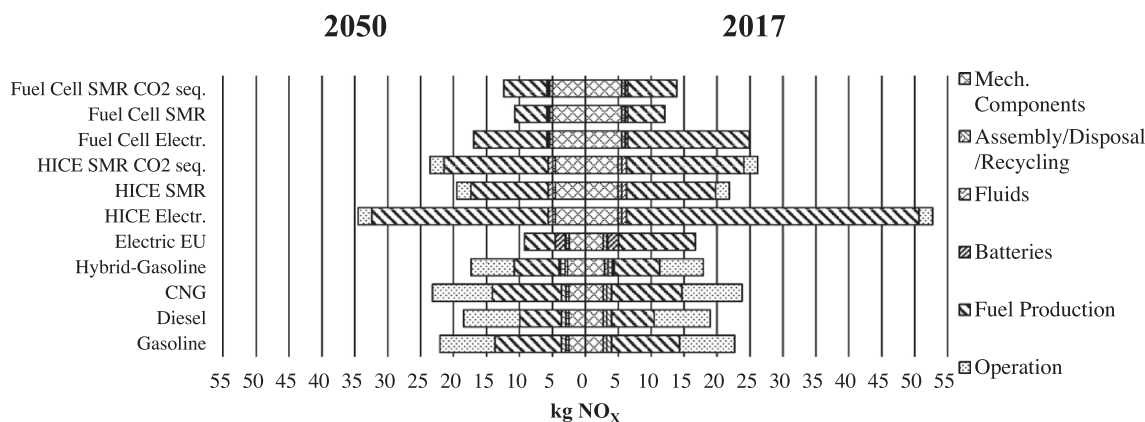


Fig. 8. Cradle-to-grave cycle, NO<sub>x</sub> emissions.

through SMR with CO<sub>2</sub> sequestration. In contrast, for conventional ICEV and HEV, the operation cycle is the most significant emissions-wise while vehicle production represents around 10% of the total life emissions. Due to the current trend towards more electrical propulsion in the automotive sector, it is possible that in the future the efforts in reducing emissions are shifted towards vehicle manufacturing.

For H<sub>2</sub>-fuelled vehicles and BEV, most of the emissions come from the fuel production cycle. The effect of H<sub>2</sub>O in the exhaust of FCV is almost negligible. In contrast, its effect on HICEV is noticeable. Particularly, in the case of a HICEV with H<sub>2</sub> produced from SMR with CO<sub>2</sub> sequestration, where it represents 5% of the total GHG-100 emissions. The noticeable difference in the emissions during the fuel production cycle between HICEV and FCV when the production technology is the same is due to the lower fuel consumption of FCV since less fuel is required for the same usage (Table 2). According to the results of greenhouse emissions in the EU 2017 scenario (Fig. 7), the interest of using HICE or FC technologies is strongly dependent on the production strategy used. In the short-term, HICEVs are competitive against fossil fuels only if H<sub>2</sub> is produced through SMR with CO<sub>2</sub> sequestration. However, if H<sub>2</sub> is produced from electrolysis with energy from the energy mix, the total emissions double those of a Diesel car during the whole life.

Regarding FCV, in the short-term, they are already competitive, with any production technology, against fossil-fuelled vehicles. If electrolysis is used, there is not a big benefit of using FCV. By combining FCV with SMR and CO<sub>2</sub> sequestration, current FCV could produce less than two-thirds of the emissions of an BEV during the whole life.

In sight of the GHG-100 emissions in the EU 2017 scenario, the short-term strategy towards the H<sub>2</sub> economy should necessarily include the spreading and development of SMR with CO<sub>2</sub> sequestration to

produce H<sub>2</sub>. Concerning the powerplant selection, FCs have the advantage of lower fuel consumption and the drawback of higher cost, which forbids their extensive usage, while HICEs have higher fuel consumption but can be easily integrated into the society due to their lower cost as a competitive option against BEVs.

As expected, the change to a more-renewable energy mix (from EU 2017 to EU 2050) in Fig. 7 affects more significantly the emissions of BEV and H<sub>2</sub> technologies with H<sub>2</sub> produced from electrolysis. With this production technology, FCV would generate half of gasoline ICEV GHG-100 emissions while HICEV would start to be competitive against conventional ICEV. The most beneficial strategy would still be producing H<sub>2</sub> with SMR and CO<sub>2</sub> sequestration. This means that the long-term strategy to move towards H<sub>2</sub>-based transport should be based on SMR with CO<sub>2</sub> capture rather than electrolysis. In this case, FCV and BEV would generate approximately similar GHG-100 during the whole life due to the higher share of clean energy available for powering BEV.

### 5.3.2. NO<sub>x</sub> emissions

NO<sub>x</sub> emissions produced by each technology (Fig. 8) must also be accounted for to assess EU objectives and H<sub>2</sub> powerplants. In the EU 2017 scenario, the less pollutant option is again the FCV whose H<sub>2</sub> is produced through SMR. This difference is significant even when compared with BEV. In contrast, BEV produce the lowest NO<sub>x</sub> emissions in the EU 2050 scenario. The shift in the most favorable technology is due to the high sensitivity of BEV emissions to the energy mix composition. In both scenarios, sequestering CO<sub>2</sub> in the central plants produce NO<sub>x</sub> emissions due to the higher energy and resources consumption it implies. If H<sub>2</sub> is produced through electrolysis, FCV would produce NO<sub>x</sub> emissions in the levels of conventional technologies in the short term. If EU objectives for 2050 are accomplished, FCV NO<sub>x</sub> emissions would be less than those produced by gasoline HEV or Diesel ICEV but still higher

than BEV.

The amount of NO<sub>x</sub> produced by HICEV during the whole life is always higher than any other technology, especially if electrolysis is used, no matter the energy mix scenario. This is because of the lower efficiency of HICE compared to FC and the high amount of NO<sub>x</sub> produced per MJ of H<sub>2</sub> during the fuel production cycle. In this case, even though NO<sub>x</sub> are low during the operation cycle and can be further reduced with the use of catalysts [31], this cycle only contributes to roughly 8% of the produced NO<sub>x</sub> emissions. The sensitivity to the energy mix is the same as for the GHG-100 results. BEV, HICEV, and FCV whose H<sub>2</sub> has been produced through electrolysis show the biggest variation when the energy mix is modified.

If the EU strategy to shift towards H<sub>2</sub> and electric vehicles was purely based on NO<sub>x</sub> emissions the approach would change from that based on GHG-100. In the short term, the most beneficial option would be to increase the amount of FCV drastically while keep increasing the amount of BEV. In the mid-term, BEV should be the predominant road transport for light-weight passenger cars. Finally, in the long-term, BEV, FCV, and HICEV with H<sub>2</sub> produced from electrolysis could coexist with an energy mix mainly based on renewable and nuclear energies.

### 5.3.3. Target consumption for HICE

HICE main limiting factor are the NO<sub>x</sub> emissions produced during fuel production. In order to reduce them, the only option, apart from improving the fuel production efficiency or using catalysts in the production process, is to decrease its fuel consumption. This could be done by hybridizing the powerplant and/or by increasing the thermal efficiency optimizing the injection and combustion processes. This last option could be achieved by adopting several solutions, such as flexible engine hardware systems (direct injection system, variable valve actuation, variable compression ratio...) or advanced combustion concepts (highly diluted combustion). In this section, the target consumption of a HICE to match the NO<sub>x</sub> emissions of an BEV during the whole life was estimated.

The NO<sub>x</sub> emissions of an BEV during the whole life in the EU 2017 scenario are 16.7 kg NO<sub>x</sub>. Considering the vehicle manufacturing emissions of a HICEV (6.3 kg NO<sub>x</sub>), the NO<sub>x</sub> emitted during the fuel production and operation cycles should be 10.4 kg NO<sub>x</sub>. With a life of 150,000 km, the target NO<sub>x</sub> production rate would be  $6.9 \cdot 10^{-5}$  kg NO<sub>x</sub>/km to match BEV's total NO<sub>x</sub>. From the data in Fig. 8, the estimated NO<sub>x</sub> production rate of HICE using SMR with CO<sub>2</sub> sequestration (whose GHG-100 production is similar to that of an BEV) is  $13.3 \cdot 10^{-5}$  kg NO<sub>x</sub>/km. Assuming that the amount of NO<sub>x</sub> is proportional to the fuel consumption, which is realistic if the engine is correctly calibrated and/or catalysts are used because most of the NO<sub>x</sub> emissions come from the fuel production cycle, the fuel consumption should decrease by 48%, from 58.7 kWh/100 km to around 30 kWh/100 km. This value is hardly reachable in real driving with a PFI HICE even though H<sub>2</sub> increases the thermal efficiency due to its high reactivity and flame speed. However, the fuel consumption of state-of-the-art Diesel HEV is 3.3 l/100 km (33 kWh/100 km). Therefore, this consumption could only be expected (if reachable) with a DI HICE integrated into a serial hybrid vehicle architecture as the range extender, where the HICE is mostly operating at peak efficiency points and the smart energy management may improve the overall efficiency.

## 6. Conclusions

In this study the GHG-100 and NO<sub>x</sub> emissions have been estimated for FCV, HICEV, BEV, gasoline HEV, and Diesel, gasoline and CNG ICEV considering a life span of 150,000 km. The fuel production, vehicle manufacturing, and operation cycles were included in the LCA. The emissions were calculated based on the EU 2017 and EU 2050 energy mixes in order to assess the suitability of the current EU objectives to increase the renewable energy share in the energy mix to advance towards the H<sub>2</sub> economy. Electrolysis, SMR with and without CO<sub>2</sub>

sequestration were considered to produce H<sub>2</sub>.

Among the H<sub>2</sub> production strategies considered in this study, SMR with CO<sub>2</sub> sequestration was the best option to minimize GHG-100 while the option without CO<sub>2</sub> sequestration minimizes NO<sub>x</sub> probably due to the extra resources and energy required to capture the CO<sub>2</sub>. Therefore, the ideal production technology would be SMR with CO<sub>2</sub> sequestration with NO<sub>x</sub>-reducing catalysts at the exhaust of the SMR plant. Transportation via tube trailer from central plants minimized the emissions because those produced by pre-treating H<sub>2</sub>O locally at each refueling station outweighed those produced by the trailers transporting the H<sub>2</sub> tanks to the refueling stations. This production and transport strategies are the most optimum both in EU 2017 and EU 2050 scenarios because the renewable energy share in the energy mix is not high enough to make electrolysis less contaminant than SMR.

FCV with SMR and CO<sub>2</sub> sequestration produce lower GHG-100 emissions than any other propulsion technology in the EU 2017 scenario but slightly higher GHG-100 than BEV with the EU 2050 energy mix. Similarly, FCV with SMR without CO<sub>2</sub> sequestration produce the lowest NO<sub>x</sub> in 2017 but BEV overcome them in the EU 2050 scenario. In none of the scenarios, H<sub>2</sub> produced from electrolysis produced both lower GHG-100 and NO<sub>x</sub> than from SMR with CO<sub>2</sub> sequestration. However, in EU 2050, electrolysis might start to be competitive against fossil-fuelled ICEVs in both GHG-100 and NO<sub>x</sub>. Therefore, EU renewable energy production objectives are not enough to produce all the H<sub>2</sub> from electrolysis. SMR with CO<sub>2</sub> sequestration should be used instead if these objectives are not redefined upwards.

Emissions produced by HICEV with SMR and CO<sub>2</sub> sequestration were superior in terms of GHG-100 and inferior in NO<sub>x</sub> than fossil-fuelled technologies. Although if electrolysis was used, given the electricity mixes, using fossil fuels would produce much less GHG-100 and NO<sub>x</sub> emissions than HICE. Using the most optimum H<sub>2</sub> technology, in order to match the emissions of HICEV and BEV in the EU 2017 scenario, it would be necessary to decrease the fuel consumption of HICE to around 30 kWh/100 km. This might be achievable if DI HICE were used in a hybrid range extender vehicle architecture.

Even though the effect of water as a greenhouse gas was included, its effect was almost negligible when using FCV, if HICEV are used its effect is noticeable. With HICEV, the H<sub>2</sub>O effect on global warming might represent 5% of the total GHG-100 emissions if SMR with CO<sub>2</sub> sequestration is used to produce H<sub>2</sub>.

This LCA study confirms how the optimum strategy to reduce GHG-100 and NO<sub>x</sub> emissions depends on the energy mix. In the short-term, H<sub>2</sub> production through SMR with CO<sub>2</sub> strategy should be extended and FCV in the market increased through cost reduction. It would be recommendable to develop NO<sub>x</sub> catalyst for SMR plants and thus introduce DI HICEV in the market whose total life cycle emissions are competitive against BEV. In the mid-term (EU 2050), FCV and BEV should coexist because of their complementary characteristics. H<sub>2</sub> should still be produced in SMR central plants with CO<sub>2</sub> sequestration. In the long term, when renewable energies compose most of the energy mix, electrolysis would produce fewer emissions than SMR and therefore producing all the H<sub>2</sub> through electrolysis would be plausible to reduce emissions. In this case, HICEV, FCV, and BEV could coexist, although FCV would probably dominate the market of H<sub>2</sub> technologies due to their lower fuel consumption.

## 7. Policy implications statement

With the study, the authors intended to elaborate recommendations to optimize the rate of decrease in emissions produced by the transport sector according to the EU 2017 and 2050 scenarios. Promoting the purchase of such vehicles through actions such as tax reduction, focused on the most optimum technologies in the short, mid and long term, would probably minimize the GHG-100 and NO<sub>x</sub> emissions in Europe. Additionally, measures are to be taken to gradually increase the renewable energy share in the European electricity mix. However, until

the renewable energy share is enough, the road to H<sub>2</sub> economy should be based on H<sub>2</sub> production through SMR with CO<sub>2</sub> sequestration.

### CRedit authorship contribution statement

**J.M. Desantes:** Conceptualization, Methodology, Supervision. **S. Molina:** Resources, Methodology, Data curation. **R. Novella:** Investigation, Formal analysis, Writing - review & editing. **M. Lopez-Juarez:** Investigation, Software, Writing - original draft.

### Declaration of Competing Interest

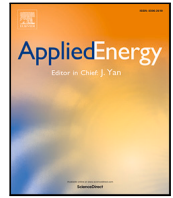
The authors declare that they have no known competing financial interests or personal relationships that could have appeared to influence the work reported in this paper.

### Acknowledgments

This research has been partially funded by FEDER and the Spanish Government through project RTI2018-102025-B-I00 (CLEAN-FUEL).

### References

- European Commission, A Clean Planet for all - A European long-term strategic vision for a prosperous, modern, competitive and climate neutral economy, Com (2018) 773; 2018. p. 114. URL:[https://ec.europa.eu/clima/sites/clima/files/docs/pages/com\\_2018\\_733\\_en.pdf](https://ec.europa.eu/clima/sites/clima/files/docs/pages/com_2018_733_en.pdf)[https://ec.europa.eu/clima/sites/clima/files/docs/pages/com\\_2018\\_733\\_en.pdf?utm\\_campaign=AktuellHållbarhet-Direkten\\_181129\\_Username&utm\\_medium=email&utm\\_source=Eloqua&elqTrackId](https://ec.europa.eu/clima/sites/clima/files/docs/pages/com_2018_733_en.pdf?utm_campaign=AktuellHållbarhet-Direkten_181129_Username&utm_medium=email&utm_source=Eloqua&elqTrackId).
- Fuel Cells & Hydrogen (FCH), Hydrogen Roadmap Europe - a Sustainable Pathway for the European Energy Transition, 1st Edition, Publications Office of the European Union; 2019. doi:10.2843/341510.
- International Energy Agency, CO<sub>2</sub> Emissions from Fuel Combustion, Tech. rep.; 2019. URL:<https://www.iea.org/reports/co2-emissions-from-fuel-combustion-2019>.
- European Environmental Agency (EEA), Greenhouse gas emissions from transport in Europe, Tech. rep., European Environmental Agency (EEA), Copenhagen; 2019. URL:<https://www.eea.europa.eu/data-and-maps/indicators/transport-emissions-of-greenhouse-gases/transport-emissions-of-greenhouse-gases-12>.
- Boningari T, Smirniotis PG. Impact of nitrogen oxides on the environment and human health: Mn-based materials for the NO<sub>x</sub> abatement, Current Opinion in Chemical Engineering 13(x):2016;133–141. doi:10.1016/j.coche.2016.09.004. URL: doi: 10.1016/j.coche.2016.09.004.
- European Commission, EU Reference Scenario 2016, Tech. rep., European Commission; 2016. doi:10.2833/9127. URL:[https://ec.europa.eu/energy/sites/ener/files/documents/ref2016\\_report\\_final-web.pdf](https://ec.europa.eu/energy/sites/ener/files/documents/ref2016_report_final-web.pdf) [accessed on 25 August 2017].
- Verhelst S, Wallner T. Hydrogen-fueled internal combustion engines. Prog Energy Combust Sci 2009;35(6):490–527. <https://doi.org/10.1016/j.pecs.2009.08.001>.
- Zamel, N, Li X. Life cycle comparison of fuel cell vehicles and internal combustion engine vehicles for Canada and the United States. J Power Sour 162(2 SPEC. ISS. ):2006:1241–53. doi:10.1016/j.jpowsour.2006.08.007.
- Pehnt M. Life-cycle analysis of fuel cell system components. In: Handbook of fuel cells, vol. 4; 2003, Ch. 94. p. 1293–317. doi:10.1002/9780470974001.f312108.
- Suwanmanee U, Saebea D, Hacker V, Assabumrungrat S, Arpornwichanop A, Authayanun S. Conceptual design and life cycle assessment of decentralized power generation by HT-PEMFC system with sorption enhanced water gas shift loop. Energy Conv Manage 2018;171(April):20–30. <https://doi.org/10.1016/j.enconman.2018.05.068>. URL: <https://doi.org/10.1016/j.enconman.2018.05.068>.
- Safari F, Dincer I. A review and comparative evaluation of thermochemical water splitting cycles for hydrogen production. Energy Conv Manage 205(October 2019):2020;112182. doi:10.1016/j.enconman.2019.112182. URL: <https://doi.org/10.1016/j.enconman.2019.112182>.
- Shahid UB, Bicer Y, Ahzi S, Abdala A. Thermodynamic assessment of an integrated renewable energy multigeneration system including ammonia as hydrogen carrier and phase change material energy storage. Energy Conv Manage 2019;198(July):111809. <https://doi.org/10.1016/j.enconman.2019.111809>. URL: <https://doi.org/10.1016/j.enconman.2019.111809>.
- Evangelisti S, Tagliaferri C, Brett DJ, Lettieri P. Life cycle assessment of a polymer electrolyte membrane fuel cell system for passenger vehicles. J Cleaner Prod 2017;142:4339–55. <https://doi.org/10.1016/j.jclepro.2016.11.159>. URL: <https://doi.org/10.1016/j.jclepro.2016.11.159>.
- Elgowainy A, Reddi K, Wang M. Life-Cycle Analysis of Hydrogen On-Board Storage Options, Argonne National Laboratory. URL:[http://www.hydrogen.energy.gov/pdfs/review13/an034\\_elgowainy\\_2013\\_o.pdf](http://www.hydrogen.energy.gov/pdfs/review13/an034_elgowainy_2013_o.pdf).
- García Sánchez JA, López Martínez JM, Lumbreras Martín J, Flores Holgado MN, Aguilar Morales H. Impact of Spanish electricity mix, over the period 2008–2030, on the Life Cycle energy consumption and GHG emissions of Electric, Hybrid Diesel-Electric, Fuel Cell Hybrid and Diesel Bus of the Madrid Transportation System. Energy Conv Manage 2013;74:332–43. <https://doi.org/10.1016/j.enconman.2013.05.023>.
- Sherwood SC, Dixit V, Salomez C. The global warming potential of near-surface emitted water vapour. Environ Res Lett 2018;13(10):104006. <https://doi.org/10.1088/1748-9326/aae018>. URL: <https://doi.org/10.1088/1748-9326/aae018>.
- IPCC, Climate Change 2014, Tech. rep., Cambridge; 2015. URL:[https://www.cambridge.org/core/product/identifier/CBO9781139177245A012/type/book\\_part](https://www.cambridge.org/core/product/identifier/CBO9781139177245A012/type/book_part).
- European Commission - Eurostat, Energy balances; 2017. URL:<https://ec.europa.eu/eurostat/web/energy/data/energy-balances>.
- Boyden A, Soo VK, Doolan M. The environmental impacts of recycling portable lithium-ion batteries. Procedia CIRP 2016;48:188–93. <https://doi.org/10.1016/j.procir.2016.03.100>. URL: <https://doi.org/10.1016/j.procir.2016.03.100>.
- Notter DA, Kouravelou K, Karachalios T, Daletou MK, Haberland NT. Life cycle assessment of PEM FC applications: Electric mobility and  $\mu$ -CHP. Energy Environ Sci 2015;8(7):1969–85. <https://doi.org/10.1039/c5ee01082a>.
- Keoleian G, Miller S, Kleine RD, Fang A, J.sley, Life Cycle Material Data Update for GREET Model - Report No. CSS12-12, Tech. rep.; 2012. URL:[http://css.snre.umich.edu/css\\_doc/CSS12-12.pdf](http://css.snre.umich.edu/css_doc/CSS12-12.pdf).
- Transport Canada, GMC Sierra 1500 Hydrogen Internal Combustion Engine (HICE ) Test Results Report (June).
- Hass H, Huss A, Maas H. Well-to-Wheels analysis of future automotive fuels and powertrains in the European context: Tank-to-Wheels Appendix 1 - Version 4.a, 2014. doi:10.2790/95839.
- US DOE, Technology Assessment of a Fuel Cell Vehicle: 2017 Toyota Mirai Energy Systems Division, US DOE -Energy Systems Division. URL: [www.anl.gov](http://www.anl.gov).
- Lampert D, Cai H, Wang Z, Wu M, Han J, Dunn J, et al. Development of a Life Cycle Inventory for Water Consumption Associated with the Production of Transportation Fuels, Tech. rep., Argonne National Laboratory - Energy Systems Division; 2015.
- Hogerwaard J, Dincer I, Naterer GF. Experimental investigation and optimization of integrated photovoltaic and photoelectrochemical hydrogen generation. Energy Conv Manage 207(January):2020;112541. doi:10.1016/j.enconman.2020.112541. URL: <https://doi.org/10.1016/j.enconman.2020.112541>.
- Nagapurkar P, Smith JD. Techno-economic optimization and environmental Life Cycle Assessment (LCA) of microgrids located in the US using genetic algorithm. Energy Conv Manage 181(December 2018):2019;272–91. doi:10.1016/j.enconman.2018.11.072. URL: doi: 10.1016/j.enconman.2018.11.072.
- Antzara A, Heracleous E, Bukur DB, Lemonidou AA. Thermodynamic analysis of hydrogen production via chemical looping steam methane reforming coupled with in situ CO<sub>2</sub> capture. Energy Procedia 63(May 2015):2014;6576–89. doi:10.1016/j.egypro.2014.11.694.
- Farid A, Gallarda J, Mineur B, Bradley S, Ott W, Ibler M. Best available techniques for hydrogen production by steam methane reforming, IGC document. URL:<http://www.eiga.eu>.
- Dai Q, Kelly JC, Elgowainy A. Vehicle Materials: Material Composition of U.S. Light-duty Vehicles, Tech. Rep. September, Argonne National Laboratory: Energy Systems Division; 2016.
- Kawamura A, Yanai T, Sato Y, Naganuma K, Yamane K, Takagi Y. Summary and progress of the hydrogen ICE truck development project. SAE Int J Commer Veh 2009;2(1):110–7. <https://doi.org/10.4271/2009-01-1922>.



# Optimization and sizing of a fuel cell range extender vehicle for passenger car applications in driving cycle conditions

S. Molina, R. Novella<sup>\*</sup>, B. Pla, M. Lopez-Juarez

CMT-Motores Térmicos, Universitat Politècnica de València, Camino de vera s/n, 46022 Valencia, Spain

## ARTICLE INFO

### Keywords:

Fuel cell vehicle  
Plug-in  
Range-extender  
Driving cycle  
Sizing  
Optimization

## ABSTRACT

Aiming to reduce global warming and emissions in general, cleaner technologies are the spotlight of research and industry development. Among them, fuel cell vehicles (FCV) are gaining interest to decarbonize the transport sector. Plug-in FCV or FCV in range-extender configuration (FCREx) is an interesting option to reduce the total cost of ownership (TCO) and the energy usage per km. The aim of this study was to generate design spaces of FCREx by varying the FC stack maximum power output, the battery capacity, and the H<sub>2</sub> tank capacity to understand the implications of this architecture in range, consumption, and cost (estimated with a WLTP driving cycle). Unlike other studies, the approach was focused on a novel architecture for passenger vehicles and was focused on the development of the validated FC system model and the energy management strategy (EMS) optimization for each design, based on the Pontryagin Minimum Principle (PMP). Consumption was found to decrease with increasing battery capacity and FC maximum power due to the higher efficiency of the systems. The design spaces showed how with 5 kg of H<sub>2</sub> and ≥50 kWh of battery capacity the maximum range of FCREx could be over 700 km. The results of this study showed how FCREx architecture could provide overall energy consumption saving up to 6.8% and H<sub>2</sub> consumption saving ranging from 16.8% to 25%, compared to current commercial FCVs. The optimum FCREx design, not only based on performance, should have ~30 kWh of battery capacity and ≥80 kW of FC maximum power to minimize manufacturing costs while maximizing efficiency.

## 1. Introduction

With the growing interest in low environmental impact technologies for mobility, hydrogen fuel cell vehicles (FCVs) are getting relevant and have gained market share in the automotive industry [1]. This technology is not only relevant because it is relatively carbon-free, but also since the fuel (H<sub>2</sub>) has many advantages as an energy carrier (Section 2.1), relative to electricity for battery electric vehicles (BEVs).

As in any relatively new technology application, there exist several system architecture variations of the same technology that may improve or worsen the capabilities and performance of FCVs. This is the case of plug-in FCVs or FCVs in range-extender configuration (FCREx). FCREx configuration is a combination of BEVs and FCVs and has not yet been extensively explored for light passenger vehicles but has high potential to improve energy usage and may be the solution to extend the range of FCVs until enough H<sub>2</sub> refueling stations are built [2]. At present, the only architecture that was considered for light-duty passenger vehicles is that combining an FC system with a low-capacity battery. As such, the performance of FCREx architecture for passenger

vehicles and how it changes with systems sizing remains unexplored, thus neglecting the potential of an FCV architecture that may be key in the context of low availability of hydrogen refueling stations.

The sizing of FCREx is relatively more complex than that of a conventional FCV since the battery capacity also affects significantly the optimum energy management strategy of the vehicle systems, the cost, and the range. As such, for this type of vehicles, it is imperative to provide a detailed and wide analysis on the performance, range, and cost of systems for different combinations of FC system, battery capacity, and H<sub>2</sub> tank storage in order to understand the real potential and limits of such configuration, relative to simple FCVs.

In the literature, most of the studies focus on sizing non-plug-in FCV components [3], and those focused on FCREx [4] are not oriented towards light passenger vehicles or do not consider the same parameters as those in this study. Therefore, there is a clear lack of data regarding the sizing of FCREx systems for light-duty passenger cars.

The state-of-the-art research about FCREx for passenger vehicles is limited. As a consequence, it is difficult to assess the state-of-the-art focusing only on light-duty applications. Mainly, the recent related

<sup>\*</sup> Corresponding author.

E-mail address: [rinoro@mot.upv.es](mailto:rinoro@mot.upv.es) (R. Novella).

URL: <http://www.cmt.upv.es> (R. Novella).

research lines have been focused on the use of FCReX on bus and heavy-duty applications and on the energy management optimization of different FCV architectures to maximize performance. The studies focused on the use and sizing of FCReX architecture for bus applications use different EMS such as the CDCS (charge depleting and charge sustaining strategy) or two-step algorithms based on dynamic programming to analyze and optimize the vehicle costs and performance. With this, it was concluded that to minimize  $H_2$  in FCReX the priorities are in order: reducing auxiliary power, braking energy recovery, increase FC stack efficiency, and decreasing battery losses [5]. Furthermore, following these methodologies, it was found that the optimum systems sizing design for city buses should be close to 150 Ah for the battery capacity and 40 kW for the FC system maximum power output [6]. Nonetheless, the conclusions extracted from these studies are only applicable to city buses and the performance results are far from those expected for an FCReX light passenger vehicle.

Similar to city bus application, FCReX architecture was also explored for urban logistics vehicles, using tools such as convex programming or fuzzy logic controllers to solve the sizing problem. The combination of FC systems together with moderate-capacity batteries showed that the range of urban logistics vehicles could be extended with respect to BEV and the  $H_2$  consumption decreased by half [7]. Differently from the city bus application, the optimum battery capacity was estimated to be around 29 kWh, while the optimum FC stack maximum power depended on  $H_2$  price [8]. The dependence of FC sizing with  $H_2$  cost to minimize the TCO showed how sensitive the performance of FCReX vehicles is to FC stack sizing since higher FC stack maximum power implies lower  $H_2$  consumption due to the higher system efficiency.

Among the heavy-duty applications, the use of FC for trucks is considered to provide the most advantages with respect to BEV and ICEV trucks due to the high range and carbon-free emissions. FCReX architecture is very compatible with these heavy-duty vehicles since it enables flexible operation and lower consumption. Recent research showed that using FCReX architectures for trucks could reduce the TCO by 1.3% with respect to conventional FCV architectures [9], but the result is still dependent on  $H_2$  costs. Furthermore, different EMS were explored and compared for FCReX trucks considering 8°C-HTC-HT and 7°C-WTVC Chinese truck driving cycles, concluding that convex-optimization-based EMS could provide minimal  $H_2$  consumption and be used in on-line driving. FCReX architecture was also used in mining truck applications, where the decrease in emissions is critical to ensure the safety of mining operations, given the small space and the potential gases build-up. For these vehicles, with an optimized FC-battery hybrid powertrain design the battery life was extended, the  $H_2$  consumption reduced, and the mining cost decreased by 8.7% [10].

Complementary to the FCReX-focused research lines, there have also been several studies also focused on EMS optimization using driving cycles simulations or conventional FCV systems sizing to improve fuel economy and system durability, but they used other components such as supercapacitors [11] or low-capacity batteries [12].

In light of the studies presented that represent the state-of-the-art of FCReX, it is worth noting that most of the use low-order models to express the FC system performance such as simple and constant polarization curves [10,11], simple polynomials [8,13] or simply straight lines expressing constant FC efficiency [12] that do not capture the physics behind the FC performance variation with operating conditions. In most of these studies, the FC system management was not optimized nor validated, while most of the research was focused on EMS optimization. This implies that the results were only partially-optimized and could be further improved.

The overview of the state-of-the-art research shows that currently, FCReX architecture has mostly been considered for heavy-duty applications and captive fleets such as urban logistics vehicles. Sizing studies for this architecture and applications already exist, but the conclusions and optimal designs do not apply to passenger vehicles. Furthermore,

sizing studies focused on the use of FC for passenger applications do not consider FCReX architecture.

In conclusion, the literature regarding the sizing of FCReX is still limited, particularly for light passenger vehicles, and mostly omit the fundamental behavior and optimization of the FC system.

### 1.1. Knowledge gaps and contributions

From the analysis of the state-of-the-art, some conclusions can be extracted to provide an idea of the knowledge gaps in the literature:

1. FCReX architecture has been explored for heavy-duty vehicles such as city buses or trucks but the literature focused on using this architecture for light-duty passenger cars is limited.
2. Most of the studies do not provide the space designs generated from their sizing analyses. The results are usually based on the optimum design based on the criteria of each particular study. Generating and showing the space designs is very important to provide an estimation of the capabilities of a system, given a wide range of design combinations.
3. Range is usually not estimated for the different designs produced in the sizing analyses. In the case of FCV and FCReX, there is an actual need to understand and quantify how the sizing of the components affects the range and consumption. By showing the range estimation in design spaces, it is possible to provide passenger car manufacturers an estimation of the preliminary design they should aim for with a chosen range.
4. Most of the studies consider the FC system maximum net output power, the battery capacity, or the  $H_2$  mass in the deposit, but very few consider these three parameters simultaneously as sizing parameters and, in the case they do, the target vehicle is a city bus instead of a light-duty passenger car.
5. The studies usually used FC system models that are not validated or, in the cases where they were validated or obtained experimentally, have not been optimized previously. Frequently, the optimization of each design was performed by optimizing only the EMS, which has a significant impact on consumption and costs reduction but does not focus on prior-optimizing the FC system behavior. Therefore, the sizing analyses usually omit the fundamental behavior and optimization of the FC system.
6. Sizing and EMS optimization are strongly coupled to provide a representative benchmarking of different designs. Some studies use the same EMS for different designs even though the load demand and the system efficiencies also change with load.
7. The resulting optimum designs from the sizing studies were not compared against commercial FCV to prove the increase in fuel economy or overall performance.

The motivation and contribution of this paper provide an understanding of the performance and costs of vehicles with FCReX architecture depending on the systems sizing and to identify how the battery capacity, the FC stack maximum power, and the  $H_2$  tank capacity should be dimensioned depending on the target range and/or consumption. To fulfill these objectives, space designs for light-duty passenger FCReX were generated and analyzed considering as sizing variables the FC stack maximum power, the battery capacity, and the  $H_2$  tank capacity (knowledge gaps 1, 2, 3 & 4). Unlike other studies, the FC stack model was validated at different operating conditions, the BoP operation was optimized, and the EMS between the FC stack and the battery was optimized independently for each design with the PMP (knowledge gaps 5 & 6). This means that the optimization of the FCReX was performed comprising the FC system operation and the EMS. The resulting FC system model was fully-scalable. The design spaces showing the range, the estimated systems cost, and the  $H_2$  consumption were generated considering the WLTP driving cycle WLTC class 3b since the power-to-mass ratio of most of the designs was over 34 (this WLTC driving cycle was also chosen so that the final results can

be compared against current commercial FCVs). Finally, state-of-the-art commercial FCVs were compared against equivalent-in-range optimum FCREx designs to understand the capabilities of this FCV architecture (knowledge gap 7).

## 1.2. Document outline

This study comprises the following parts: introduction (Section 1), theoretical foundations (Section 2), methodology (Section 3), BoP operating conditions optimization (Section 4), FCREx systems sizing (Section 5), and conclusions (Section 6). In the Introduction and the theoretical foundations sections, the objectives, background, and motivation of the study are defined and explained. The simulation tools and procedures were described in the methodology section. The results are presented and discussed in BoP operating conditions optimization and FCREx systems sizing sections, where the optimum operating conditions and energy balance of the FC system and the consequences of varying the FCREx design are analyzed respectively. Finally, the main conclusions of this study were summarized in the conclusions section.

## 2. Theoretical foundations

### 2.1. $H_2$ as energy carrier

Hydrogen can offer numerous benefits if used as an energy carrier in most sectors. The main advantages of this fuel are its carbon-free emissions when burned or used in an FC, the possibility of producing it through different production strategies such as electrolysis or steam methane reforming (SMR), and its higher energy density in terms of mass and volume than batteries [1,14,15]. However, there is not such a thing as the perfect fuel, therefore  $H_2$  has also some disadvantages if compared against batteries or conventional fuels.

Regarding the energy production sector,  $H_2$  can be used effectively to decarbonize the gas grid. Biogas is expected not to be available at the required scale and full electrification with heat pumps would be very expensive for old buildings and would produce such seasonal imbalances in power demand that a large-scale power storage mechanism, such as  $H_2$ , would be required. Using  $H_2$  as an energy carrier could maximize the efficiency of energy usage in the electric grid by absorbing the seasonal energy imbalances. Furthermore, its gas properties and storage versatility enable low-cost long-range renewable energy transportation through pipelines, ships, or trucks, compared to power transmission lines. The transport of  $H_2$  could be even further optimized to reduce transportation costs and  $CO_2$  emissions if it is first converted to any liquid e-fuel such as methanol or ethanol through  $CO_2$  sequestration. These fuels, if produced from  $H_2$ , can also be used directly in ICE producing neutral  $CO_2$  emissions [16–18].

In the transportation sector,  $H_2$  has higher energy density than batteries, thus enabling long-range displacements (>500 km), and lower cradle-to-grave emissions than hydrocarbon-fueled vehicles [19], given the large variety of  $H_2$  production strategies. Furthermore, FC systems can be easily scaled with significantly lower specific weight and power density than batteries. This makes  $H_2$  the only option to decarbonize the operation of heavy-duty vehicles, ships, trains, and aircraft while it is a perfect fuel to complement and coexist with batteries and/or neutral  $CO_2$  emissions ICE for light-duty vehicles, enabling high-range, carbon-free passenger cars [1,14].

### 2.2. FC vehicles: non-plug-in FCV and FCREx

Fuel cell vehicles can be classified according to many criteria such as the fuel storage method (pressurized  $H_2$  or liquid carriers to be reformed/cracked), the power system structure (direct or indirect), or the battery size (plug-in or non-plug-in). Despite all the possible classifications, it is relevant to remark how all of them are equivalent to a serial hybrid electric vehicle. Currently, the commercial FCVs Honda

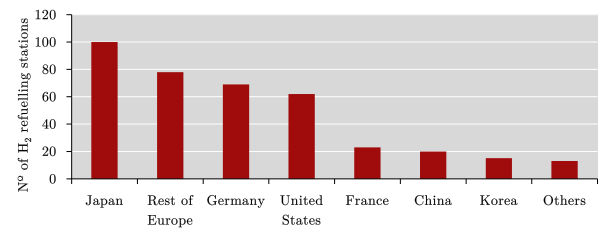


Fig. 1. Hydrogen refueling stations in different countries in 2018 [14].

Clarity, Toyota Mirai, and Hyundai Nexo have an indirect-type power architecture,  $H_2$  stored at 700 bar of pressure, and have small batteries (non-plug-in). Regarding the power system structure and the fuel storage of these vehicles, it is understandable to choose the indirect-type power architecture to reduce the size of the fuel cell system and compressed  $H_2$  because this technology has been reliably demonstrated (high TRL) [20]. However, despite the absence of light-duty plug-in vehicles in the market, they must not be discarded since they can offer significant benefits compared to non-plug-in vehicles. These benefits are mainly lower degradation rate, potentially higher performance, increased operational flexibility, and lower TCO and cradle-to-grave emissions.

Plug-in FCVs operate using the FC like a range extender (FCREx) because both the FC and the battery can minimize power and battery state-of-charge (SOC) fluctuations. The power fluctuations that the FC stack suffers in non-plug-in vehicles operation and frequent start and stop increase their degradation [21,22], thus leading to a decrease in performance and increase of user costs. Analogously, in-depth battery discharge or very high SOC also lead to decreased durability and performance. Therefore, keeping battery SOC in moderate and stable levels increases its life and reduces user maintenance costs [23].

Recent technological assessments of commercial FCVs show that state-of-the-art FC systems are capable of presenting highly dynamic behavior, enough to satisfy the power requirements of aggressive driving cycles with small batteries [24]. However, highly dynamic behavior induces an additional cost in performance, apart from degradation. That is why, the stable operation of FCREx could, besides, contribute to reducing  $H_2$  consumption.

The bigger batteries of FCREx allow for a more flexible operation, enabling purely electrical mode and hybrid mode, depending on the user requirements. This is especially important in the current situation, where the price of  $H_2$  is far above that of electricity and there are few  $H_2$  refueling stations across the world (Fig. 1). In this case, these vehicles could operate as battery electric vehicles (BEV) in cities, where 100 km of range is enough since the vehicle can be charged overnight, and use the FC to extend the range for extra-urban movements with an approximate range of 500 km.

Finally, the TCO may be lower for an FCREx if the battery is not over-dimensioned. TCO includes the price of the vehicle, the insurance, the cost of fuel or energy source, the maintenance, and various taxes and fees. Assuming that insurance and taxes/fees are fundamentally the same for FCREx and non-plug-in FCV, FCREx could reduce the TCO due to various reasons. First, since the battery capacity is comparatively higher, the FC system maximum net power can be reduced. Hence, the stack and all the components of the FC system should have lower power requirements and should be cheaper. However, this could be outweighed by the increase in the production cost of a larger battery. Second,  $H_2$  is currently more expensive than electricity if produced through electrolysis with the same electricity mix, therefore the operation costs of an FCV may be greater than those of a BEV. Using a mix of electricity and  $H_2$  is an option to reduce the TCO of FCV. The option of obtaining  $H_2$  from steam methane reforming, which should be considerably cheaper than from electrolysis, is not considered because this process produces  $CO_2$  emissions and therefore it is not the long-term solution to sustain the vehicle portfolio of the  $H_2$  economy [19].

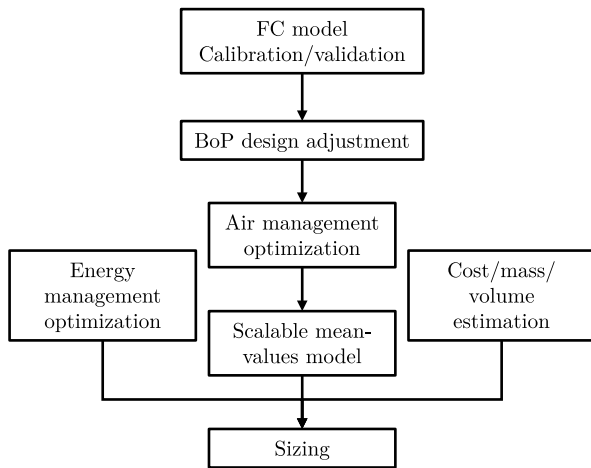


Fig. 2. Methodology flow chart.

### 3. Methodology

Studies such as optimization or sizing of vehicle systems must be carried out using simulation tools capable of representing reliably the physics of the target system. The software GT-Suite v2020 was used to perform this study. GT-Suite is a 0D–1D modeling tool widely used in the automotive industry. As such, it is capable of reproducing high fidelity numeric results based on energy, momentum, and mass conservation equations coupled with empirical correlations. 0D–1D modeling software is suitable for sizing and optimization studies since they can produce reliable results at the expense of low computational cost. However, especially for FC systems, they must be calibrated and validated with experimental data.

As such, the first step in this study was to calibrate and validate the GT-Suite FC model using experimental data [25,26]. Then, a model for the BoP of the FC system was adjusted to match the flow requirements of the FC stack. Next, the air management strategy of the resulting model, describing the FC system (BoP and FC stack), was optimized in steady conditions. The results from this optimization were then used to develop a mean-values model in order to reduce the computational cost of the complex model by sacrificing the FC system dynamics. For the sizing, the energy management strategy between the FC system and the battery was optimized to minimize  $H_2$  consumption and the variation of the SoC of the battery for each design independently. GT-Suite was connected to MATLAB Simulink to perform the energy management strategy optimization. Finally, parameters such as the system costs, weight, the vehicle range, and  $H_2$  consumption were estimated for different FCEx designs whose FC system net power,  $H_2$  tank, and battery capacities were varied along the defined design space. This methodology is represented in Fig. 2.

#### 3.1. FC model description

The polarization curve of the FC stack model used in this study is defined as follows:

$$V_{FC} = V_{OC} - V_{act} - V_{ohm} - V_{conc} \quad (1)$$

$$V_{OC} = \frac{-\Delta\bar{g}_f}{2F} \quad (2)$$

$$V_{act} = \begin{cases} \frac{R_{gas}T}{2F} \left( \frac{i}{i_0} \right) \\ \frac{R_{gas}T}{2\alpha F} \ln \left( \frac{i}{i_0} \right) \end{cases} \quad (3)$$

$$V_{ohm} = R I \quad (4)$$

$$V_{mt} = -C \ln \left( 1 - \frac{i}{i_l} \right) \quad (5)$$

where  $V_{OC}$  is the open voltage circuit and  $V_{act}$ ,  $V_{ohm}$  and  $V_{mt}$  are the activation, ohmic and mass transport losses. Advanced losses modeling was used to include the sensitivity of the ohmic resistance and the exchange current density to the FC operating conditions. The ohmic resistance  $R_{ohm}$  was modeled according to [27] by considering the change in the ionic conductivity of the membrane as a function of the membrane water content, temperature, and membrane properties:

$$\sigma_{30} = 0.005139w - 0.00326(w > 1) \quad (6)$$

$$\sigma(T_{cell}) = \exp \left[ 1268 \left( \frac{1}{303} - \frac{1}{273 + T_{cell}} \right) \right] \quad (7)$$

$$R_{ohm} = \int^{t_m} \frac{dz}{\sigma} \quad (8)$$

where  $w$  is the local membrane water content,  $\sigma_{30}$  and  $\sigma(T_{cell})$  are the protonic conductivity of the membrane at 30°C and at  $T_{cell}$  respectively,  $T_{cell}$  is the cell temperature, and  $t_m$  is the membrane thickness.

Analogously, the exchange current density was modeled as a function of the FC temperature, the oxygen partial pressure, the electrochemical activation energy, the electrode roughness and the reference exchange current density  $i_{0,ref}$  [28].

$$i_0 = i_{0,ref} a_c L_c \left( \frac{p_{O_2}}{p_{O_2,ref}} \right)^{\gamma_c} \exp \left[ \frac{-E_{act}}{RT} \left( 1 - \frac{T}{T_{ref}} \right) \right] \quad (9)$$

where  $a_c L_c$  is the electrode roughness (defined by the material properties),  $p_{O_2}$  is the oxygen partial pressure,  $\gamma_c$  is the pressure dependency factor of the electrochemical reaction,  $E_{act}$  is the activation energy of the electrochemical reaction,  $R$  is the ideal gas constant, and  $T$  is the stack temperature.

The parameters that can be used to calibrate this formulation of the polarization curve (Section 3.2) are the mass transport loss coefficient  $\alpha$ , the exchange current density  $i_{0,ref}$ , the limiting current density  $i_l$  and the open circuit losses, already included into  $V_{OC}$ .

Although this model was calibrated to experimental data, it still has some limitations that are not relevant for this study. For example,  $N_2$  crossover was not modeled since the simulations of the WLTC 3b driving cycle only last 30 min (computational time), so the effect of  $N_2$  on performance and degradation is minimum in such a short time frame. Furthermore, FC degradation was not modeled because the performance deviation due to degradation in such a short time frame is negligible. Therefore, the designs that were simulated in this study represent the maximum realistic performance of the systems. The evaluation of the degradation of the systems with the design and the EMS is out of the scope of this study.

#### 3.2. FC model validation/calibration

The calibration of an FC stack model with experimental data is critical. Given the definition of the polarization curve, there are several coefficients and parameters that need to be calibrated (Eq. (1)). As such, there are several possibilities for the same polarization curve and, depending on the value of these parameters, the sensitivity of the polarization curve to boundary conditions changes. In order to validate and calibrate properly a FC stack model, it is mandatory to have data about how the polarization curve changes with temperature and pressure, i.e., the calibration should be valid for a wide range of operating conditions.

The experimental data from [25,26] was used to calibrate the FC stack model. These data were measured from a 80 cells, 20 kW PEMFC experimental facility under temperature, stoichiometry and pressure-controlled conditions. Active surface area was assumed to be 250 cm<sup>2</sup>. Also, the polarization curve was measured at different cathode pressure and temperature. Therefore, the data is sufficient not only to capture the polarization curve but to capture and calibrate the sensitivity to temperature and pressure of the model.



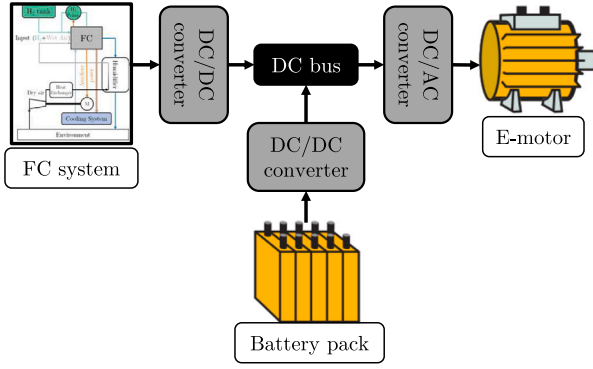


Fig. 5. Powerplant electronic configuration.

no overheating is produced in the battery. However, due to the lack of data, the effect of temperature on the battery was not accounted for. Finally, the DC/DC converter for the battery and the DC/AC converter for the electric motor were modeled with a constant conversion efficiency of 95%.

### 3.3.3. Vehicle body

An FCREx vehicle requires relatively high storage capacity to allocate the FC system, the H<sub>2</sub> tanks and the battery. As such, a vehicle body similar to that of Hyundai Nexo has been used in this study. After preliminary calculation, the vehicle has enough space to store relatively high-size batteries, given the trunk volume. The vehicle dry mass without the FC system, the H<sub>2</sub> tanks and the battery was estimated as 1400 kg, with a frontal area of 2.58 m<sup>2</sup> and a drag coefficient of 0.329, based on Hyundai Nexo technical specifications [31].

The vehicle electrical architecture was decided to be indirect (Fig. 5). This configuration, although it could be less efficient than the direct configuration, allows to increase the FC lifetime since it is protected from the electric fluctuations of the system bus and to downsize the FC system thanks to the DC/DC converter it is connected to [20]. As mentioned before, the conversion efficiency of each DC/DC or DC/AC converters was assumed constant and equal to 95% to account for these power losses.

The device powering the shaft is an electric motor with 120 kW of maximum power whose torque–power curve provides highly-enough torque even at high load. The connection between the e-motor and the shaft was set as a direct drive.

### 3.4. Energy management strategy

The energy management in a powertrain with different energy sources, essentially consists of finding the sequence of power split that fulfills the design criteria with minimum cost [32]. It is a key aspect governing, to a great extent, the performance of the complete system [33]. In this sense, an inappropriate power split strategy may affect the benchmark between different sizing combinations, therefore leading to a biased decision on which is the best powertrain sizing. Optimal Control (OC) is a tool specially suited to develop the energy management strategy in a benchmark study such as the one presented in this paper, since it naturally provides the optimal energy split for every powertrain considered. Accordingly, all the architectures under investigation will be compared in the best possible scenario [34].

In line with the previous idea, the OC problem consisting of finding the powertrain control policy that minimizes a cost index over the considered driving cycle has been solved for every architecture assessed. Regarding the control variable, considering the powertrain model described in previous sections, and particularly the energy balance in the DC bus see Fig. 5, leads to:

$$P_{dem} = P_{batt} + P_{FC} \quad (10)$$

where the electrical power required by the motor to propel the vehicle ( $P_{dem}$ ) can be supplied by the battery ( $P_{batt}$ ), the FC ( $P_{FC}$ ), or a combination of both. Note that the evolution of  $P_{dem}$  only depends on the driving cycle and therefore taking the FC power as control variable ( $u = P_{FC}$ ) the electrical power demanded (or delivered) to the battery ( $P_{batt}$ ) can be obtained as:

$$P_{batt} = P_{dem} - u \quad (11)$$

Concerning the optimization objective, the fuel consumption (H<sub>2</sub>) has been chosen as cost to be minimized, although similarly, the fuel cost, the total energy consumed or CO<sub>2</sub> emissions associated to battery charging or H<sub>2</sub> production could be used.

Considering the chosen control variable and optimization criteria, the problem can be formally defined as finding the control law  $u(t)$  over time  $t$  that minimizes the cost:

$$J = \int_{t_0}^{t_f} P_f(u(t), t) dt \quad (12)$$

where  $P_f$  is the fuel (H<sub>2</sub>) power consumed depending on the control variable ( $u$ ), in the case at hand, the electrical power delivered by the FC. Observe that as  $P_f$  is proportional to the fuel consumption, minimizing Eq. (12) will naturally minimize fuel consumption. The detailed FC model described in Sections 3.1 and 3.3.1 was simplified to a table ( $P_f = P_f(u)$ ) providing the fuel power  $P_f$  depending on the electrical power delivered by the FC, i.e. the control variable  $u$ .

Considering the univocal relation between  $u$  and  $P_f$ , the only state in the system is the energy stored in the battery ( $E_b$ ) whose dynamic equation is:

$$\dot{E}_b = -P_b \quad (13)$$

being  $P_b$  the variation in the battery state of energy (which is considered positive when the battery is being discharged and negative when the battery is being charged). Note that  $P_b$  can be calculated from  $P_{batt}$  and the battery model described in Section 3.3.2.

Finally, regarding the optimization constraints, as grid charging is not considered, and all the energy should ultimately come from the FC, the net battery charge variation in a long enough cycle should be zero to assess the battery charge sustaining and to allow a fair comparison between the powertrains considered. This is included in the optimization problem as:

$$\int_{t_0}^{t_f} P_b(u(t), E_b(t), t) dt = 0 \quad (14)$$

Pontryagin's Minimum Principle allows solving the global optimization problem defined in Eqs. (12)–(14) as a sequence of local optimization problems. In particular, the PMP states that if  $u^*$  and  $E_b^*$  are the optimal trajectories of the control and battery energy over the driving cycle, then:

$$H(u^*, E_b^*, \lambda^*, t) \leq H(u, E_b, \lambda, t) \quad \forall u \in U, t \in [t_0, t_f] \quad (15)$$

where  $H$  is the Hamiltonian function, defined as:

$$H = P_f - \lambda \dot{E}_b = P_f(u(t), t) + \lambda(t) P_b(u(t), E_b(t), t) \quad (16)$$

Note that because  $P_f$  and  $P_b$  share the same units, the co-state  $\lambda$  is dimensionless. PMP identifies the evolution of  $\lambda$  with the variation of the Hamiltonian ( $H$ ) with respect to the state ( $E_b$ ):

$$\dot{\lambda} = \frac{\partial H}{\partial E_b} \quad (17)$$

Replacing Eq. (16) into (17) and introducing  $P_{batt}$  yields:

$$\dot{\lambda} = \lambda \frac{\partial P_b}{\partial E_b} = \lambda P_{batt} \frac{\partial (P_b/P_{batt})}{\partial E_b} \quad (18)$$

where the electrical power provided by the battery ( $P_{batt}$ ), according to expression (11), depends on  $u(t)$  but not on  $E_b$ . The ratio  $P_b/P_{batt}$  represents the battery efficiency. Since the sensitivity of the battery parameters (open circuit voltage and internal resistance) on variations in

**Table 2**  
Energy management main characteristics.

Control input ( $u$ )	Fuel cell power	$P_{FC}$
State	Energy in the battery	$E_b$
Objective	Fuel minimization	Eq. (12)
Constraint	Charge sustaining	Eq. (14)
Algorithm	PMP	

**Table 3**  
Mass, volume and cost data [36–41].

System	Data used to estimate Mass–Volume	Cost
FC system	Linear correlation:	40/kW <sub>net</sub>
	• Estimated 175 kg and 286 l for a 30 kW system • 250 kg and 614 l for a 70 kW system	– 36 €/kW <sub>net</sub>
H <sub>2</sub> tank	0.045 kg H <sub>2</sub> /kg system	333/kg H <sub>2</sub>
	0.030 kg H <sub>2</sub> /l system	– 300 €/kg H <sub>2</sub>
Battery	220 Wh/kg	156/kWh
	600 Wh/l	– 140 €/kWh

$E_b$  is small,  $\lambda$  can be assumed constant for the considered system [35]. Therefore, the optimization problem is reduced to choose the proper constant value of  $\lambda$  which satisfies the problem constraint (Eq. (14)). An extensive review of the application of PMP to the Energy Management of Hybrid Electric Vehicles can be found in [32] and references within.

As in the current work the driving cycle is known in advance,  $\lambda$  can be found by any iterative method, testing different values of  $\lambda$  until the constraint (Eq. (14)) is satisfied. As an initial guess to the value  $\lambda$ , one can note that, applying the condition of minimum to Eq. (16) leads to:

$$\lambda = - \frac{\left( \frac{\partial P_f}{\partial u} \right)}{\left( \frac{\partial P_b}{\partial u} \right)} \quad (19)$$

where terms in numerator and denominator are related to the efficiencies of FC and battery respectively, and the denominator is clearly negative due to Eq. (11). In this sense, the ratio between FC and battery average efficiencies is a good first guess for  $\lambda$ .

Table 2 summarizes the details of the Energy Management Strategy

### 3.5. Mass, volume and cost estimation

The data to estimate the mass, volume and systems cost was obtained from different sources (Table 3). Data about the systems mass had a direct impact in the simulation since it determined the vehicle total mass. In contrast, volume and cost data were only estimated for post processing purposes. Volume data was used to ensure that the H<sub>2</sub> tank and battery systems were small enough to fit in the rear part of the vehicle by reducing the space of the trunk. Cost estimation was performed with current data when possible or with data from DOE objectives when not public data was available. The final systems cost was used to understand which design offered the lowest production cost.

## 4. BoP operating conditions optimization

Prior to the sizing of the FC system, it is necessary to optimize the operating conditions of the BoP. There are several parameters affecting the performance of the FC stack such as the stoichiometry, the pressure, the temperature and the relative humidity at both the anode and the cathode. Among these parameters, the cathode stoichiometry and pressure have a major effect on the FC system performance since their values are coupled with the compressor consumption, which is significantly higher than that of the H<sub>2</sub> recirculating pump or the coolant pump. As such, in this study, the optimization of the BoP was performed

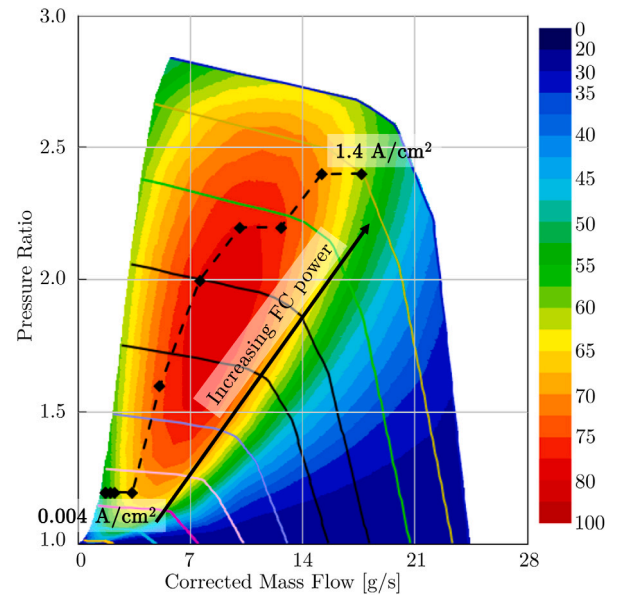


Fig. 6. Parametrized compressor map with optimum operating conditions.

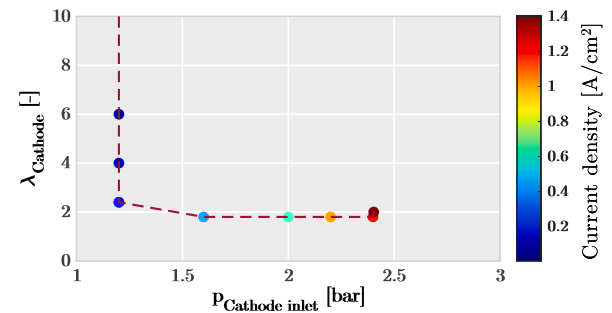


Fig. 7. Optimum cathode inlet pressure and stoichiometry at different current densities (load).

by optimizing the air management strategy with the FC stack load to maximize the FC system efficiency. The optimization was performed in steady-state conditions with some restrictions to avoid operating conditions during transient operation that may harm the integrity of the FC. As such, the cathode stoichiometry was always kept equal or over 1.8 to avoid cathode starvation during abrupt load increases, the anode pressure was always kept over the cathode pressure with a  $\Delta p$  limited to 0.3 bar and the minimum cathode inlet pressure was set to 1.2 bar to overcome the pressure losses of the FC stack and auxiliary devices and ensure atmospheric pressure at the outlet of the system.

Regarding the other parameters affecting the FC stack performance, some additional constraints were added:

- Anode stoichiometry was always 3 to avoid anode starvation and increase H<sub>2</sub> diffusion through the anode gas diffusion layer (GDL), thus maximizing the FC efficiency. This stoichiometry was kept this high because the energy consumption of the H<sub>2</sub> pump which controls it has a minor effect on the overall FC system.
- The relative humidity at the inlet of the cathode was 80% for any condition, i.e., the increase in temperature and pressure due to the compressor was taken into account to calculate the relative humidity.
- Coolant temperature at the outlet of the FC stack was kept to 70 °C.

All these parameters were controlled by means of PID controllers as explained in Section 3.3.1.

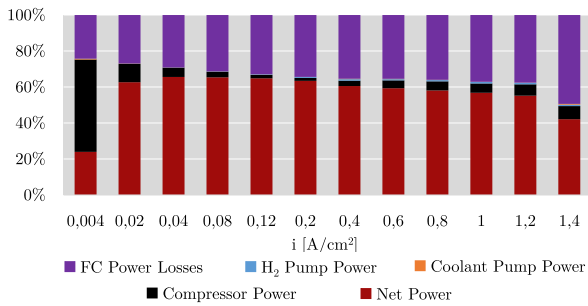


Fig. 8. FC system optimum power distribution as a function of the current density.

Table 4  
BoP management optimization characteristics.

Methodology	Design of experiments	
Control input ( $u$ )	Cathode inlet pressure	$p_{cath}$
	Cathode stoichiometry	$\lambda_{cath}$
Objective	Efficiency maximization	$\eta_{FC\text{system}}$
Constraints	Security: Section 3.3.1	
	Performance: Section 4	

The optimization was performed for the baseline design. Since this optimization is intended to be scalable, in this section the load is expressed in terms of the current density so that it is common for all the designs (Fig. 7). In order to optimize the BoP operating conditions, the stoichiometry and the cathode inlet pressure were varied in the range of 1.8 to 60 (the highest values correspond to extremely low load) and from 1.2 to 2.5 bar (to preserve mechanical integrity) respectively. A summary of the main characteristics of the optimization process can be found in Table 4.

From Fig. 6 it is possible to conclude that the optimum air management strategy of an FC system, as in ICE, is that minimizing the compressor wasted energy, i.e., for a given cathode stoichiometry (mass flow) the optimum compressor pressure ratio is that offering the maximum efficiency. This implies that the effect of increasing the FC stack fuel efficiency with air pressure has a relatively low impact on the optimization of the BoP operating conditions.

Analogously, Fig. 7 shows how for low loads high cathode stoichiometry was required to avoid compressor surge and the corresponding inefficiency. High pressure at high load was required only to optimize the compressor efficiency given a mass flow rate. However, as soon as the compressor can offer low stoichiometry without suffering from surge (from 0.2–0.4 A/cm<sup>2</sup>), the cathode stoichiometry converges towards the self-imposed lower limit of 1.8, thus minimizing the compressor mass flow rate and power consumption. From this, it is possible to conclude that the driving factor when optimizing the air management strategy of an FC system is the compressor power consumption and efficiency, outweighing the increase in FC stack efficiency with cathode pressure and stoichiometry.

The optimum power distribution of the FC system is shown in Fig. 8. The red bar, representing the FC system net power (FC stack power minus the power consumption of the auxiliary devices), also represents the FC system efficiency. The other bars represent the power losses due to different causes such as the FC stack inefficiencies and the power consumption of the BoP (mostly compressor power consumption). As such, the curve described by joining the red bars represents the polarization curve of the FC system efficiency. In this graph it is possible to differentiate four operating regions depending on the current density:

- Ultra-low load ( $i \approx 0.004$  A/cm<sup>2</sup>): the compressor consumes most of the power provided by the FC stack while the FC efficiency is maximum because ohmic losses are negligible. The FC system efficiency is the lowest. This region is similar to the idle condition for ICE. If available, a solution to increase the idle performance of

an FC system could be to use RAM air, i.e., air directly introduced to the FC stack by bypassing the compressor to avoid the pressure loss under the low-load condition and compressed when stopped due to the relative speed between the air and the vehicle.

- Low load ( $i \in [0.02, 0.04]$  A/cm<sup>2</sup>): compared to the previous region the FC stack losses increase because ohmic losses begin to have a noticeable effect. However, FC system efficiency grows with load because the FC electrical power increases significantly compared to the compressor power.
- Medium load ( $i \in [0.04, 0.4]$  A/cm<sup>2</sup>): FC system efficiency is maximized (desired operating conditions) since FC losses are moderate while the compressor power is minimized. Overall system efficiency could reach over 60%. Note that the efficiencies obtained here do not include the loss in power in the DC–DC converters and that the BoP operation was optimized and dimensioned according to the FC maximum power. This explains the slightly higher values of the efficiency in this study.
- High load ( $i \in [0.4, 1.4]$  A/cm<sup>2</sup>): FC losses are almost constant up to 1.2 A/cm<sup>2</sup> because compressor pressure ratio increases with load. Around 1.4 A/cm<sup>2</sup> mass transport losses increase significantly leading to higher FC stack inefficiency. Furthermore, overall FC system efficiency decreases with load because for a given cathode stoichiometry increasing the current density means increasing the required air mass flow rate, thus increasing the compressor power consumption.

#### 4.1. Development of the mean values model

For analyses that require a high number of simulations, the computational cost is often a limitation. In order to carry out a sizing study, it is imperative to simulate numerous designs following a *Design of Experiments* methodology. The simulation of a WLTP driving cycle considering all the FCEx systems lasts about 4 h, making the sizing study to last about 10 months. In order to reduce the computational cost, the FC system was simplified to a mean values model, i.e., it was substituted with a map containing the steady performance and operating conditions at different loads. This model, widely used in ICE research [42,43], interpolates linearly between previously-calculated points with relatively low error. Due to the steady nature of the model, some deviation between the complete and the mean values model was expected, especially considering the slow thermal dynamics of fuel cells affecting their transient performance.

Despite the deviation, this approach was based on a validated model under different conditions of pressure, temperature, and stoichiometry of an FC stack integrated into a BoP whose air management strategy was optimized. As such, the simplified model was capable of reproducing the actual FC system operation with simplified dynamics, providing much higher fidelity results than other approaches where the whole FC system was oversimplified to a single polarization curve without including the BoP power demand and the inefficiencies associated with driving cycle conditions. The mean values model produces lower H<sub>2</sub> consumption since the FC system is always working in pseudo-steady conditions, therefore the inefficiencies associated with transient operation such as slow thermal dynamics are not considered. Furthermore, the energy usage distribution in both models only presents a significant deviation in the FC system losses (Fig. 9) due to the error caused by model simplification. The energy usage for other purposes such as produce brake power or charge the battery with the FC stack was almost identical since the same energy management strategy was used for both models. Still, the deviation was relatively low and was accepted to reduce the computational cost from 4 h to 50 s per case.

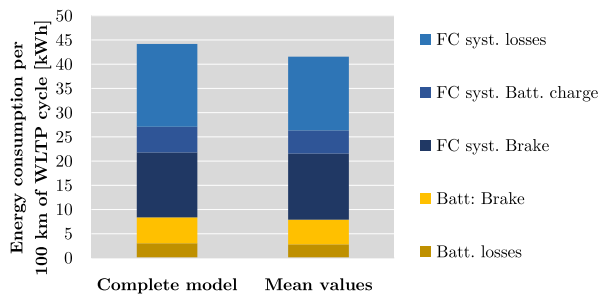


Fig. 9. Energy usage distribution comparison between the complete and the mean values models.

## 5. FCREx systems sizing

The global space design consisted of varying 3 independent design parameters: the FC stack maximum power, the battery capacity, and the capacity of  $H_2$  tanks. As such, the results in Figs. 10–12 have 1 out of 3 parameters fixed. In the case of Fig. 12, the fixed parameter is the tank capacity which was set accordingly to get a specific vehicle range with an error of  $\pm 20$  km. Battery capacity was varied within 30 and 60 kWh, FC stack power within 20 and 100 kW and  $H_2$  mass in tanks within 1 and 5 kg. The ratio between the energy stored in the battery and that stored as  $H_2$  is indicative of the  $H_2$  usage to cover the whole range. The results provided in these figures were affected by the error when simplifying the complete model to the mean values model. Therefore, the actual values of range may be slightly lower than those presented in Figs. 10 and 12.

Along this discussion, different FCREx designs are compared against state-of-the-art FCV with commercial applications. The FCV are referred as FCV1 and FCV2, and their performance data and characteristics can be found at [31] and [24], respectively.

Fig. 10 shows the range,  $H_2$  consumption and system cost as a function of the battery capacity and the  $H_2$  tank capacity with 20 and 82 kW FC stacks. Range was calculated considering the operation with the battery until SOC=0.3, then operation with optimum energy management strategy as explained in Section 3.4 until  $H_2$  depletion, followed finally by operation until full battery discharge. In Fig. 10, FC stack power was the fixed design parameter in the analysis since it has the lowest influence in the range compared with the other two sized parameters. However, increasing the FC stack power implies a higher vehicle range.

When the FC stack maximum power increases, the FC system operates under lower current density for the same load. According to Fig. 8, this means higher FC system efficiency since the stack operates mostly in the medium current density region, i.e., lower  $H_2$  consumption. The higher efficiency at lower current density is justified by the lower electrochemical losses and BoP power consumption. On one hand, both ohmic and activation losses decrease with the current density since the flow of protons through the membrane and the intensity of the surface reaction per unit of surface at the catalyst layer decrease, thus decreasing the losses associated with the membrane protonic conductivity (ohmic losses) and the activation overpotential required to start the electrochemical reaction (activation losses). On the other hand, since the compressor was scaled with the FC maximum power, despite the required mass flow may increase, the relative compressor energy consumption decreases since the FC stack is more efficient (see Fig. 8). Opposite to this effect, this also implies increasing the FC system weight, hence the vehicle weight. The increase in weight also had the effect of increasing the required load, therefore  $H_2$  consumption. The results in the left-side and central graphs on Fig. 10 show that the increase in FC system efficiency outweighs the increase in the vehicle weight, thus increasing range and decreasing  $H_2$  consumption as the FC stack maximum power increases. The left-side graphs also

show how the range changes with the energy stored in the battery and the energy stored as  $H_2$  respectively. With 20 kW PEMFC, if an iso-range line is drawn from the X axis at 2 kg of  $H_2$  (66.6 kWh as  $H_2$ ) it would cross the Y axis at about 50 kWh of energy stored in the battery. This means that from the design of 30 kWh battery and 1 kg of  $H_2$ , it would be necessary to increase the energy stored as  $H_2$  by 33.3 kWh to get the same increase in range as increasing the battery capacity by 20 kWh. Therefore, in terms of energy utilization and performance, increasing the energy stored in the battery is more efficient to improve range than increasing it in the form of  $H_2$  due to the higher efficiency of batteries. This additional benefit was also found with those designs whose FC maximum power was 82 kW but it was less significant since the FC efficiency increased. Despite this, the weight, space and cost restriction of batteries makes it currently impossible to achieve ranges similar to those of FCVs with BEVs for passenger vehicles. As such, to minimize energy and  $H_2$  consumption in FCVs the battery capacity should be moderate and not reduced to the minimum as current commercial FCVs, in other words, the FCREx architecture could also be used to maximize the energy utilization in FCVs and thus minimize consumption and maximize range.

The two central graphs of Fig. 10 indicate a similar decrease in  $H_2$  consumption when the FC stack maximum power increases. As explained before, this is due to the outweigh of the FC system efficiency increase against the increase in required power when the vehicle weight increases. In this case,  $H_2$  consumption was calculated as  $H_2$  mass stored in the tank divided by the total range of the vehicle. Therefore, this definition is representative of the total performance of the vehicle, not only of the FC+battery mode, and is of the utmost importance given the current scenario with limited  $H_2$  refueling stations across the globe.

As explained before, increasing the  $H_2$  mass in the tank also increased the range. However, it also increased the  $H_2$  consumption due to the vehicle increase in weight. This was produced because increasing the stored fuel mass did not have any effect on the efficiency of the systems directly, but increased the required power for a given operation due to the extra weight. In contrast, increasing the battery capacity dramatically decreases  $H_2$  consumption since it implies that a greater part of the range was covered only with the battery, which implied that the range increased while the stored fuel mass was kept constant.  $H_2$  consumption for all the designs with 82 kW PEMFC were below 0.9 kg  $H_2$ /100 km. The fuel consumption of FCV1 [31] (state-of-the-art FCV) is 0.95 kg  $H_2$ /100 km (31.6 kWh/100 km) considering 6.33 kg of  $H_2$  stored and a range of 666 km (WLTP). Compared to this vehicle, in the design space shown in Fig. 10, the equivalent-in-range FCREx design with minimum  $H_2$  consumption (4.97 kg of  $H_2$ , a battery of 44.5 kWh and 82 kW FC stack) had a  $H_2$  consumption of 0.79 kg  $H_2$ /100 km and a total energy consumption of 31.56 kWh/100 km. Hence, this equivalent-in-range design compared to FCV1 data is capable of achieving around 16.8% saving in  $H_2$  consumption and similar overall energy consumption to cover the whole range. This comparison allows highlighting the potential of FCREx, which could provide similar performance in terms of energy utilization and range with lower  $H_2$  consumption and the possibility to use different driving modes depending on  $H_2$  availability.

The right-hand side pair of graphs of Fig. 10 show the overall energy consumption of each design with FCREx architecture. Energy consumption was calculated as the total energy stored in the vehicle (considering both the  $H_2$  and the battery) over the total range. Increasing the FC maximum power implied a dramatic decrease in energy consumption. This indicated that the FC system, compared to the battery, was the most limiting system in terms of performance since it had lower efficiency. The effect of increasing the battery and the  $H_2$  tank capacities on energy consumption was the same as that noticed on  $H_2$  consumption. However, the effect of increasing the battery size of decreasing energy consumption was lower since for  $H_2$  consumption the  $H_2$  mass in the tank was kept constant. From these data, FCREx manufacturers should avoid having low-power FC

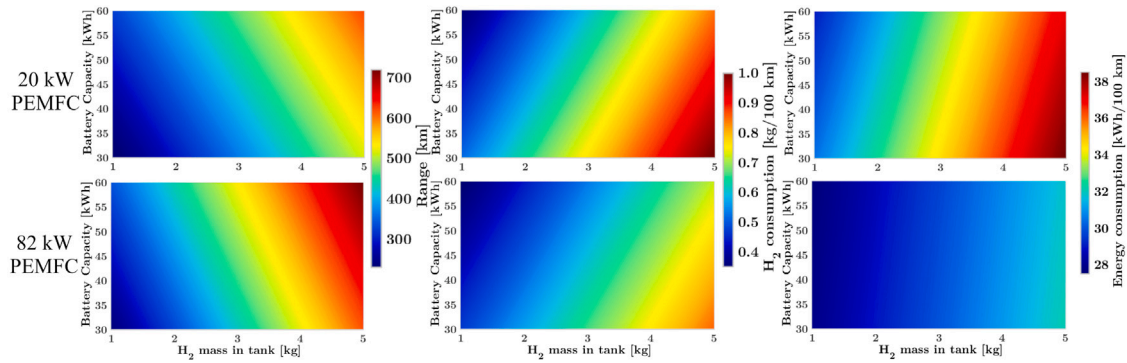


Fig. 10. Range,  $H_2$  consumption and systems cost of FCEx with 20 and 82 kW PEMFC.

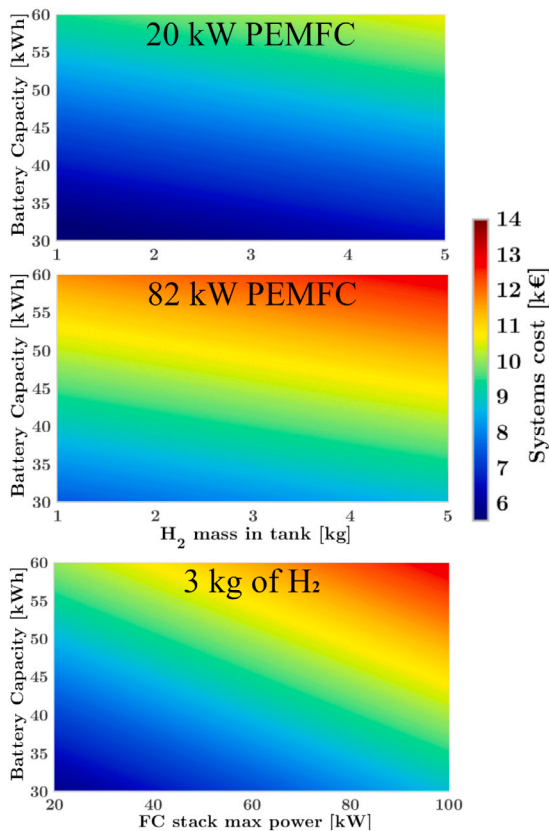


Fig. 11. Total cost variation of the FC system, battery and  $H_2$  tank for a FCEx architecture considering the designs with 20 kW PEMFC, 82 kW PEMFC and 3 kg of  $H_2$  as fixed variables.

stacks in their designs in order to maximize the energy utilization and range. Furthermore, FCEx also allow lower FC stack maximum power compared to FCV for the same range and performance.

The graphs in Fig. 11 show the total cost variation of the FC system, the battery and the  $H_2$  tank. The two first graphs show the cost variation when extending the vehicle range by using batteries or  $H_2$  tank capacity. Analogously, the cost variation when increasing the maximum FC stack power and the battery capacity was showed in the third graph since these two parameters have the greatest effect on  $H_2$  and energy consumption. From these results, increasing the energy stored in the vehicle was significantly more expensive if it was done by increasing the battery capacity rather than increasing the  $H_2$  tank capacity. This implies that the purchase cost of any BEV with the same range as any FCV should be much higher, which could allow higher  $H_2$

price to have the same TCO. For the designs with 82 kW PEMFC (second graph) increasing the  $H_2$  capacity from 1 kg to 5 kg with a battery of 30 kWh was equivalent in costs to increasing the battery capacity from 30 kWh to 40 kWh with 1 kg of  $H_2$ . These two designs with equivalent cost offered significantly different performance in terms of consumption and range. The design with 5 kg of  $H_2$  and 30 kWh of battery capacity had a range,  $H_2$  and energy consumption of 616 km, 0.85 kg  $H_2$ /100 km and 32.1 kWh/100 km, respectively. In contrast, the design with 1 kg of  $H_2$  and 40 kWh of battery capacity had a range,  $H_2$  and energy consumption of 272 km, 0.43 kg  $H_2$ /100 km and 27.8 kWh/100 km, respectively. These designs are diametrically opposed and offer such different performance and range since the ratio of energy stored as  $H_2$  to the total energy stored, including that in the battery, is completely different. This ratio was identified as another deciding factor for potential FCEx manufacturers that may change depending on the vehicle application. For the same volume of the systems, if this ratio is low (low  $H_2$  stored), the range is significantly reduced together  $H_2$  and energy consumption. This implies much more efficient energy usage to cover a given range, thus reducing operating costs. This architecture could be interesting for captive fleets applications such as those founds at ports and airports or for low-power vehicles, thus reducing the refueling/recharging time of these vehicles compared to BEV. In contrast, if the ratio is high, FCEx could be suitable for passenger vehicles by providing a great-enough range together with a flexible operation (battery for city driving and FC+battery for long rides) and low  $H_2$  consumption compared to commercial FCVs. Finally, the results in Fig. 11 showed that increasing the FC stack maximum power also had a significant impact on the vehicle production cost. Therefore, for any car manufacturer, the final choice of the FC stack maximum power should consider the vehicle application, the increase in price and the decrease in  $H_2$  consumption to minimize the TCO.

In Fig. 12, the space design for 500, 600, and 700 km of range FCEx are shown. In this case, the mass of  $H_2$  in the tank was fixed depending on the battery capacity to provide enough on-board energy to achieve the target range ( $\pm 20$  km). As such, it is possible to see that FCEx could potentially reach a range of about 700 km with 5 kg of on-board  $H_2$ , a battery of  $>50$  kWh and a FC maximum power  $>30$  kW if its operation was optimized. All the designs whose systems specifications were lower than these could not reach a range of 700 km due to the lack of on-board energy or the low efficiency of the systems. However, this range or slightly superior range seems to be the current limit for FCEx since the required space to have 5 kg of  $H_2$  and a battery of  $>50$  kWh may only be achievable for high size passenger vehicles.

Based on the results of this study, a properly designed and optimized FCEx could reach a range of 500 km with barely 3.76 kg of  $H_2$  and a battery of 30 kWh (155.3 kWh of stored energy, i.e., 31.06 kWh/100 km of energy consumption and 0.75 kg  $H_2$ /100 km of  $H_2$  consumption). Compared to FCV2, which has a range of approximately 500 km with 5 kg of  $H_2$  (166.5 kWh, i.e., 33.3 kWh/100 km and 1 kg  $H_2$ /100 km of energy and  $H_2$  consumption), this implies a much

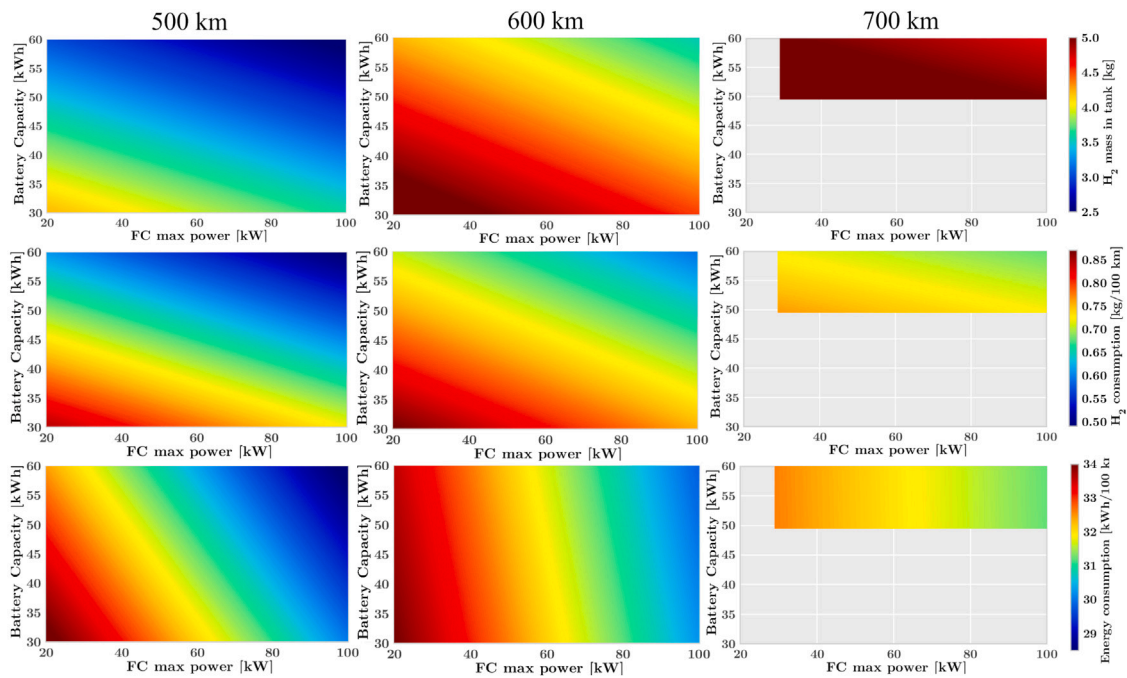


Fig. 12. Design spaces showing H<sub>2</sub> consumption and required H<sub>2</sub> mass capacity for FCREx with 500, 600, 700 km of range.

more efficient energy usage around 6.8% in energy saving and around 25% in H<sub>2</sub> consumption saving. As a consequence, FCREx could offer much lower operation costs.

The benefit obtained after optimizing both FCV1 and FCV2 converted into an FCREx architecture and imposing the same total range is higher in the case of the FCV2. In this case the savings in energy usage are higher (over 6% saving against no saving), and the reason is the higher fraction of the total energy stored in the battery (30 kWh out of 155.3 kWh against 44.5 kWh out of 210.15 kWh). This provides a higher optimization potential since the fraction of energy used from the battery to cover the given range increases, therefore the overall vehicle efficiency also increases accordingly.

As seen in Fig. 12, increasing the FC stack maximum power decreases H<sub>2</sub> consumption (second row of graphs in Fig. 12). As such, the space design shows that higher FC stack maximum power could reduce the amount of H<sub>2</sub> stored to reach the same range (first row of graphs in Fig. 12), hence reducing the operation cost but increasing the manufacturing costs. Energy consumption presents different sensitivity with the battery capacity depending on the vehicle range. For FCREx designs with 500 km of range, the decrease in energy consumption with the increase in battery capacity (due to the higher battery efficiency) is lower than for designs with 600 km of range. This happens since the ratio of stored H<sub>2</sub> with respect to the total on-board energy must increase to reach higher ranges, hence a higher part of the range is covered using only H<sub>2</sub> thus decreasing the influence of battery capacity over energy consumption. The final design of any FCREx should consider this to minimize the TCO. Based on the design spaces in Fig. 12 and more detailed data about the total cost of a single FCREx production, it would be possible to produce analogous graphs showing the TCO. With the data in hand, the minimum TCO would probably be located at moderate values of battery capacity (cheaper operation with only electricity from the battery) and relatively high FC stack maximum power to reduce the H<sub>2</sub> consumption. Of course, the optimum design to minimize the TCO depends on the H<sub>2</sub> price. If H<sub>2</sub> is cheap, the optimum would move towards lower FC stack power, lower battery capacity and higher H<sub>2</sub> tank capacity to reduce manufacturing costs while if it is expensive, it would move towards higher FC stack power, higher battery capacity and lower H<sub>2</sub> tank capacity. Estimating the TCO is a difficult task which depend on the H<sub>2</sub> cost, therefore on the location

of the refueling station among other factors, and on the vehicle usage in general, i.e., if the vehicle is used mainly in cities (pure electric mode) and occasionally for long trips (FC+battery mode) or otherwise. This estimation is out of the scope of this study and could provide an meaningful and interesting analysis about the benefits, in terms of TCO, of FCREx against equivalent FCVs and BEVs.

As can be noticed along the discussion of results, obtaining an optimum design for FCREx passenger vehicles was not the objective of this study. Nonetheless, the generation of the design spaces enabled to understand the implications of changing the systems sizing in terms of range, production costs and consumption. Only in terms of performance, the optimum design would be that with a battery capacity of 60 kWh and a FC stack maximum power of 100 kW (Figs. 12), and the H<sub>2</sub> tank capacity would be adjusted according to the desired range. Nonetheless, this design would also imply higher manufacturing costs, compared to lower FC power designs. Following this reasoning, the optimum FCREx design would not only depend on performance factors but on the TCO, as discussed, and the cradle-to-grave emissions, which would depend significantly on the H<sub>2</sub> production pathway and the systems sizing. For this reason, the main outcomes of this study are the design spaces themselves together with the performance evaluation of FCREx architectures compared to current commercial FCVs, and the identification of the optimum systems sizing: moderate battery capacity (~30 kWh) and moderate-to-high FC stack maximum power ( $\geq 80$  kW). Although the maximum performance was achieved for 60 kWh batteries, the increase in systems costs almost doubled when increasing the battery capacity from 30 kWh to 60 kWh (Fig. 11). For that reason, the optimum design, as a trade-off between TCO and performance would most probably have a battery of 30 kWh in these design spaces. Finally, as H<sub>2</sub> prices drop and the FC systems become more efficient, it would be possible to reduce the FC stack maximum power output without significant variation in performance and operation costs to reduce manufacturing costs.

### 5.1. Results application and usefulness

The results presented in this paper can be of interest for the research community and the industry for various reasons. First, any individual from research centers or industry who wants to know which would be

the optimal H<sub>2</sub> and/or energy consumption and range of a given FCREx design could directly use the design spaces (Figs. 10–12) to obtain fair and direct information. These results could be used directly in the first stages of the FCREx vehicle development process to down select an initial architecture that would be refined with costs and emissions associated data. TCO and cradle-to-grave emissions could also be obtained from H<sub>2</sub> and energy consumption data. Furthermore, the benefit of this architecture was highlighted against commercial FCVs, showing that the lower the total range, the higher the benefit in consumption of FCREx compared to FCV (see FCV1 and FCV2 comparisons). The maximum achievable range for a FCREx passenger with 5 kg of H<sub>2</sub> was also calculated (700 km), showing that FCREx architecture is suitable for passenger car application. All in all, the results presented in this study can be used extensively in both scientific research and industry applications.

## 6. Conclusions

In this study different space designs for FCREx vehicles were generated showing the range, the systems cost and the H<sub>2</sub> consumption. In order to generate such spaces a validated FC stack model was used and integrated into a FC system. The BoP operation was optimized at steady conditions. In this optimization, 3 regions of operation were identified, with the maximum FC system efficiency on the medium-load region. For these regions, the energy distribution to each component was discussed in detail. Then, the FC system model was simplified to a mean values model to reduce the computational time of a driving cycle simulation from 4 h to 50 s to make the generation of the design spaces feasible. The energy management strategy was optimized for each design using the mean values model by solving the optimal control problem with the Pontryagin Minimum Principle.

The overall design space comprised the FC stack power ranging from 20 to 100 kW, the battery capacity ranging from 30 to 60 kWh and the H<sub>2</sub> tank capacity from 1 to 5 kg of H<sub>2</sub> at 700 bar. Additional design subspaces were also generated by fixing the FC maximum power to 20/82 kW or the range to 500, 600, 700 km by adjusting the battery and H<sub>2</sub> tank capacities to the corresponding values.

The main findings and contributions of this study are based on the understanding of the change in performance and capabilities of FCREx with the systems sizing and the identification of the benefits of FCREx architectures compared to conventional ones. Furthermore, the design spaces are a contribution themselves (Figs. 10–12), since they can be directly use in the first stages of FCREx design and for scientific research, as explained in Section 5.1.

Regarding the performance of FCREx vehicles (Figs. 10 and 12), it was identified how, in general terms, increasing both the battery capacity and the FC maximum power decreases H<sub>2</sub> and energy consumption since the systems efficiency increase. Among these two sizing parameters, consumption is more sensitive to the FC maximum power since most of the energy stored in the FCREx vehicle was in the form of H<sub>2</sub>. In this sense, the ratio consisting of the energy stored as H<sub>2</sub> over the total on-board energy in the vehicle was identified as an important parameter for potential FCREx manufacturers. For a fixed volume of the systems (available space), if this ratio is low, the range is significantly reduced together with H<sub>2</sub> and energy consumption (suitable for captive fleets and low-power vehicles applications). In contrast, if the ratio is high, FCREx could be suitable for passenger vehicles since they could offer great-enough range together with flexible operation (battery for city driving and FC+battery for long displacements) and lower H<sub>2</sub> consumption than conventional FCVs. The maximum range for FCREx could be around 700 km due to space constraints in passenger vehicles and the relation between the vehicle weight and overall efficiency.

In order to understand the benefit in performance of FCREx against conventional FCVs, equivalent-in-range FCREx designs were compared against state-of-the-art FCVs with commercial application (FCV1 & FCV2). From this comparison, it was concluded that FCREx architecture

could provide a more efficient energy usage, hence lower H<sub>2</sub> consumption, meaning a potential decrease in the TCO. The design with a FC stack of 82 kW, 4.97 kg of H<sub>2</sub> and 44.5 kWh stored in the battery was equivalent in range to the FCV1 and offered 16.8% saving in H<sub>2</sub> consumption and similar overall energy consumption. Compared to the FCV2, the overall energy usage of the equivalent-in-range FCREx (3.76 kg of H<sub>2</sub> and 30 kWh of energy in the battery) was around 6.8% lower. Therefore, FCREx architecture could significantly decrease H<sub>2</sub> and energy consumption compared to conventional FCV.

The findings of this study, relative to the increase in performance of these vehicles with FCREx architecture, are of great relevance regarding the resources and energy utilization aspect. The combination of a high-efficiency system such as batteries together with a high specific energy system such as H<sub>2</sub> FC implies a clean, feasible, and efficient passenger road transport without many penalties.

In terms of systems costs (Fig. 11), it was concluded that increasing the range of FCREx was significantly cheaper by increasing the H<sub>2</sub> tank capacity rather than by increasing the battery capacity, due to the high manufacturing costs of batteries. In this sense, the total costs of the systems almost doubled when increasing the battery capacity from 30 kWh to 60 kWh. Therefore, in order to minimize manufacturing costs, it was recommended to reduce the battery capacity to the minimum to ensure enough operation with the battery mode (30 kWh).

The recommended range of optimum FCREx designs was with minimum but high-enough battery capacity (30 kWh) to reduce production costs and moderate-to-high FC maximum power ( $\geq 50$  kW) to maximize performance (operation costs) since the H<sub>2</sub> and energy consumption was more sensitive to FC maximum power than to battery capacity. Still, an optimum design was not selected from the design spaces since it may depend on other factors such as H<sub>2</sub> or electricity price (key to calculate the TCO) and cradle-to-grave emissions.

To conclude, due to the lower energy and H<sub>2</sub> usage than FCVs and the possibility of using electricity to cover part of the range, FCREx is a promising vehicle architecture that could reduce the TCO and cradle-to-grave emissions compared to equivalent-in-range FCVs and BEVs.

## CRedit authorship contribution statement

**S. Molina:** Conceptualization, Methodology, Supervision. **R. Novella:** Investigation, Formal analysis, Writing - review & editing. **B. Pla:** Resources, Methodology, Software, Data curation. **M. Lopez-Juarez:** Investigation, Validation, Software, Writing - original draft.

## Declaration of competing interest

The authors declare that they have no known competing financial interests or personal relationships that could have appeared to influence the work reported in this paper.

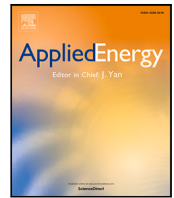
## Acknowledgments

This research has been partially funded by FEDER, Spain and the Spanish Government through project RTI2018-102025-B-I00 (CLEAN-FUEL) and through the University Faculty Training (FPU) program.

## References

- [1] Fuel Cells & Hydrogen (FCH). Hydrogen roadmap Europe - a sustainable pathway for the European energy transition. 1st ed. Publications Office of the European Union; 2019, p. 70. <http://dx.doi.org/10.2843/341510>.
- [2] Lane B, Shaffer B, Samuelsen S. A comparison of alternative vehicle fueling infrastructure scenarios. *Appl Energy* 2020;259(June 2019):114128. <http://dx.doi.org/10.1016/j.apenergy.2019.114128>.
- [3] Feroldi D, Carignano M. Sizing for fuel cell/supercapacitor hybrid vehicles based on stochastic driving cycles. *Appl Energy* 2016;183:645–58. <http://dx.doi.org/10.1016/j.apenergy.2016.09.008>.

- [4] Pourabdollah M, Egardt B, Murgovski N, Grauers A. Convex optimization methods for powertrain sizing of electrified vehicles by using different levels of modeling details. *IEEE Trans Veh Technol* 2018;67(3):1881–93.
- [5] Xu L, Ouyang M, Li J, Yang F, Lu L, Hua J. Optimal sizing of plug-in fuel cell electric vehicles using models of vehicle performance and system cost. *Appl Energy* 2013;103:477–87. <http://dx.doi.org/10.1016/j.apenergy.2012.10.010>.
- [6] Xu L, Mueller CD, Li J, Ouyang M, Hu Z. Multi-objective component sizing based on optimal energy management strategy of fuel cell electric vehicles. *Appl Energy* 2015;157:664–74. <http://dx.doi.org/10.1016/j.apenergy.2015.02.017>.
- [7] Lü X, Wang P, Meng L, Chen C. Energy optimization of logistics transport vehicle driven by fuel cell hybrid power system. *Energy Convers Manage* 2019;199(June):111887. <http://dx.doi.org/10.1016/j.enconman.2019.111887>.
- [8] Wu X, Hu X, Yin X, Li L, Zeng Z, Pickert V. Convex programming energy management and components sizing of a plug-in fuel cell urban logistics vehicle. *J Power Sources* 2019;423(March):358–66. <http://dx.doi.org/10.1016/j.jpowsour.2019.03.044>.
- [9] Sim K, Vijayagopal R, Kim N, Rousseau A. Optimization of component sizing for a fuel cell-powered truck to minimize ownership cost. *Energies* 2019;12(6). <http://dx.doi.org/10.3390/en12061125>.
- [10] Feng Y, Dong Z. Integrated design and control optimization of fuel cell hybrid mining truck with minimized lifecycle cost. *Appl Energy* 2020;270(March):115164. <http://dx.doi.org/10.1016/j.apenergy.2020.115164>.
- [11] Gaikwad SD, Ghosh PC. Sizing of a fuel cell electric vehicle: A pinch analysis-based approach. *Int J Hydrogen Energy* 2020;45(15):8985–93. <http://dx.doi.org/10.1016/j.ijhydene.2020.01.116>.
- [12] Hu Z, Li J, Xu L, Song Z, Fang C, Ouyang M, et al. Multi-objective energy management optimization and parameter sizing for proton exchange membrane hybrid fuel cell vehicles. *Energy Convers Manage* 2016;129:108–21. <http://dx.doi.org/10.1016/j.enconman.2016.09.082>.
- [13] Wu X, Hu X, Yin X, Peng Y, Pickert V. Convex programming improved online power management in a range extended fuel cell electric truck. *J Power Sources* 2020;476(2019):228642. <http://dx.doi.org/10.1016/j.jpowsour.2020.228642>.
- [14] International Energy Agency. The future of hydrogen. Tech. rep., 2019. <http://dx.doi.org/10.1787/1e0514c4-en>.
- [15] Verhelst S, Wallner T. Hydrogen-fueled internal combustion engines. *Prog Energy Combust Sci* 2009;35(6):490–527. <http://dx.doi.org/10.1016/j.pecs.2009.08.001>.
- [16] Benajes J, Antonio G, Monsalve-Serrano J, Balloul I, Pradel G. Evaluating the reactivity controlled compression ignition operating range limits in a high-compression ratio medium-duty diesel engine fueled with biodiesel and ethanol. *Int J Engine Res* 2017;18:60–88. <http://dx.doi.org/10.1177/1468087416678500>.
- [17] García A, Monsalve-Serrano J, Villalta D, Lago Sari R, Gordillo Zavaleta V, Gaillard P. Potential of e-Fischer Tropsch diesel and oxymethyl-ether (OMeX) as fuels for the dual-mode dual-fuel concept. *Appl Energy* 2019;253:113622. <http://dx.doi.org/10.1016/j.apenergy.2019.113622>.
- [18] García A, Monsalve-Serrano J, José Sanchís E, Fogué-Robles Á. Exploration of suitable injector configuration for dual-mode dual-fuel engine with diesel and OMeX as high reactivity fuels. *Fuel* 2020;280:118670. <http://dx.doi.org/10.1016/j.fuel.2020.118670>.
- [19] Desantes JM, Molina S, Novella R, Lopez-Juarez M. Comparative global warming impact and NOX emissions of conventional and hydrogen automotive propulsion systems. *Energy Convers Manage* 2020;221:113137. <http://dx.doi.org/10.1016/j.enconman.2020.113137>.
- [20] Teng T, Zhang X, Dong H, Xue Q. A comprehensive review of energy management optimization strategies for fuel cell passenger vehicle. *Int J Hydrogen Energy* 2020;45(39). <http://dx.doi.org/10.1016/j.ijhydene.2019.12.202>.
- [21] Sun Z, Wang Y, Chen Z, Li X. Min-max game based energy management strategy for fuel cell/supercapacitor hybrid electric vehicles. *Appl Energy* 2020;267:115086. <http://dx.doi.org/10.1016/j.apenergy.2020.115086>.
- [22] Zhang H, Li X, Liu X, Yan J. Enhancing fuel cell durability for fuel cell plug-in hybrid electric vehicles through strategic power management. *Appl Energy* 2019;241(January):483–90. <http://dx.doi.org/10.1016/j.apenergy.2019.02.040>.
- [23] Wikner E, Thiringer T. Extending battery lifetime by avoiding high SOC. *Appl Sci (Switzerland)* 2018;8(10). <http://dx.doi.org/10.3390/app8101825>.
- [24] Argonne National Laboratory. Technology assessment of a fuel cell vehicle: 2017 toyota mirai energy systems division. US DOE -Energy Systems Division; 2017.
- [25] Corbo P, Migliardini F, Veneri O. Experimental analysis and management issues of a hydrogen fuel cell system for stationary and mobile application. *Energy Convers Manage* 2007;48(8):2365–74. <http://dx.doi.org/10.1016/j.enconman.2007.03.009>.
- [26] Corbo P, Migliardini F, Veneri O. Experimental analysis of a 20 kWe PEM fuel cell system in dynamic conditions representative of automotive applications. *Energy Convers Manage* 2008;49(10):2688–97. <http://dx.doi.org/10.1016/j.enconman.2008.04.001>.
- [27] Terada I, Nakagawa H. Polymer electrolyte fuel cell. *Kobunshi* 2008;57(7):498–501. <http://dx.doi.org/10.1295/kobunshi.57.498>.
- [28] Murschenhofer D, Kuzdas D, Braun S, Jakubek S. A real-time capable quasi-2D proton exchange membrane fuel cell model. *Energy Convers Manage* 2018;162(January):159–75. <http://dx.doi.org/10.1016/j.enconman.2018.02.028>.
- [29] Ballard. FCvelocity – 9SSL product specification. 2011.
- [30] Rabbani RA. Dynamic performance of a PEM fuel cell system. In: DTU mechanical engineering. DCAMM special report (no. S154), 2013.
- [31] Hyundai. Hyundai nexo - technical specifications. p. 0–2.
- [32] Onori S, Serrao L, Rizzoni G. Hybrid electric vehicles: Energy management strategies. Springer; 2016.
- [33] Sciarretta A, Guzzella L. Control of hybrid electric vehicles. *IEEE Control Syst Mag* 2007;27(2):60–70.
- [34] Luján JM, Guardiola C, Pla B, Reig A. Cost of ownership-efficient hybrid electric vehicle powertrain sizing for multi-scenario driving cycles. *Proc Inst Mech Eng D* 2016;230(3):382–94.
- [35] Serrao L, Onori S, Rizzoni G. ECMS as a realization of Pontryagin's minimum principle for HEV control. In: 2009 American control conference. IEEE; 2009, p. 3964–9.
- [36] Ballard. Product data sheet - FCMove-HD. 2016.
- [37] Ballard. Product data sheet - FCvelocity-MD. 2016.
- [38] US Department Of Energy. DOE Technical targets for fuel cell systems and stacks for transportation applications. 2015.
- [39] US Department Of Energy. DOE Technical targets for onboard hydrogen storage for light-duty vehicles. 2015.
- [40] Howell D, Cunningham B, Duong T, Faguy P. Overview of the DOE VTO advanced battery R&D program. Tech. rep., U.S. Department Of Energy; 2016, p. 24.
- [41] BloombergNEF. 2019 battery price survey. Tech. rep., 2019.
- [42] Luján JM, Guardiola C, Pla B, Reig A. Optimal control of a turbocharged direct injection diesel engine by direct method optimization. *Int J Engine Res* 2019;20(6):640–52.
- [43] Payri F, Guardiola C, Pla B, Blanco-Rodríguez D. A stochastic method for the energy management in hybrid electric vehicles. *Control Eng Pract* 2014;29:257–65. <http://dx.doi.org/10.1016/j.conengprac.2014.01.004>.



# Impact of fuel cell range extender powertrain design on greenhouse gases and NO<sub>x</sub> emissions in automotive applications

J.M. Desantes, R. Novella\*, B. Pla, M. Lopez-Juarez

CMT-Motores Térmicos, Universitat Politècnica de València, Camino de vera s/n, 46022 Valencia, Spain

## ARTICLE INFO

### Keywords:

Hydrogen  
Fuel cell vehicle  
Range-extender  
Driving cycle  
Sizing  
LCA

## ABSTRACT

Fuel cell (FC) technologies for mobility are gaining interest as promising options to decarbonize the transport sector in line with the current progress towards the H<sub>2</sub> economy. Previous studies show how the fuel cell range extender (FCREx) powertrain architecture can offer flexible and efficient operation along with the potentially low total cost of ownership (TCO) in passenger car applications. Cradle-to-grave emissions of these vehicles have not been estimated, nor their variation with the components sizing or the H<sub>2</sub> production pathway analyzed. In this study, the life cycle assessment (LCA) and sizing methodologies were combined to address these knowledge gaps. The design spaces were generated by varying the FC maximum power, the battery capacity and the H<sub>2</sub> tank capacity and by simulating the resulting designs with the WLTC 3b driving cycle. Then, the lifetime H<sub>2</sub> and energy consumption results and design parameters were calculated and used as inputs to estimate the greenhouse gases (GHG) and NO<sub>x</sub> emissions on the manufacturing and fuel production cycles. From the results, it was proven how considering steam methane reforming (SMR) with carbon capture and storage (CCS) as the H<sub>2</sub> production pathway could decrease by 60% and 38% GHG-100 and NO<sub>x</sub> emissions respectively, with respect to electrolysis where electricity is generated with the EU mix. The optimum design, in terms of emissions, was found to be with low-moderate battery capacity and moderate-high FC maximum power in contrast to the optimum design for performance, which had high battery capacity and high FC stack power.

## 1. Introduction

The use of H<sub>2</sub> in fuel cells (FC) for mobility and power generation application has been continuously growing during the last decade since it is an effective enabling technology for the decarbonization of these sectors [1]. Apart from H<sub>2</sub>, there are different choices to also fulfill this objective: batteries and e-fuels. Batteries are more efficient than fuel cells, but their low energy density limits the battery-electric vehicles' (BEV) range capabilities (200–400 km), imply prohibitive costs for those with high range and have excessively long charging time [2]. E-fuels can be generated from H<sub>2</sub> and captured CO<sub>2</sub>, thus enabling long-range displacements and CO<sub>2</sub>-neutral emissions [3]. However, CO<sub>2</sub> and other emissions are released in-situ, thus increasing local pollution in cities. In contrast, H<sub>2</sub> FC vehicles (FCV) enable long-range displacements (500–800 km), high-efficiency energy utilization, fast refueling, low cradle-to-grave emissions and pollution decentralization [4].

The tank-to-wheel emissions produced by H<sub>2</sub>-fueled engines or FC are mostly composed of H<sub>2</sub>O vapor, which allows the decentralization of emissions. Nonetheless, due to certain factors such as the lack

of infrastructure, the difficulties of H<sub>2</sub> distribution and the multiple production pathways available to produce H<sub>2</sub>, the cradle-to-grave emissions when using H<sub>2</sub> as an energy vector may be significant. Depending on the production pathway, H<sub>2</sub> can be classified according to different colors: black when it is produced from electrolysis whose energy has been obtained from fossil fuels, gray when it is obtained from steam methane reforming (SMR), blue when the production pathways are either electrolysis from nuclear power or SMR with carbon capture and storage (CCS) technologies, and green when it is obtained from electrolysis with electricity generated from renewable sources. Among this spectrum, green H<sub>2</sub> implies the lowest cradle-to-grave emissions, yet it requires large infrastructure and is not achievable in the short-term on a large scale. Furthermore, in terms of costs, blue H<sub>2</sub> is a significantly cheaper option than green H<sub>2</sub>, thus being the optimal production pathway to extend the use of H<sub>2</sub> until enough infrastructure to produce green H<sub>2</sub> is developed [5]. Due to the unfeasible short-term application of green H<sub>2</sub>, this study only considers black, gray and blue H<sub>2</sub>. Furthermore, the choice of considering blue H<sub>2</sub> rather

\* Corresponding author.

E-mail address: [rinoro@mot.upv.es](mailto:rinoro@mot.upv.es) (R. Novella).

URL: <http://www.cmt.upv.es> (R. Novella).

<https://doi.org/10.1016/j.apenergy.2021.117526>

Received 23 February 2021; Received in revised form 27 July 2021; Accepted 1 August 2021

Available online 13 August 2021

0306-2619/© 2021 The Authors.

Published by Elsevier Ltd.

This is an open access article under the CC BY-NC-ND license

(<http://creativecommons.org/licenses/by-nc-nd/4.0/>).

than green H<sub>2</sub> was motivated to avoid any bias in the present study towards fuel cell vehicles since two energy sources are considered to power FCVs in this study: H<sub>2</sub> and electricity. As such, it could be argued that considering green H<sub>2</sub> and electricity from the common mix (EU, USA, China, ...) would result in a biased study since the additional renewable energy required to produce H<sub>2</sub> could be used to decarbonize the electricity mix, thus making the use of electricity produce lower emissions than the use of H<sub>2</sub>. Even though green H<sub>2</sub> is not considered as the main production pathway due to the reasons previously explained, an appendix was added to understand the effect of considering an even lower-emission production pathway than H<sub>2</sub>. The emissions associated with each type of H<sub>2</sub> were compared to understand the implications considering high-emissions production pathways.

In recent years, several FCV has been released to the market (Honda Clarity, Toyota Mirai, and Hyundai Nexa). Shallowly, the architecture of these vehicles is composed of a low-capacity battery with a high-power FC system. This architecture is mainly designed to use the FC system to power the vehicle during most of the operation with the battery as a supporting power source. Nevertheless, this configuration is not suitable for the current scenario with a such low number of refueling stations worldwide [6]. In previous work, the authors of the present study proposed the previously unexplored use of FC systems as a range-extender (FCREx) in passenger vehicles [7]. This architecture has previously been considered for other types of vehicles such as trucks, captive fleets, or city buses, yet not for light-duty passenger cars. FCREx configuration consists of a moderate-capacity battery together with a moderate-to-high FC stack maximum power and offers many advantages such as flexible operation (BEV and FCREx modes), significantly lower total cost of ownership (TCO), potentially lower cradle-to-grave emissions and lower energy consumption, compared to conventional FCV [4,7].

Other research lines include alternative FCV architectures such as those with fuel processors to obtain H<sub>2</sub> from liquid fuels such as ethanol [8] to extend even further the vehicle range given the extra consumption of auxiliary components [9]. Although these alternative architecture have been proved to be interesting to extend the range of FCVs, they require additional components and lower-capacity batteries than the architecture proposed in this study, which follows the range-extender concept.

The sizing studies of passenger FCV are usually limited to low-capacity batteries of super-capacitors [10] ( $\leq 5$  kWh) and high-power FC stacks [11]. In contrast, for the sizing of a FCREx vehicle, the ranges of battery capacity and FC stack power must change and the H<sub>2</sub> tank capacity must be included since, along with the battery, is the main source of energy and affects the range of the vehicle. As such, for FCREx sizing studies, the sizing parameters must be the battery capacity, the FC stack maximum power and the H<sub>2</sub> since they have a direct impact on cradle-to-grave emissions, electricity and H<sub>2</sub>, vehicle range, and TCO.

The state-of-the-art for FCREx is represented by limited literature and the only application of FCREx architecture to heavy-duty vehicles or captive fleets. In the literature regarding the use of the FCREx configuration for city buses, Xu et al. [12] analyzed different designs of FCVREx in terms of costs and range for city buses using the CDCCS (charge depleting and charge sustaining strategy). They concluded that to minimize H<sub>2</sub> in FCVREx the priorities are in order: reducing auxiliary power, braking energy recovery, increase FC stack efficiency and decreasing battery losses. In further studies [13], they used a two-step algorithm based on dynamic programming to obtain a quasi-optimal solution to the sizing problem. With this approach, they concluded that a battery of 150 Ah and an FC system maximum power output of 40 kW were optimal for fuel economy and systems durability for an FC city bus.

Apart from city buses, this architecture has also been considered for captive fleets, where the refueling and recharging infrastructure is always close to the operating zone of the vehicle, and trucks. In this sense, Wu et al. [14] used convex programming to solve the sizing

problem for urban logistics FCVREx. They concluded with an optimum battery capacity of 29 kWh and an FC stack maximum power and usage dependent on the hydrogen price but did not include the mass of hydrogen stored as a variable for the sizing since urban logistics vehicles do not need a high range. They followed their research by considering the FCVREx architecture in trucks [15], showing that convex programming methods could provide minimal H<sub>2</sub> consumption in 8°C-HTC-HT and 7°C-WTVC Chinese truck driving cycles.

As commented before, other authors have also considered the sizing of FCV with conventional configurations. Following this line of research, Gaikwad et al. [16] used a pinch-based analysis for sizing the FC system together with a supercapacitor considering the WLTC class 3 driving cycle, concluding that the FC size must be at least equal to the average power demand for a given cycle while the supercapacitor capacity is only limited to a minimum value if regenerative braking is considered. Hu et al. [17] performed a sizing analysis of the Lithium battery of an FCV passenger car with multi-objective real-time EMS considering fuel economy and system durability to reduce the life cycle cost. However, the maximum battery capacity considered was 24 Ah, not enough to provide normal operation in the pure-electric mode for a reasonable range. Therefore, it cannot be considered an FCREx.

There has been extensive work in the last decade about the use of life cycle assessment (LCA) methodologies to estimate the cradle-to-grave emissions of H<sub>2</sub>-based fuels and technologies. LCA studies are an important tool that serves as a base of comparison to understand the environmental impact of technologies in different sectors [18], scenarios [19], and even costs [20]. Nonetheless, this LCA study focuses on estimating the cradle-to-grave emissions rather than in costs given the current growth of the H<sub>2</sub>-related technologies and the huge variation in their costs during the previous and following years. None of the studies focused on LCA for H<sub>2</sub> technologies consider the use of FCREx architecture for passenger vehicles. The recent research found in the literature shows how e-fuels (or H<sub>2</sub>-based synthetic fuels) have gained interest due to the neutral CO<sub>2</sub> emissions their usage implies [21]. Nonetheless, it has been proved that the use of H<sub>2</sub> produced through electrolysis from renewable sources could decrease the greenhouse gas emissions (GHG) significantly more than e-fuels while if it is produced through SMR the H<sub>2</sub> cost could be lower than the e-fuels cost [22]. In this regard, the direct use of H<sub>2</sub> in FC has also been proven to have clear advantages in terms of well-to-wheel efficiency, GHG-100 and other pollutant emissions, and fuel cost for light-duty passenger vehicles [23].

The studies regarding the emissions associated with the H<sub>2</sub> value chain are mostly focused on a very specific part of the cradle-to-grave process such as H<sub>2</sub> production [24] and distribution [25], FC stack production and recycling [26], and storage [27]. Those focused on the general cradle-to-grave process show how FC vehicles could significantly reduce the GHG emissions with respect to conventional ICEV [28] and even BEV [4] if H<sub>2</sub> is produced through SMR with CCS. In the literature, only Dimitrova et al. [29] considered the environmental impact of a vehicle with a solid-oxide FC (SOFC) operating as a range-extender. Nevertheless, none of them considers the use of Proton Exchange Membrane FC (PEMFC) as a range-extender in FCREx vehicles nor the variation of the environmental impact of FCREx vehicles with design and H<sub>2</sub> production pathway.

### 1.1. Knowledge gaps

In light of the previous studies, some conclusions can be extracted to provide an idea of the knowledge gaps in the literature:

1. The studies about the use of FCREx architecture for light-duty passenger vehicles are limited since most of the research has been focused on the use of this configuration of heavy-duty vehicles or captive fleets.

2. No data was found about the lifetime  $H_2$  and overall energy consumption of FCREx passenger vehicles nor about how they change with the sizing of the battery, the  $H_2$  tank capacity and the FC stack maximum power.
3. The environmental impact, in terms of GHG and  $NO_x$  emissions, of FCREx vehicles with PEMFC technology has not been assessed yet. Not to mention the application of this architecture to passenger vehicles.
4. Most of the studies focus on a specific vehicle or design but do not consider the variability of the environmental impact with the sizing of the components. There is no information about how the cradle-to-grave emissions of FCREx vehicles change with the components sizing. The combination of LCA with sizing methodologies is a novelty itself.
5. There are no studies about how the cradle-to-grave emissions of a vehicle with two power sources comprising the powerplant such as FCREx change with the  $H_2$  production pathway.
6. There is a lack of research about how the cradle-to-grave emissions of an FCV change if it is designed for a different target range.
7. The performance of FCREx has only been assessed in terms of  $H_2$  consumption, but no data about the optimum design in terms of cradle-to-grave emissions is available. Also, there is no information about whether the optimum FCREx design in terms of performance coincides with the optimum design that minimizes cradle-to-grave emissions.

In conclusion, the literature regarding the sizing of FCREx is still limited, particularly for passenger vehicles, and mostly omits the fundamental behavior and optimization of the FC system while do not pay attention to the cradle-to-grave emissions implication. Also, there is no study combining both sizing and LCA methodologies to understand the design implications both in terms of emissions, lifetime fuel or energy carriers consumption, and performance. This study combines both LCA and sizing methodologies to understand the impact of FCREx design on performance and emissions and to provide recommendations about the future design choices for this type of FCV.

## 2. Contribution and objectives

This study intends to address all the knowledge gaps listed above. In order to do so, the LCA and sizing methodologies are combined. With the sizing methodology, the  $H_2$  and energy lifetime consumption are calculated for FCREx passenger vehicles, thus allowing to analyze the energy carriers utilization and its variation with the components sizing (knowledge gaps 1, 2). With the design spaces obtained from this combination in terms of GHG-100 and  $NO_x$  emissions, it is intended to analyze and understand how the cradle-to-grave, fuel cycle and manufacturing cycle GHG-100 and  $NO_x$  emissions change with the FCREx design, the target range and the  $H_2$  production pathway (knowledge gaps 3, 4, 5 and 6). Special attention is paid to blue  $H_2$  since it is the lowest pollutant production pathway that is feasible in the short term. In this case, the relative emission-production of the vehicle manufacturing and fuel production cycles with respect to the total emissions are analyzed to understand the relative importance of each cycle of the cradle-to-grave process to minimize GHG-100 and  $NO_x$  emissions. With the data at hand, the optimum FCREx design in terms of emissions and consumption are compared to understand if they overlap or are different in order to understand which factors affect the sizing of the optimum FCREx design (knowledge gap 7). Finally, it will be possible to elaborate recommendations for the FCREx design process-based, not only on performance but also on cradle-to-grave emissions. These recommendations are not only focused on how the FCREx should be designed, but also on how it should be taken action on the fuel production and vehicle manufacturing processes to minimize the cradle-to-grave emissions of FCREx efficiently.

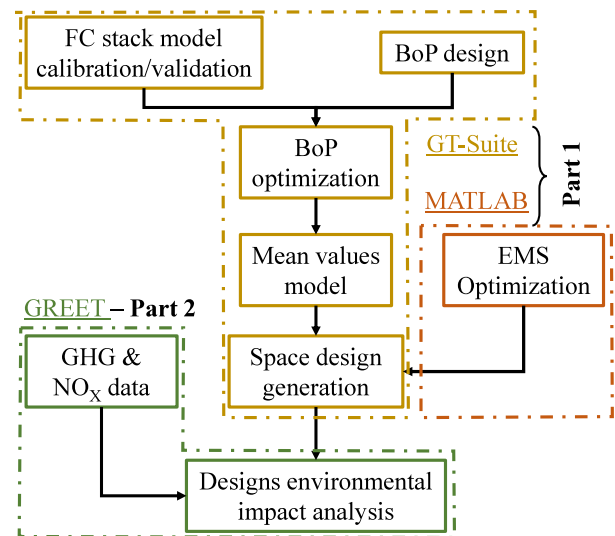


Fig. 1. Methodology schematic, simulation tools and differentiated parts.

## 3. Methodology

In this section, the methodology applied to perform this study is described. It can be divided into two different parts: the FCREx modeling (part 1) and the LCA (part 2) methodologies. Fig. 1 shows a schematic of the methodological procedure followed. Albeit the two parts are equally important to obtain the results of this study, the explanation of the FCREx model is simplified since previous studies contain extensive and detailed information about the FCREx modeling procedure [7]. For the LCA methodology, FCREx design and  $H_2$ /electricity consumption data were used as inputs from the simulations performed following the first part of the methodology.

### 3.1. FC vehicle model description

This model was developed in previous studies to understand the performance in terms of consumption and range of FCREx architecture in WLTC 3b cycles with different designs [7]. The model was implemented in the commercial simulation platform GT-Power. This software is extensively used in the automotive industry to simulate thermo-fluiddynamic systems by numerically solving the mass, energy, species and momentum conservation equations, among others. The FC model was calibrated to experimental results using genetic algorithms with an overall error lower than 2% (Fig. 2). The experimental data used were extracted from [30,31]. They consisted of the polarization curves of a 20 kW FC stack at the following conditions:

- $T_{stack} = 346 \text{ K}$  &  $p_{cath in} = 1.3 \text{ bar}$
- $T_{stack} = 346 \text{ K}$  &  $p_{cath in} = 2.5 \text{ bar}$
- $T_{stack} = 305 \text{ K}$  &  $p_{cath in} = 1.3 \text{ bar}$

Furthermore, the behavior of the model to cathode stoichiometry was also validated with data from the same papers. Unlike other studies, the FC model was validated at different operating conditions of pressure, temperature and stoichiometry so that the results obtained from simulations such as driving cycles, where the FC temperature and the air management are constantly changing with the operating conditions, are meaningful and representative.

Once the FC stack model was validated, it was integrated into a fully scalable balance of plant (BoP), thus forming an FC system (Fig. 3) which includes: a  $H_2$  recirculating pump, an electric compressor, a cooling circuit, a heat exchanger after the compressor and a cathode inlet humidifier. This BoP was designed and optimized to maximize the



**Table 1**  
Energy management description and main characteristics.

Control input ( $u$ )	Fuel cell power	$P_{FC}$
State	Energy in the battery	$E_b$
Objective/Cost function	H <sub>2</sub> consumption minimization	$J = \int_{t_0}^{t_f} P_f(u(t), t) dt$ (1)
Constraint	Battery charge sustaining	$\int_{t_0}^{t_f} P_b(u(t), E_b(t), t) dt = 0$ (2)
Algorithm	Pontryagin's Minimum Principle (PMP)	

it is necessary to find the sequence of power split that complies with the systems requirements with minimum cost [35]. In a study like the present one, where different designs whose optimum EMS is different are compared, ensuring that each design operates with the best performance is mandatory to eliminate any bias. Optimal control (OC) is a tool developed specifically for benchmarking studies since it provides the optimal power split sequence for every powertrain considered. This tool was used to ensure that the designs are compared in the best-case scenario [36].

The overall description of the EMS optimizer can be found in Table 1. The cost function  $J$  (Eq. ) is the result of integrating along the simulation time the H<sub>2</sub> power consumed ( $P_f$ ) which is controlled through the control variable  $u$ . In the case of FCReX vehicles, the driving mode that uses the FC system must ensure that the energy in the battery ( $E_b$ ) or the state of charge of the battery (SOC) is sustained. As such, this condition is imposed as a constraint for the EMS (Eq. ) by means of the power consumed by the battery ( $P_b$ ) integration.

In order to solve the OC problem, Pontryagin's Minimum Principle (PMP) was applied. It allows solving an integral optimization problem as a set of differential optimization problems. The PMP states the necessary conditions for optimal trajectories in the control and state of a dynamic system. In particular, PMP applied to the case at hand implies:

$$H(u^*, E_b^*, \lambda^*, t) \leq H(u, E_b, \lambda, t) \forall u \in U, t \in [t_0, t_f] \quad (3)$$

where  $u^*$  and  $E_b^*$  are the optimal trajectories of the control and state of the problem and  $H$  is the Hamiltonian function, defined as:

$$H = P_f - \lambda \dot{E}_b = P_f(u(t), t) + \lambda(t) P_b(u(t), E_b(t), t) \quad (4)$$

According to the PMP, the dimensionless co-state  $\lambda$  varies with the evolution of  $H$  respect to the state  $E_b$ :

$$\dot{\lambda} = \frac{\partial H}{\partial E_b} \quad (5)$$

Combining with Eq. (4):

$$\dot{\lambda} = \lambda \frac{\partial P_b}{\partial E_b} = \lambda P_{batt} \frac{\partial (P_b/P_{batt})}{\partial E_b} \quad (6)$$

The ratio  $P_b/P_{batt}$  represents the inverse of the battery efficiency (power consumed over power provided). If the battery state of charge is controlled around its design range, and the variation of the efficiency with its energy level  $E_b$  is small. Therefore, according to Eq. (6), the co-state  $\lambda$  can be assumed constant [37]. This implies that the OC problem can be solved with the PMP by iteratively looking for the value of  $\lambda$  that fulfills the required constraint (Eq. (2)). A more detailed description of the EMS optimization algorithm can be found in previous studies [7].

### 3.1.3. Sizing: design spaces generation

Regarding the sizing procedure, three key design parameters were varied to cover a wide range of FCReX designs: FC stack maximum power output, H<sub>2</sub> tank capacity, and battery capacity. Among these parameters it was shown how the former had the lowest effect on range but the greatest effect on H<sub>2</sub> consumption while the other two had significant effect on range and overall energy consumption [7]. The limits within which these parameters were varied are:

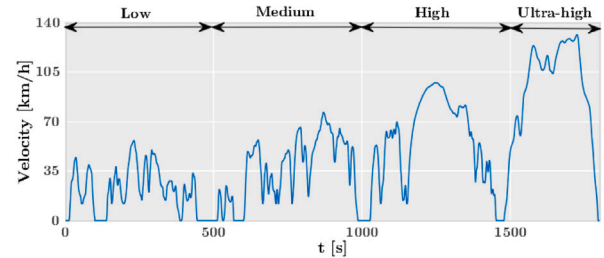


Fig. 4. Worldwide harmonized Light vehicles Test Cycles (WLTC) 3b cycle description. Low, medium, high and ultra-high dynamics regions are indicated.

- FC stack maximum power  $\in [20, 100]$  kW
- H<sub>2</sub> tank capacity  $\in [1, 5]$  kg
- Battery capacity  $\in [30, 60]$  kWh

The lower limit for the battery capacity (30 kWh) was chosen from preliminary simulations so that it ensures enough operable range in the battery mode with such vehicle body and systems. The mass and volume of each system was added to the total mass and varied for each design, i.e., two different simulations with different FCReX systems sizing have different weight and has influence over the vehicle consumption. The volume was also estimated to ensure that the H<sub>2</sub> tank and the battery could fit in the rear part of the vehicle at the expense of trunk space. The data used in the sizing are in Table 2.

The data about H<sub>2</sub> and electricity consumption were estimated by simulating the FCReX vehicles with the WLTC 3b driving cycle, corresponding to a power-to-mass ratio  $\geq 34$  for all the possible designs considered with an electric motor of 120 kW. The WLTC 3b driving cycle is characterized by four different regions of operation: low, medium, high, and ultra-high dynamics regions (Fig. 4). Even though this comprises a significant number of driving conditions, it is still not fully representative of real driving. Given the designs and vehicle considered in this study, the brake power consumption in this cycle is around 12.4 kWh/100 km. The range was estimated by first operating the vehicle with the battery until SOC = 0.3, then the operation in FCReX mode following the battery charge-sustained criteria explained in Section 3.1.2 with optimum EMS until H<sub>2</sub> depletion, followed by operation with the battery until charge depletion. The criteria of considering the battery SOC = 0.3 for FCReX mode is based on the philosophy behind range-extender vehicles, whose main operation could be in battery mode until low SOC is achieved when the range-extender powerplant is activated to enable charge-sustaining operation. Considering higher SOC would lead to lower battery losses and thus to the under-prediction of H<sub>2</sub> consumption.

### 3.2. Life cycle assessment

This section, together with its corresponding subsections, is focused on explaining the LCA methodology after obtaining the H<sub>2</sub> and electricity consumption data as inputs (Fig. 6). Most of the emissions-related data were obtained from the GREET<sup>®</sup> model v2019 as well as from other data sources in the literature. The emissions data for each H<sub>2</sub> production pathway are those obtained [4] for the scenario with the

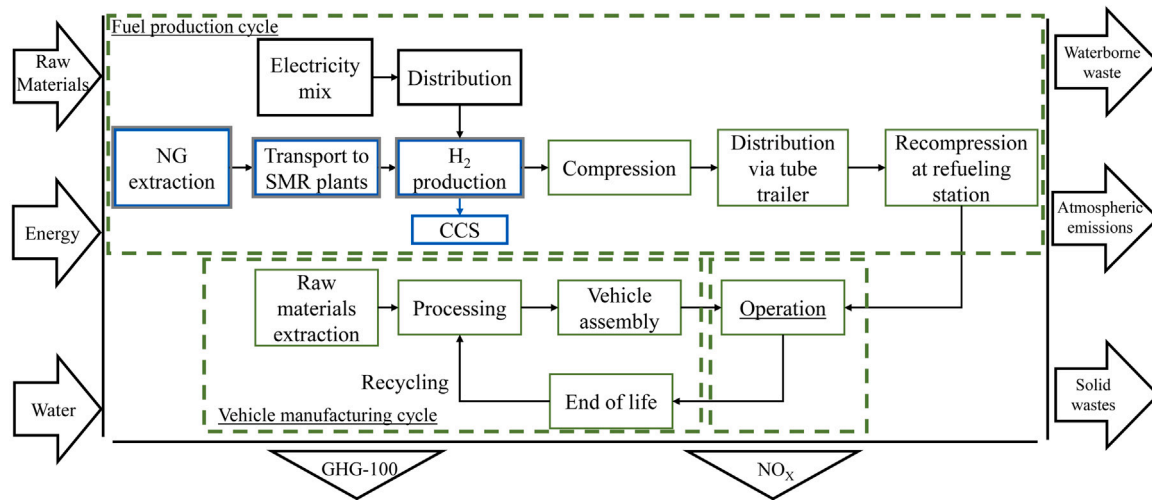


Fig. 5. System boundaries and elementary flows for the cradle-to-grave process considering electrolysis, SMR and SMR with CCS as the H<sub>2</sub> production pathways. Processes unique to electrolysis production pathway are in black, those unique to SMR are in gray, and those unique to SMR with CCS are in blue.

Table 2

Data used to calculate the mass and volume of the systems [38–41]. These data were integrated into the FCV model to increase its weight depending on the powertrain design.

System	Data used to estimate Mass - Volume
FC system	Linear correlation: <ul style="list-style-type: none"> <li>• Estimated 175 kg and 286 l for a 30 kW system</li> <li>• 250 kg and 614 l for a 70 kW system</li> </ul>
H <sub>2</sub> tank	0.045 kg H <sub>2</sub> /kg system 0.030 kg H <sub>2</sub> /l system
Battery	220 Wh/kg 600 Wh/l

current EU electricity mix so that the results are representative of the short-term scenario. In this LCA analysis, all the pathways involved in the cradle-to-grave process were considered, i.e., the LCA analysis comprises the fuel production cycle, the vehicle manufacturing cycle and the operation cycle.

### 3.2.1. System boundaries

A schematic of the system boundaries and the elementary flows considered in this study for the cradle-to-grave process considering electrolysis, steam methane reforming (SMR) and SMR with carbon capture and storage (CCS) is shown in Fig. 5. In the present study, despite many outputs of the cradle-to-grave process such as waterborne waste and other emissions such as SO<sub>x</sub> were calculated, the analysis only considers the GHG-100 and NO<sub>x</sub> emissions as the system outputs.

### 3.2.2. Functional unit

The functional unit in this study was changed according to the process under analysis to improve readability. The functional unit for the emissions in the vehicle manufacturing cycle was 1 unit of such vehicle. For the emissions produced in the fuel production cycle, the functional unit was 120,000 km of vehicle average useful life. This life was set slightly lower than the commonly used for hydrocarbon-fueled ICEV (150,000 km) since the batteries and FC durability are lower. Finally, in the cradle-to-grave process, the functional unit was both 1 unit of vehicle and 120,000 km of useful life, i.e., the total emissions during the vehicle life.

In the case of Section 3.2.4, where the life cycle inventories are presented, in the case of the fuel production cycle, the emissions are given in terms of kWh of energy source, since different energy

sources are being considered (H<sub>2</sub> and electricity). These values are then multiplied by the total life H<sub>2</sub> and electricity consumption (Fig. 6) to obtain the fuel production cycle emissions along the whole vehicle life.

The values of Table 4 are given as a function of the component sizing parameter (kWh of energy stored in the case of the battery and the H<sub>2</sub> tank and kW of maximum stack power for the FC system) so that they can be directly converted into emissions by knowing the sizing parameters.

### 3.2.3. Impact categories

In the present study, GHG-100 was the main impact category considered since the main objective of extending the use of FCV is to reduce the global warming impact of the transport sector. GHG-100 is an impact category that represents the global warming potential of different gases over a period of time of 100 years. According to this category, each greenhouse gas has assigned a value of global warming potential (GWP) that represents the relative effect on global warming of 1 g of such gas compared to the effect of 1 g of CO<sub>2</sub>. The GHG-100 were calculated by taking into account CO<sub>2</sub>, CH<sub>4</sub> and N<sub>2</sub>O emissions with their GWP of 1, 28, and 265 kg CO<sub>2</sub> equivalent, respectively [42]:

$$GHG-100 = m_{CO_2} \cdot GW P_{CO_2} + m_{CH_4} \cdot GW P_{CH_4} + m_{N_2O} \cdot GW P_{N_2O}$$

where  $m_{CO_2}$ ,  $m_{CH_4}$  and  $m_{N_2O}$  are the CO<sub>2</sub>, CH<sub>4</sub> and N<sub>2</sub>O mass emissions, respectively.

Furthermore, NO<sub>x</sub> emissions, although they are not an impact category, were also calculated due to the harmful effects they pose to human health, as well as, their effect on ozone depletion at high altitudes and ozone generation at low altitudes.

### 3.2.4. Life cycle inventory

The life cycle inventory (LCI) data was mainly extracted from GREET® v2019 model, although some data was corrected and added from the literature. This model is extensively used in the automotive industry and has been the source of data of many studies [14,43–45]. In this section, unless otherwise specified, the presented data was obtained from GREET® model.

The life cycle inventory can be separated according to the part of the cradle-to-grave process it is used to provide data: fuel production cycle, vehicle manufacturing cycle and operation cycle (Fig. 5).

#### Fuel production cycle LCI

The fuel production cycle comprises all the processes from the raw material extraction until the vehicle refueling. It can be also referred

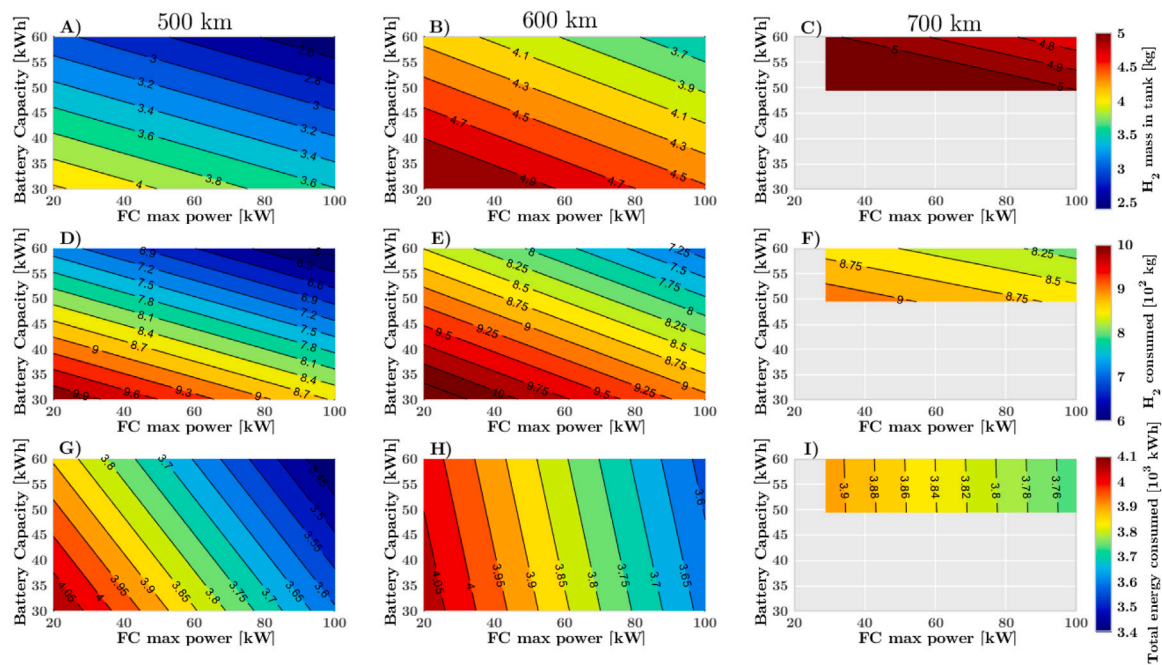


Fig. 6. Design spaces for 500, 600, and 700 km of range FCREx. Contours show: H<sub>2</sub> mass in tank to achieve the target range (1st row), H<sub>2</sub> consumed along the whole life (2nd row), and NO<sub>x</sub> total energy consumed along the whole life, including H<sub>2</sub> and electricity in the operation cycle (3rd row).

Table 3

Fuel cycle LCI data: GHG-100 and NO<sub>x</sub> emissions. Functional unit is kWh of energy source (H<sub>2</sub> or electricity produced).

Production pathway	GHG-100 emissions [kg CO <sub>2</sub> eq./kWh]	NO <sub>x</sub> emissions [kg/kWh]
H <sub>2</sub> -Electrolysis (black)	0.489	5.1 · 10 <sup>-4</sup>
H <sub>2</sub> -SMR (gray)	0.343	1.5 · 10 <sup>-4</sup>
H <sub>2</sub> -SMR w/ CCS (blue)	0.111	2.0 · 10 <sup>-4</sup>
Electricity	0.316	3.6 · 10 <sup>-4</sup>

as the well-to-tank process. As explained before, three different H<sub>2</sub> pathways were considered: electrolysis with electricity from the current EU electricity mix, SMR and SMR with CCS. In these three pathways, the H<sub>2</sub>, after being produced, is compressed and distributed via tube trailers to be re-compressed at the refueling station (Fig. 5). These production pathways along with the distribution procedure and the EU electricity mix were considered since they represent the closest-to-present scenario. Green H<sub>2</sub> and distribution via pipeline are not considered due to the large infrastructure it needs to be feasible at a reasonable scale, which means they are not feasible at the short-term. In contrast, producing H<sub>2</sub> with distributed electricity or through SMR with or without CCS is relatively immediate since most of the H<sub>2</sub> at the present is produced through SMR, whose plants can be adapted to include CCS strategies. In the case of CCS technology, a CO<sub>2</sub> sequestration capacity of 90% was assumed, based on the literature data [46].

Apart from H<sub>2</sub>, there is another energy source in FCREx vehicles: electricity stored in the battery. The GHG-100 emissions per kWh of electricity were obtained from [47] assuming a 6.5% of distribution and transmission losses [48]. Table 3 shows the GHG-100 and NO<sub>x</sub> emissions per kWh of energy source for each production pathway, considering all the processes described. Total emissions were calculated with a refueling efficiency of 1.

Vehicle manufacturing cycle LCI

The emissions produced in the vehicle manufacturing cycle are subjected to significant changes in this study since the vehicle design

Table 4

Vehicle manufacturing cycle LCI: GHG-100 and NO<sub>x</sub> emissions. Emissions given per unit of sizing parameter.

System	GHG-100 emissions [kg CO <sub>2</sub> eq.]	NO <sub>x</sub> emissions [kg]
Battery capacity [kWh]	26.07	3.9 · 10 <sup>-2</sup>
FC stack power [kW]	7.84	8.7 · 10 <sup>-3</sup>
H <sub>2</sub> tank capacity [l/kg H <sub>2</sub> ]	424	4.9 · 10 <sup>-1</sup>
H <sub>2</sub> tank capacity [kWh]	12.73	1.46 · 10 <sup>-2</sup>

changes. The emissions associated with the production of each component were scaled to those corresponding to a 1400 kg vehicle body. The vehicle manufacturing cycle comprises the manufacturing of mechanical components (transmission system, chassis, traction electric motor, electronic controller, vehicle body and vehicle tire replacement), the assembly, disposal and recycling (ADR) processes, the fluids manufacturing (brake, transmission, coolant, windshield and adhesives), the battery (NMC111 Li-ion), the FC system and the H<sub>2</sub> tank (type IV carbon fiber for 700 bar). The data associated with the recycling of the FC system and the H<sub>2</sub> were not included since emissions associated with the FC stack recycling are negligible [49] and there is not enough data in the literature about the emissions produced during the recycling of H<sub>2</sub> high-pressure tanks. The emissions data for the components whose specifications change in the design spaces (sizing) are given in Table 4 per unit of sizing parameter. The sizing parameters, or those controlled to modify the components sizing, are the FC stack maximum power (kW) the battery capacity (kWh) and the H<sub>2</sub> tank capacity (kWh of H<sub>2</sub> or kg of H<sub>2</sub>).

The raw materials (inputs in Fig. 5) considered for the manufacturing of such vehicles were steel, aluminum, magnesium, zinc, copper wires, glass, plastic product, styrene-butadiene rubber, carbon-fiber-reinforced plastic, lithium and other vehicle materials. The emission associated with the processing of raw materials and the extraction of elementary materials such as sand water, bauxite ore, zinc ore, etc,

were considered while those generated during the transport of such materials to the manufacturing plants were neglected [50].

#### Operation cycle LCI

The operation cycle can also be called the tank-to-wheel process. Different from conventional ICE vehicles, the emissions produced by FCV and their effect on the environment are minimal. The only significant tank-to-wheel emission of FC systems is H<sub>2</sub>O. In this study, the H<sub>2</sub>O emissions of the FCREx vehicles when operating in the range-extender mode and their effect on global warming were considered. For that purpose, the effective global warming potential of water was set as 5·10<sup>-4</sup> kg CO<sub>2</sub> eq. [51]. This value is the result of two contrary effects of near-surface emitted water vapor: the effect of water as a GHG-100 emission and the decrease in temperature due to the formation of low-altitude clouds that increase the atmosphere reflectance.

#### 4. Limitations of the study

Before presenting the results obtained and the discussion, it is important to highlight the limitations of this study derived from the hypotheses and methodologies applied:

- The results of this study are applicable to SUV-type passenger vehicles since they represent an important fraction of the vehicle fleet and their size enables the coexistence of moderate-capacity batteries together with FC systems.
- Europe and United States technology level are assumed to be similar (GREET<sup>®</sup> model) while the main difference is the electricity mix.
- The emissions produced in the manufacturing processes of the machines and devices used to generate the energy sources and the vehicles are not considered. This is negligible with respect to the whole-life emissions of a vehicle since the same machine is constantly used in the industry to produce other vehicles or generate H<sub>2</sub>.
- The results do not present any uncertainties study since most of the data sources for the emissions did not have them included [4, 42,47,50,51]. Furthermore, including uncertainties in the design spaces of this study would only lead to the misunderstanding of the results.

#### 5. Results and discussion

In this section, the results obtained after applying the methodology and combining the LCA data with the space design results is shown. First, the design spaces were shown as a function of the H<sub>2</sub> mass in the tank, and the GHG-100 and NO<sub>x</sub> emissions produced during the manufacturing cycle for each design (Fig. 6) to provide an idea about the considered designs and the implication of such designs in the manufacturing cycle emissions (Section 5.1). Then, GHG-100 emissions produced in the fuel production cycle and in the cradle-to-grave process by each design were analyzed for 500, 600, and 700 km of range FCREx considering SMR with CCS as the H<sub>2</sub> production pathway. This analysis was repeated for a 600 km of range FCREx considering different H<sub>2</sub> production pathways: electrolysis with electricity from the EU mix, SMR and SMR with CCS (Section 5.1.1). The same results were also extracted and discussed for NO<sub>x</sub> emissions (Section 5.1.2).

As explained in Section 3.1.3, the design spaces were generated as a function of the battery capacity, the FC maximum power output, and the H<sub>2</sub> tank capacity. All the maps representing the design spaces in this section were shown as a function of the battery capacity (Y axis) and the FC maximum power output (X axis). The H<sub>2</sub> tank capacity was fixed to achieve a target range (500, 600 or 700 km) depending on the design space that is shown.

#### 5.1. Design spaces description and energy carriers lifetime consumption

In this section, the design spaces in terms of H<sub>2</sub> tank capacity, H<sub>2</sub> and total energy consumed along the life as a function of the battery capacity and the FC stack maximum power output are shown in Fig. 6 for FCREx designs with a range of 600, 500 and 700 km. These design spaces are explained so that the tendencies of how the H<sub>2</sub> tank capacity and consumption change with the design and the target range. Then, GHG-100 and NO<sub>x</sub> emissions in the manufacturing cycle for these design spaces are shown in Fig. 7 and discussed. This section is intended to provide a detailed explanation of the energy consumption characteristics of each design and how they change when the sizing of the main components under study is modified.

Different powertrain component sizing has a significant effect on both the performance of the vehicle in terms of consumption and range and on the emissions produced in the cradle-to-grave process. Among the impacts the powertrain design has on emissions, it is possible to differentiate two effects. First, there is a direct effect on the emissions produced during the manufacturing of the vehicle. Second, an indirect effect due to the fact that a different powertrain design may affect significantly the H<sub>2</sub> or electricity consumption of the vehicle, thus requiring a lower or higher amount of energy during the whole vehicle life. As such, the second effect only increases the emissions coming from the fuel production cycle, since using H<sub>2</sub> or electricity from batteries to drive a vehicle does not produce any GHG-100 or NO<sub>x</sub> emissions during the operation cycle. Nevertheless, in the case of FCREx, there is a third effect coming from the complexity and versatility of the powertrain since it is composed of two power sources: a battery and an FC system. The third effect is also indirect and affects significantly the fuel production cycle since, in this case, there are two types of fuels (H<sub>2</sub> and electricity) and the total percentage of H<sub>2</sub> or electricity utilization along the whole life depends on the proportion of energy in the vehicle stored in the tank or in the battery. Therefore, the fuel production cycle could also be affected by the relative amount of fuel produced as H<sub>2</sub> or as electricity since the emissions generated in the H<sub>2</sub> production pathway could be significantly larger than those emitted to produce electricity.

Fig. 6 shows in the first row (graphs A–C) how the H<sub>2</sub> tank capacity was modified according to the battery capacity and the FC maximum power output to achieve the target range (calculated using the WLTC 3b driving cycle). In the second row (graphs D–F) the amount of H<sub>2</sub> consumed along the 120,000 km of life is shown while in the third row (graphs G–I) shows the total energy consumed along the whole life, including both H<sub>2</sub> in the tank and the electricity in the battery. All these results were calculated from previous studies [7].

FCREx design and performance change significantly depending on the range (Fig. 6). In the case of the design, it was calculated that the maximum range for FCREx could be around 700 km, given the significant weight of this vehicle that includes two combined powertrains. Nonetheless, with the minimum battery capacity that was considered (30 kWh) it would be possible for these vehicles to achieve a range of 500 km with 3.6–4 kg of H<sub>2</sub> and a range of 600 km with 4.5–4.9 kg of H<sub>2</sub>. The range of 700 km would only be achievable with a battery capacity ≥50 kWh, an FC maximum power output >30 kW and approximately 5 kg of H<sub>2</sub>. As the H<sub>2</sub> tank increase with the target range, given a fixed battery capacity and FC maximum power, the overall vehicle weight increases without increasing the efficiency of the systems, hence both H<sub>2</sub> and total energy consumption increase with target range (Fig. 6, D–I). As such, it is important to note that depending on the application and the target range for which the vehicle is designed, the energy and H<sub>2</sub> consumption may be affected. This is critical and must be taken into account by FCV designers and manufacturers since, unlike conventional vehicles, changing the tank capacity of an FCREx vehicle may have a significant impact on consumption.

As the battery capacity increases in the FCREx architecture, the H<sub>2</sub> tank capacity decreases since the fraction of the range that can be

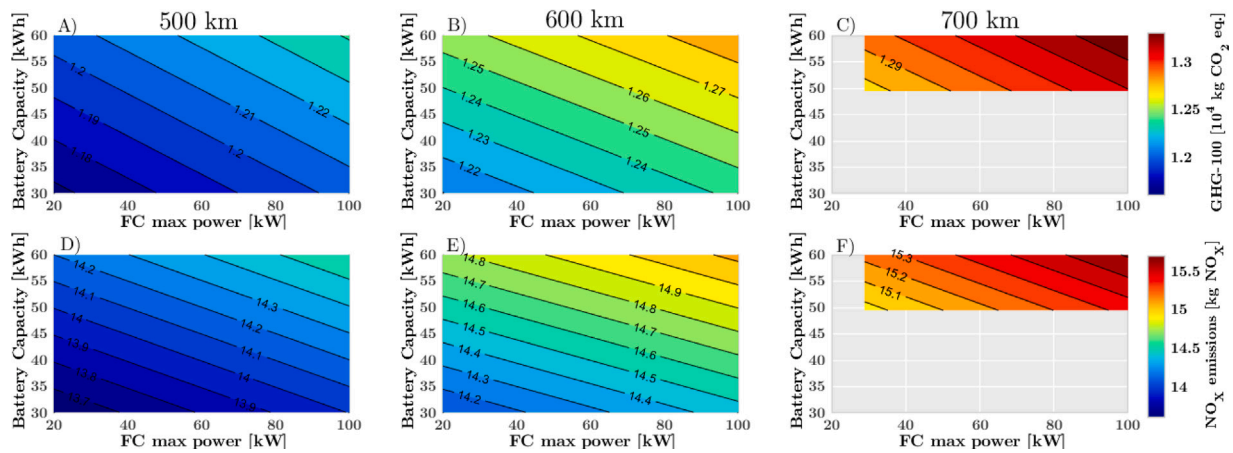


Fig. 7. Design spaces for 500, 600, and 700 km of range FCREx: GHG-100 emissions in the manufacturing cycle (1st row), and  $\text{NO}_x$  in the manufacturing cycle (2nd row). Functional unit is 1 vehicle. Life is set to 120,000 km.

covered with the battery alone increases, thus allowing the decrease in the  $\text{H}_2$  mass for a fixed range (Fig. 6, A–C). As a consequence, the required amount of  $\text{H}_2$  to cover 120,000 km also decreases with increasing battery capacity (Fig. 6, D–F). Furthermore, the higher the share of energy produced from the battery increases the overall system efficiency, given the higher efficiency of the battery compared to that of the FC system. Therefore, the overall vehicle efficiency increase despite the higher vehicle weight, thus decreasing the total energy consumed to cover 120,000 km as the battery capacity increases (Fig. 6, G–I). It is important to note here that the decrease in the  $\text{H}_2$  consumed is not due to an increase in the FC system efficiency. In fact, the higher vehicle weight implies higher brake power demand along the driving cycle, meaning that the FC system would operate at higher current densities, thus decreasing the efficiency. Rather, the decrease in  $\text{H}_2$  comes from the lowest requirement of  $\text{H}_2$  to cover a certain range, since the distance that can be covered only with the battery increases.

The main effect of increasing the FC maximum power was to increase the FC system efficiency since, for the same power demand, a higher-power FC stack operates with lower current density, thus decreasing the electrochemical losses associated with the FC stack operation and the BoP power consumption. This implies that  $\text{H}_2$  consumption decreases with increasing FC maximum power despite the increase in vehicle weight, hence decreasing the required  $\text{H}_2$  tank capacity (Fig. 6, A–C), the  $\text{H}_2$  and total energy consumed along the lifetime (Fig. 6, D–I). Differently from what was explained in the previous paragraph, the trend of decreasing  $\text{H}_2$  consumption, in this case, is motivated by an increase in the FC system efficiency along the driving cycle. When increasing the FC stack maximum power the range that can be covered using the battery alone is slightly reduced, given the increase in the vehicle weight. Nonetheless, this seems to be compensated by the increase in the FC system efficiency.

It is important to note that, while the iso- $\text{H}_2$ -consumed lines are parallel between graphs with different target range (Fig. 6, D–F), in the case of the total energy consumption these lines do not present the same slope between graphs (G–I). This happens because as the target range, the amount of required  $\text{H}_2$  increases, thus increasing the fraction of energy stored as  $\text{H}_2$ . If the fraction of the total energy as  $\text{H}_2$  increases, the vehicle efficiency and overall consumption would be more sensitive to increases in efficiency produced over the FC system. This explains why the iso-lines in graphs G–I in Fig. 6 become more vertical as the target range increases, implying higher sensitivity to the FC maximum power output compared to the battery capacity. Therefore, for high-range FCREx, it would be more beneficial in terms of overall energy consumption to target high-power FC stack designs.

From these results, the optimum design of FCREx passenger vehicles in terms of consumption and performance was found to have high battery capacity and high FC stack maximum power. This result suggests

that, only in terms of performance, the FCREx nor the conventional FCV architectures are optimum, but a compromise between these two must be achieved. However, the results of this study also indicate that the optimum design in terms of performance may not be implementable into passenger vehicles due to available space and TCO reasons. In contrast, cradle-to-grave emissions may be optimum with the optimum-performance design depending on the  $\text{H}_2$  production pathway and the vehicle manufacturing process emissions.

As commented before, the first effect of FCREx design on emissions is derived from the increase in emissions coming from the vehicle manufacturing cycle. This is shown in Fig. 7 in terms of GHG-100 (A–C) and  $\text{NO}_x$  emissions (D–F). When comparing designs with the same battery capacity and FC maximum power output but different range, those with higher range imply higher GHG-100 and  $\text{NO}_x$  emissions since the  $\text{H}_2$  tank capacity increases, thus producing more emissions during its manufacturing process. However, the relative increase of GHG-100 emissions with target range is more significant compared to  $\text{NO}_x$  because GHG-100 emissions in the manufacturing process of  $\text{H}_2$  tanks scale more with its capacity than  $\text{NO}_x$ . Both increasing the battery capacity and the FC maximum power imply higher emissions since the increase in emissions produced when manufacturing higher-capacity batteries and higher-power FC stacks outweighs the decrease in emissions due to the decrease in the required  $\text{H}_2$  tank capacity shown in Fig. 6, graphs A–C. Note how the emissions shown in Fig. 7 are significantly high compared to those produced in the manufacturing cycle of any fossil-fueled conventional ICE vehicle since the emissions coming from the battery, the FC system, and the  $\text{H}_2$  tanks are large compared to the emission required to produce an ICE vehicle. This difference is expected to decrease with time as the  $\text{H}_2$ -based technologies become more mature and the industry producing them is more developed, thus reducing the costs and emissions due to economies of scale. Nevertheless, the manufacturing cycle is just one part of the cradle-to-grave process, hence the fuel production cycle should also be accounted for (the emissions during the operation cycle are almost negligible and are only GHG-100).

### 5.1.1. Global warming emissions

In this section, the design spaces were expressed as a function of GHG-100 emissions for the fuel production cycle and the cradle-to-grave process. First, the design spaces for the FCREx vehicles with a target range of 600 km were plotted considering different  $\text{H}_2$  production pathways (Fig. 8): electrolysis with the current EU electricity mix, and SMR with and without CCS. With these data, how the emissions vary for a fixed design space when changing the  $\text{H}_2$  production pathway is discussed. Then, the design spaces for FCREx with a range of 500, 600 and 700 km for the fuel cycle and the cradle-to-grave associated

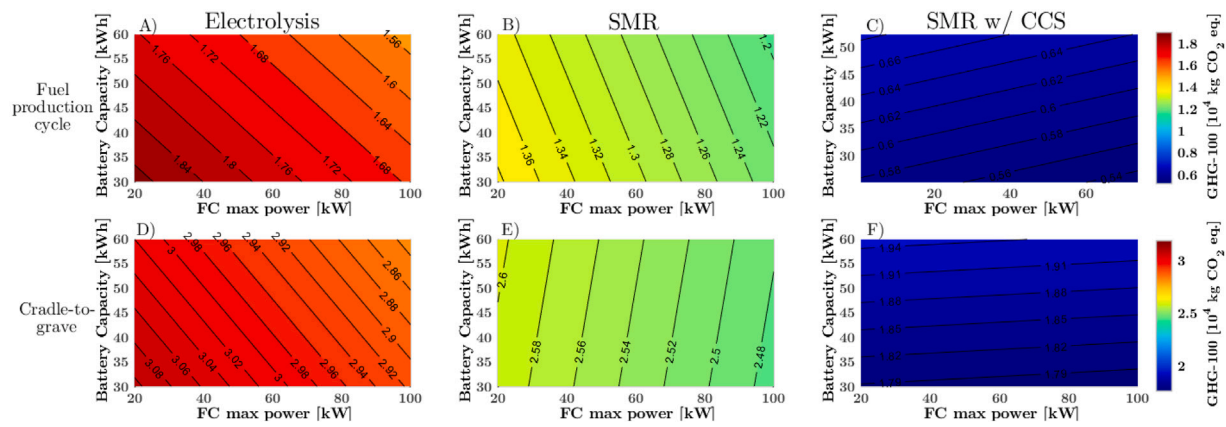


**Fig. 8.** Design spaces for 600 km of range FCReX: GHG-100 emissions produced in the fuel production cycle and in the cradle-to-grave cycle considering different H<sub>2</sub> production pathways. Functional unit is 120,000 km.

emissions were shown in Fig. 9 considering blue H<sub>2</sub> (H<sub>2</sub> produced through SMR with CCS) since most of the H<sub>2</sub> produced currently is based on SMR technology which can be improved in the short-term with CCS, thus being a more realistic option to reduce emissions in the short-term than green H<sub>2</sub> (produced solely from renewable sources).

The greatest variation of GHG-100 emissions in the graphs of Fig. 8 is produced when changing the H<sub>2</sub> production pathway. This variation in emissions is significantly higher than that produced by varying the design in terms of battery capacity or FC maximum power output, hence the change in emissions produced during the fuel production cycle per kg of H<sub>2</sub> or per kWh of electricity when changing the H<sub>2</sub> production pathway is far more relevant than the decrease in H<sub>2</sub> or electricity consumption as a consequence of changing the powerplant design. Overall, GHG-100 emissions produced in the fuel production cycle increase by ~184 % and ~111 % compared to the production pathway of SMR with CCS for electrolysis with the EU electricity mix and SMR respectively. Analogously, the overall increase in GHG-100 emissions in the cradle-to-grave process with the H<sub>2</sub> production pathway is ~60 % and ~36 % compared to SMR with CCS for electrolysis and SMR respectively. The large relative increase in emissions in the fuel production pathway and the significant increase in the cradle-to-grave process confirm how the fuel production pathway has a great influence on the total emissions. Comparing the overall GHG-100 emissions in the fuel production cycle against the total emissions they could imply around ~33 % in the case of SMR with CCS, ~51 % in the case of SMR, and ~58 % in the case of electrolysis. According to this data, it is possible to conclude that the emissions produced during the manufacturing cycle are always a significant part of those produced in the FCReX cradle-to-grave process and could be more than 50% of the total GHG-100 emissions if low-emissions production pathways such as SMR with CCS are considered. Therefore, the vehicle design would have a higher influence on total emissions if H<sub>2</sub> production pathways imply high emissions (SMR and electrolysis with the EU mix) since the emissions in the fuel production cycle are sensitive to the vehicle efficiency through fuel and electricity consumption (Fig. 6). This means that in a scenario with blue or green H<sub>2</sub> the focus to minimize cradle-to-grave emissions for FCV and FCReX should mostly shift towards the vehicle manufacturing cycle.

The slope of the iso-lines in Fig. 8 represent the sensitivity of the GHG-100 emissions produced in the fuel cycle or in the cradle-to-grave process to the FCReX design. The slope changes significantly with the H<sub>2</sub> production pathway since there are two energy carriers in the vehicle (electricity in the battery and H<sub>2</sub> in the tank) with different emissions per kWh of energy. As such, how GHG-100 emissions change with the FCReX design would depend on which energy carrier implies

more emissions per useful,<sup>1</sup> kWh of energy carrier produced. In the case of H<sub>2</sub> produced through electrolysis or SMR (Fig. 8: A,B,D & E), the production of 1 kWh<sub>useful</sub> of H<sub>2</sub> generates more emissions than 1 kWh<sub>useful</sub> of electricity due to both the higher efficiency of batteries and the lower emissions per actual kWh. Therefore, in this case, as the battery capacity increases, GHG-100 emissions in the fuel production cycle decrease (A–B). In Fig. 8 the slope of graph A's iso-lines is similar to the slope of the iso-lines in the graph showing the total H<sub>2</sub> consumption along the life (Fig. 6, graph E) since the emissions produced when generating H<sub>2</sub> through electrolysis with the EU electricity mix dominate the overall emissions in the fuel cycle. In contrast, the iso-lines of Fig. 8 graph B are similar to those in Fig. 6 graph H which represents the total energy consumption since producing 1 kWh<sub>useful</sub> of H<sub>2</sub> generates similar but higher emissions than producing 1 kWh<sub>useful</sub> of electricity for the battery. The trends of GHG-100 emissions when comparing graphs A and D (electrolysis, Fig. 8) are similar, hence the fuel production cycle dominates most of the cradle-to-grave process. In the case of SMR (graphs B and E) the trends change: increasing the battery capacity increases global emissions despite decreasing both the H<sub>2</sub> and the electricity consumed along the life. This means that if SMR is considered, GHG-100 decrease in such a way that the vehicle manufacturing cycle dominates the cradle-to-grave emissions when the battery capacity increases. Nevertheless, with both electrolysis and SMR as production pathways, cradle-to-grave emissions still decrease with FC maximum power since the efficiency of the FC system increases and most of the energy is stored as H<sub>2</sub>. Therefore, the fuel production cycle dominates the global GHG-100 when the FC maximum power changes.

Interestingly, if high-emissions production pathways for H<sub>2</sub> are considered, the optimum FCReX design in terms of cradle-to-grave emissions is found to be the same as that minimizing the H<sub>2</sub> and energy consumption (high battery capacity and high FC stack maximum power) since in this case, the fuel production cycle dominates the overall emissions (Fig. 8, graphs A & D). Hence, minimizing H<sub>2</sub> consumption also means minimizing cradle-to-grave emissions. This trend is also found for NO<sub>x</sub> emissions in the following section (Fig. 10, graphs A & D).

The trends found for SMR with CCS in the fuel production cycle are significantly different from those of the other production pathways. In the fuel production cycle (Fig. 8, graph C), the GHG-100 generated per kWh<sub>useful</sub> of H<sub>2</sub> are much lower than those per kWh<sub>useful</sub> of electricity, thus increasing the fuel cycle emissions as the battery capacity increases (amount of energy stored as electricity in the vehicle). With all the

<sup>1</sup> Useful kWh means the energy stored as electricity or H<sub>2</sub> multiplied by the mean efficiency of the corresponding system (battery or FC system).

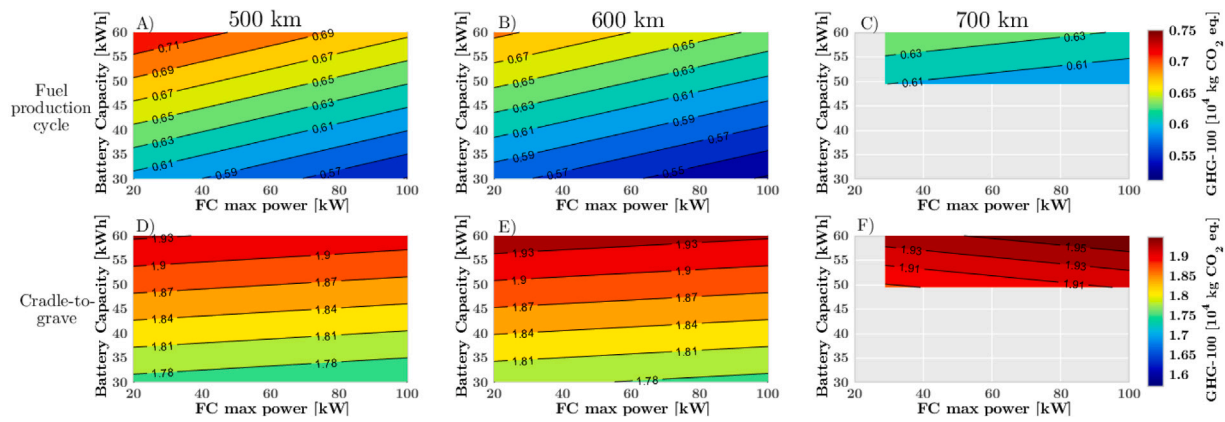


Fig. 9. Design spaces for 500, 600, and 700 km of range FCReX: GHG-100 emissions produced in the fuel production cycle and in the cradle-to-grave cycle considering SMR with CCS as  $H_2$  production pathway. Functional unit is 120,000 km.

production pathways considered, since most of the energy stored is in form of  $H_2$ , increasing the FC maximum power clearly decreases the emissions in the fuel production cycle, being SMR with CCS no exception (Fig. 8 graph F). Again, the increase of battery capacity imply higher cradle-to-grave emissions. In the case of considering SMR with CCS, the overall GHG-100 emissions are far more sensitive to battery capacity than SMR without CCS. This is due to the fact that both in the fuel cycle and the cradle-to-grave process GHG-100 emissions increase with battery capacity (both dominate the trend). This is indicative of the consequences of using low-emission fuels such as blue or green  $H_2$  to power FCV. First, the aim to reduce emissions shifts towards the vehicle manufacturing cycle since it dominates the cradle-to-grave emissions. Second, using electricity from batteries if the renewable share in the electricity mix does not improve may only increase the cradle-to-grave emissions.

Fig. 9 shows the fuel production cycle and the cradle-to-grave emissions for different target range FCReX with  $H_2$  produced through SMR with CCS. Note again how the GHG-100 emissions of blue  $H_2$  are lower than those of electricity. The graphs A–C are analogous to graph C in Fig. 8, showing how GHG-100 emissions increase with the battery capacity and decrease with the FC maximum power due to the low emissions produced in the SMR with CCS process. In these graphs, it is possible to see how the GHG-100 emissions in the fuel production cycle decrease with the target range for a fixed design. Interestingly this happens because, for a given battery capacity, as the target range increases, the amount of  $H_2$  stored increases, thus increasing the percentage of the whole life (distance) that is covered using only  $H_2$ . If GHG-100 emissions per  $kWh_{\text{useful}}$  of  $H_2$  were higher than those produced per  $kWh_{\text{useful}}$  of electricity (SMR or electrolysis) in the fuel production cycle, then the overall GHG-100 in the fuel cycle would increase with the target range.

In the case of cradle-to-grave GHG-100 emissions, increasing the range for a fixed combination of battery capacity and FC stack maximum output power increases GHG-100 emissions (Fig. 9 graphs D–F). This happens because the decrease in emissions in the fuel cycle (Fig. 9 graphs A–C) is lower than the increase in the manufacturing cycle emissions due to the need for bigger  $H_2$  tanks (Fig. 7 graphs A–C) when increasing the target range. When the target range is kept constant at 500 or 600 km, graphs D–E show how GHG-100 emissions increase with battery capacity and decrease with FC maximum power, as explained for Fig. 8, graph F. In contrast, for the design space with a target range of 700 km the emissions trend with respect to the FC maximum power changes, implying an increase in GHG-100 with this sizing parameter. The change in trend is motivated by the high weight of the FCReX with such target range, which limits the decrease in  $H_2$  consumption (Fig. 6, graph F) with the FC maximum power, making the increase in emissions in the manufacturing cycle outweigh the decrease in the fuel cycle.

From the data in Fig. 9 cradle-to-grave GHG-100 emissions may vary up to 10% depending on the components sizing and the target range FCReX are designed for. This value may seem small, but actually it is significant if it is considered that the comparison is performed between vehicles that use the same power sources ( $H_2$  and electricity) with constant production pathway and similar architecture, albeit the sizing of the components may vary.

In conclusion, the use of FCReX provides significant variability in GHG-100 emissions with the design, the target range and the  $H_2$  production pathway. Therefore, these emissions must be taken into account in the vehicle development process. With low-emission  $H_2$  production strategies, decreasing the FCReX target range and decreasing the battery size could reduce emissions since the vehicle manufacturing cycle becomes the dominant phase in the cradle-to-grave process. As such, depending on how the  $H_2$  production infrastructure evolves in the following decades, the optimum FCReX in terms of GHG-100 emissions may evolve towards moderate-to-high FC stack power and moderate-to-low battery capacities. This optimum design may imply lower-than-BEV manufacturing costs and low but not minimum  $H_2$  and total energy consumption (Fig. 6) [7]. This optimum might be in line with the optimum design in terms of TCO.

### 5.1.2. $NO_x$ emissions

$NO_x$  emissions are also analyzed in this study since they are a major concern for society due to the harmful effects of these gases on human health and ozone generation/depletion. This section follows the same structure as Section 5.1.1 but focused on  $NO_x$  emissions. Note that, differently from GHG-100, the SMR production pathway produces the least  $NO_x$  emissions (Fig. 10) since SMR with CCS requires additional resources and energy to capture the  $CO_2$  and the EU electricity mix is not renewable-enough to produce low- $NO_x$   $H_2$  from electrolysis. As a consequence, compared to the  $H_2$  production pathway SMR with CCS, overall  $NO_x$  emissions change in the fuel cycle by  $\sim 95\%$  and  $\sim -16\%$  considering electrolysis and SMR without CCS, respectively. Analogously, in the cradle-to-grave process overall  $NO_x$  emissions change by  $\sim 38\%$  and  $\sim -6\%$ . From the overall change in emissions with the production pathway, it is possible to identify that their influence is significant by much lower than for GHG-100 emissions. Given the relatively small variation in  $NO_x$  emissions and the large difference in GHG-100 emissions between SMR with and without CCS, it could be favorable to consider SMR with CCS as the optimum production pathways to reduce overall emissions (among those considered in this study).

Producing  $H_2$  from electrolysis implies much higher  $NO_x$  emissions since a significant part of the electricity mix is produced from fossil fuels. In the SMR process, the  $NO_x$  are produced in the combustion of the fuel used to heat the reactor. In this case, low- $NO_x$  burners and

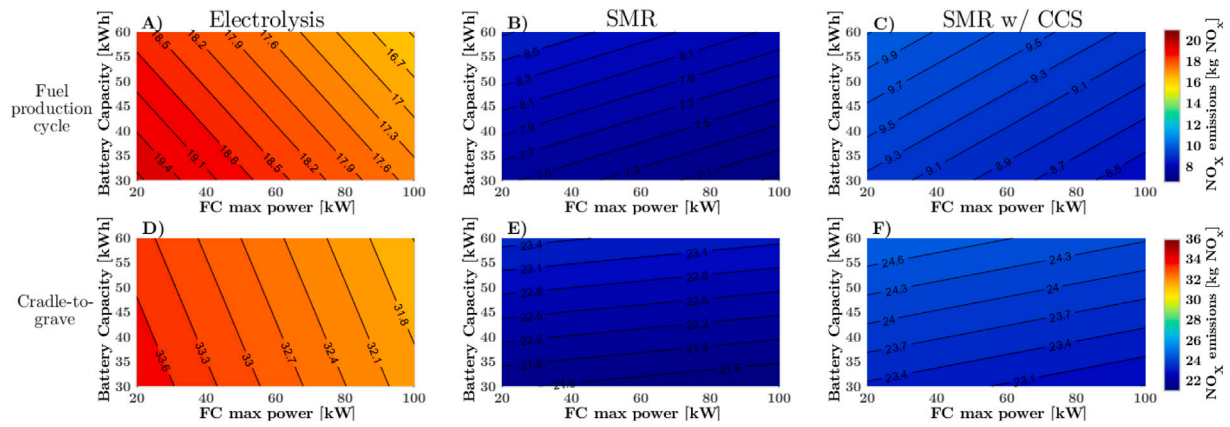


Fig. 10. Design spaces for 600 km of range FCReX: NO<sub>x</sub> emissions produced in the fuel production cycle and in the cradle-to-grave cycle considering different H<sub>2</sub> production pathways. Functional unit is 120,000 km.

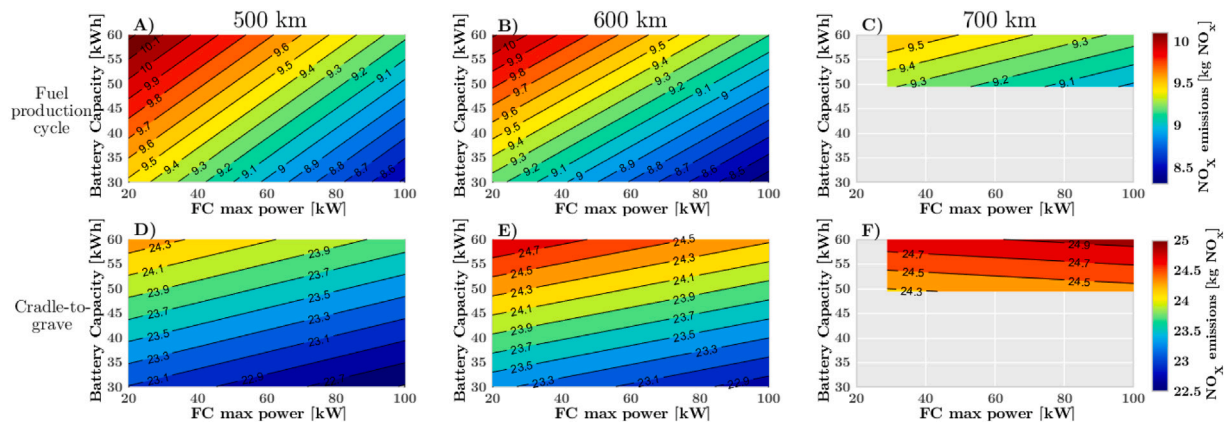


Fig. 11. Design spaces for 500, 600, and 700 km of range FCReX: NO<sub>x</sub> emissions produced in the fuel production cycle and in the cradle-to-grave cycle considering SMR with CCS as H<sub>2</sub> production pathway. Functional unit is 120,000 km.

selective catalyst reduction (SCR) exhaust gas after treatments are a feasible option to minimize NO<sub>x</sub> in SMR plants, although their use is not widely extended [52].

When H<sub>2</sub> is produced from electrolysis (Fig. 10, graphs A & D), NO<sub>x</sub> emissions decrease when increasing the FC maximum power output and the battery capacity, both in the fuel cycle (graph A) and in the cradle-to-grave process (graph D). As explained before, the evolution of NO<sub>x</sub> emissions in the fuel cycle is justified by the decrease in energy and H<sub>2</sub> consumption. The emissions produced in the H<sub>2</sub> production cycle seem to be high than that produced to generate the electricity for the battery. As a consequence, the decrease in emissions when raising the FC maximum power is more significant than when increasing the battery capacity. The trends of the fuel cycle and the cradle-to-grave process opposed to that found in the manufacturing cycle (Fig. 7, graph E), where NO<sub>x</sub> emissions increase with the FC power and the battery capacity. This means that the evolution of cradle-to-grave emissions is dominated by the fuel cycle. In this case, the fuel cycle also produces more emissions than the manufacturing cycle (16.4–19.7 kg NO<sub>x</sub> against 14.1–15.1 kg NO<sub>x</sub>), implying that the fuel production strategy dominates the global emissions both in trend and amount.

NO<sub>x</sub> emissions evolution and the amount produced are very similar in the cases of producing the H<sub>2</sub> from SMR with or without CCS (Fig. 10, graphs B, C, E & D). In the fuel cycle (graphs B & C), NO<sub>x</sub> emissions decrease with the FC stack maximum power due to the lower H<sub>2</sub> consumption. In contrast, they increase with the battery capacity since producing electricity produces more emissions than producing H<sub>2</sub>. In this sense, the fraction of energy stored as H<sub>2</sub> decreases, thus increasing the electricity usage to achieve a certain range. Regarding the

cradle-to-grave emissions, they show the same evolution with respect to design parameters as the fuel cycle, hence they are dominated by the fuel cycle emissions. Nonetheless, the emissions in the fuel cycle are significantly lower than those in the manufacturing cycle, which means that although the manufacturing cycle is responsible for most of NO<sub>x</sub> emissions, the sensitivity of the fuel cycle to the FCReX design is higher, thus dominating the trends but not the total emissions.

Complementary to Figs. 10, 11 shows the NO<sub>x</sub> emissions in the fuel cycle and the cradle-to-grave process for designs with 500, 600 and 700 km of range considering blue H<sub>2</sub> (SMR with CCS). The evolution of NO<sub>x</sub> emissions in the graphs A–C is analogous to that in Fig. 10 graph C and it is explained in the previous paragraph. For a given design, in terms of battery capacity and FC maximum power, increasing the range implies lower NO<sub>x</sub> emissions in the fuel cycle since more H<sub>2</sub> is required to increase the range and the emissions of blue H<sub>2</sub> are lower than those produced to generate electricity with the EU mix. This trend in the fuel cycle is the same found for GHG-100 emissions in Fig. 9. In the design space of 700 km, NO<sub>x</sub> emissions are less sensitive to the variation of the FC maximum power because the gain in efficiency when increasing the FC power is less significant due to the high vehicle weight. This can also be appreciated in the total H<sub>2</sub> consumption calculated for this design space (Fig. 6, graph F).

Graphs D–F of Fig. 11 show how cradle-to-grave NO<sub>x</sub> emissions, for a given combination of battery capacity and FC maximum power, increase with target range due to the additional emissions coming from requiring higher-capacity H<sub>2</sub> tanks. Furthermore, the change in NO<sub>x</sub> trend when comparing graphs D–E with graph F results from the decrease of the sensitivity of the emissions produced in the fuel cycle

with the FC maximum power, thus allowing the vehicle manufacturing cycle dominates the tendency. As such, in the design space of 700 km,  $\text{NO}_x$  emissions increase with the FC maximum power.

The variation between worst and best designs in terms of cradle-to-grave  $\text{NO}_x$  emissions can be up to 10% within the generated design spaces. This variation is similar to that found for GHG-100 emissions, which is a consequence of the same trend they follow when changing the sizing of the components.

To conclude, differently from GHG-100 emissions,  $\text{NO}_x$  emissions for FCREx seem to be mostly dominated by the fuel production process, except for the designs with a high target range (700 km) where the weight becomes an obstacle to decrease significantly  $\text{H}_2$  consumption by increasing the FC maximum power. As such, the designs offering the lowest  $\text{NO}_x$  emissions in the cradle to grave process are those with a battery of 30 kWh and high Fc maximum power, except for the design space of 700 km. The production pathway that offered the lowest  $\text{NO}_x$  was SMR without CCS since CCS process requires an extra amount of energy to enable  $\text{CO}_2$  capture. Nevertheless, the difference between SMR with and without CCS in  $\text{NO}_x$  is substantially smaller than that found for GHG-100. Therefore, looking at overall emissions, SMR with CCS may still be the optimum  $\text{H}_2$  production pathway among those considered in this study.

### 5.2. Potential of cradle-to-grave emissions decrease with FCREx architecture

From the results shown along this section, it was concluded that with low-emissions  $\text{H}_2$  production pathways (blue  $\text{H}_2$ ), the design trend to minimize cradle-to-grave emissions of FCREx vehicles should focus on decreasing the battery capacity to the minimum possible to ensure enough range in BEV mode so that the emissions produced during the manufacturing of the batteries are minimum and high FC stack maximum power to decrease  $\text{H}_2$  consumption. In other words, this trend suggests that the FCREx architecture could produce higher cradle-to-grave GHG-100 and  $\text{NO}_x$  emissions than conventional FCV architectures.

In contrast, with high-emissions  $\text{H}_2$  production pathways (electrolysis from the current EU electricity mix), the FCREx architecture could decrease significantly the GHG-100 and  $\text{NO}_x$  emissions with higher battery capacities (Figs. 8 and 10, graph D). This suggests that the interest in FCREx architecture, only regarding cradle-to-grave emissions, would depend on the balance between the emissions produced when generating electricity and those released when producing  $\text{H}_2$ . However, there is another factor that would affect significantly the cradle-to-grave emission of FCREx architecture: the emissions produced in the battery manufacturing process. Therefore, it is possible to deduce that, in the short term, if  $\text{H}_2$  is produced from the EU electricity mix, FCREx would have significant advantages over FCV in terms of emissions. In the medium and long-term it is uncertain whether FCREx or conventional FC architectures will produce lower emissions since it will depend on the rate at which the EU electricity mix, the  $\text{H}_2$  production pathways, and the battery production process are decarbonized and become cleaner. The results derived from this study will serve the FCV manufacturers to understand the performance and cradle-to-grave emissions of FCREx vehicles and their variation with the design choice regarding changes in FC stack maximum power, battery capacity and  $\text{H}_2$  tank capacity. This could also serve as a starting point for the design process of FCV vehicles with FCREx architecture to down-select a set of design choices to be further refined as the vehicle development advances. The relevance of producing such results not only lies in the benefits for FCV manufacturers but rather for society in general since the existence of these design spaces both in terms of performance and emissions could shorten significantly the FCREx vehicle process, thus accelerating the path towards the  $\text{H}_2$  economy and decreasing the environmental impact of the transport sector.

Finally, from this analysis, a set of recommendations to decrease the cradle-to-grave emissions of FCREx vehicles could be extracted. First, it is imperative to invest in decarbonizing and decreasing the overall emissions of the vehicle manufacturing process, especially battery manufacturing, since it is responsible for a significant part of the cradle-to-grave emissions. Second, the renewable share on the EU electricity mix should increase since it will have a direct impact on both electricity and  $\text{H}_2$  production. Third, in order to drastically decrease the cradle-to-grave emissions of FCV in general, it is necessary to implement CCS technology in SMR plants, since this process would allow increasing the renewable share of the EU electricity mix at a faster rate in parallel to decarbonizing the  $\text{H}_2$  production pathway which will imply a higher rate of decrease of global emissions rather than dedicating all the renewable energy infrastructure into producing green  $\text{H}_2$ . Fourth, due to the uncertainty on the cradle-to-grave emissions of FCREx caused by its use of different energy sources and powerplants, this kind of LCA analysis should be revised over time to adapt these recommendations since important changes are expected in the emissions produced in the battery manufacturing process, the EU electricity mix [53], and the  $\text{H}_2$  production pathways.

## 6. Conclusions

In this study, the design spaces,  $\text{H}_2$ , energy lifetime consumption, GHG-100 and  $\text{NO}_x$  emissions were analyzed by combining sizing with life cycle assessment (LCA) methodologies. The only impact category considered was greenhouse gases (GHG-100) since they are the emissions of the utmost scientific and social concern, although  $\text{NO}_x$  were also estimated. The design spaces, calculated in previous studies, were expressed as a function of the battery capacity, the FC stack maximum power output at the limiting current density and the  $\text{H}_2$  tank capacity. These three design parameters were related through 1D simulations of the fuel cell range-extender (FCREx) complete architecture in WLTC 3b driving cycle for the selected ranges of 500, 600 and 700 km. Furthermore, for the design space with 600 km of range, electrolysis with electricity from the current EU mix, steam methane reforming (SMR) with and without carbon capture and storage (CCS) were considered as the  $\text{H}_2$  production pathways to understand the cradle-to-grave emissions of these vehicles on different feasible-in-the-short-term  $\text{H}_2$  production scenarios. Green  $\text{H}_2$  from only renewable sources was not considered since it is not a feasible solution in the short-term and considering it would only lead to misinterpreting the actual emissions of these vehicles for the following 5–15 years.

The design spaces, the  $\text{H}_2$ , and energy consumption along the lifetime were calculated, from which it was concluded that both increasing the battery capacity and the FC stack maximum power decreased the  $\text{H}_2$  and energy consumption, hence decreasing the emissions in the fuel cycle and increasing those in the vehicle manufacturing cycle. This happened since increasing the battery capacity leads to a decrease in the  $\text{H}_2$  capacity, thus implying that a greater part of the lifetime should be covered with the battery alone, which is more efficient than the FCREx mode despite the higher weight. Furthermore, it was found that increasing the FC maximum stack power decreased the  $\text{H}_2$  consumption since the FC stack operated at lower current densities, thus increasing the FC system efficiency despite the vehicle weight increase. These results were directly used as inputs in the LCA analysis to estimate the vehicle manufacturing and fuel production cycle associated emissions.

In the cradle-to-grave process, GHG-100 emissions increase by ~60% and ~36% with electrolysis and SMR without CCS compared to SMR with CCS or blue  $\text{H}_2$ . Analogously,  $\text{NO}_x$  emissions change by ~38% and ~-6%. The decrease in  $\text{NO}_x$  emissions with SMR without CCS was justified with the extra energy and resources required to enable CCS. These data showed how sensitive the overall GHG-100 and  $\text{NO}_x$  emissions are with the  $\text{H}_2$  production pathway. For both GHG-100 and  $\text{NO}_x$  emissions, the vehicle manufacturing cycle produced most of the cradle-to-grave process, although not always this cycle dominated

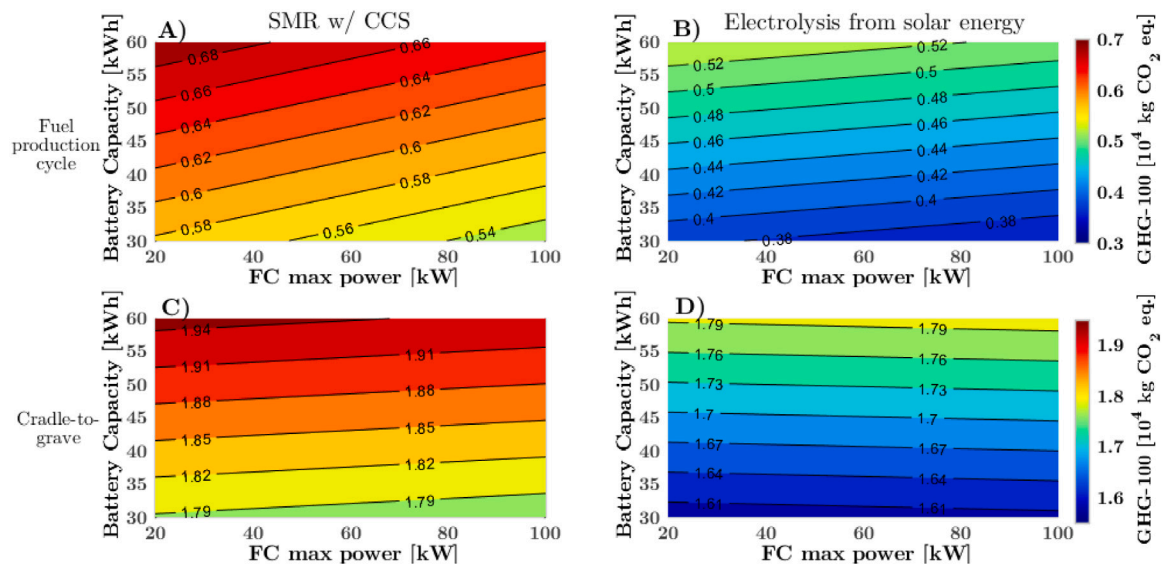


Fig. A.12. Design spaces for 600 km of range FCReX: GHG-100 emissions produced in the fuel production cycle and in the cradle-to-grave cycle considering blue (1st column) and green (2nd column) H<sub>2</sub>. Functional unit is 120,000 km.

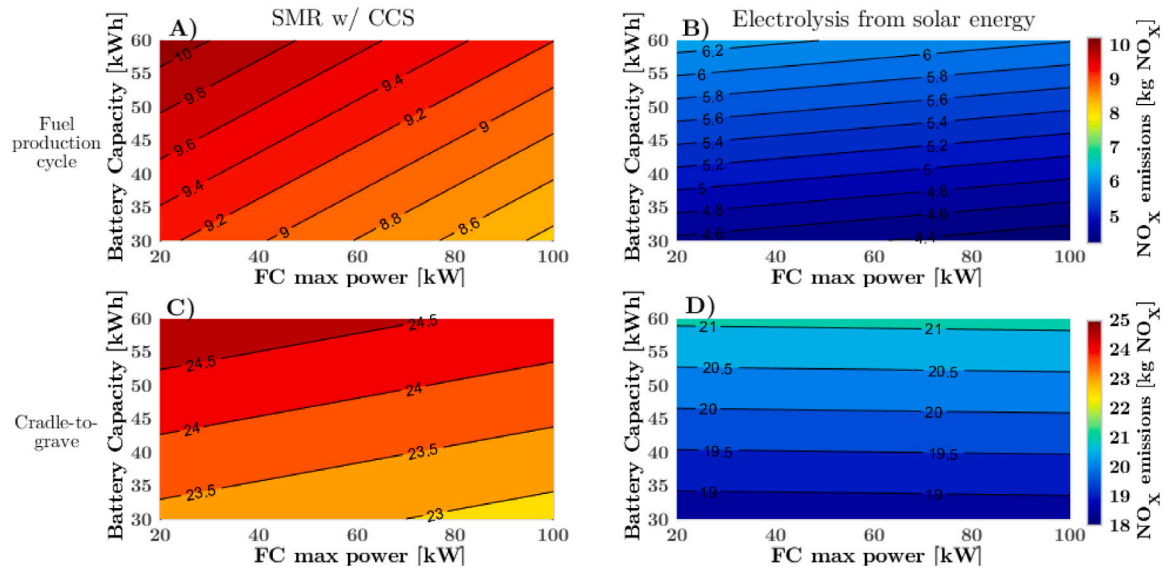


Fig. A.13. Design spaces for 600 km of range FCReX: NO<sub>x</sub> emissions produced in the fuel production cycle and in the cradle-to-grave cycle considering blue (1st column) and green (2nd column) H<sub>2</sub>. Functional unit is 120,000 km.

how the overall emissions change with the design. With the SMR with CCS as the production pathway, the manufacturing cycle dominated together with the fuel cycle the sensitivity of the cradle-to-grave process when the battery capacity increased but the trend in emissions when the FC maximum power increase was clearly dominated by the fuel cycle, except for NO<sub>x</sub> emissions in the FCReX designs with 700 km of range. Both cradle-to-grave GHG-100 and NO<sub>x</sub> emissions may vary up to 10% when comparing the worst and best design among those considered.

With blue H<sub>2</sub>, increasing the battery capacity increased NO<sub>x</sub> as well as GHG-100 emissions in both the fuel production and vehicle manufacturing cycles, despite decreasing the energy consumption, since the emissions produced in this pathway are smaller compared to those produced to generate electricity. This means that, in order to minimize overall emissions, FCReX should be designed with moderate-to-low battery capacities. Interestingly, it was found that for most of the design spaces, increasing the FC maximum power decreased overall cradle-to-grave GHG-100 and NO<sub>x</sub> emissions, as well as overall H<sub>2</sub> consumed

along the lifetime. Therefore, in terms of overall emissions and with low but not minimum H<sub>2</sub>/energy consumption, the optimum FCReX design should have a moderate-to-small battery enough to cover a certain range of operation in battery mode only and moderate-to-high FC stack maximum power in contrast to the optimum design in terms of consumption, which was found to have high battery capacity and high FC stack maximum power. Nonetheless, the fact that the performance-wise and the emissions-wise optimum designs coincide or not, depends mainly on the H<sub>2</sub> production pathway and the vehicle manufacturing process. In the case of considering high-emissions H<sub>2</sub> production pathways (electrolysis from EU mix), these optimum designs overlap because minimizing H<sub>2</sub> consumption means minimizing cradle-to-grave emissions. Although small-to-moderate battery size is recommended, there still exists a trade-off in terms of the total cost of ownership (TCO), emissions and consumption that makes FCReX a promising FCV architecture in the short-to-medium term, given the flexible operation it can offer, the high H<sub>2</sub> prices, the lower energy consumption and the low availability of H<sub>2</sub> refueling stations.

Finally, a set of recommendations were suggested to decrease the cradle-to-grave emissions of FCReX vehicles. They were: decarbonizing the battery manufacturing process, decarbonizing the EU electricity mix, prioritizing blue H<sub>2</sub> over green H<sub>2</sub> to maximize the rate of decrease of cradle-to-grave emissions, and refreshing the data of this analysis over time so that the recommendation can be adapted to the scenario in that moment, given the uncertainty on how the manufacturing and fuel production processes will evolve with time.

### CRedit authorship contribution statement

**J.M. Desantes:** Conceptualization, Project administration, Supervision. **R. Novella:** Investigation, Formal analysis, Writing – review & editing. **B. Pla:** Resources, Methodology, Software, Data curation. **M. Lopez-Juarez:** Investigation, Methodology, Validation, Software, Writing – original draft.

### Acknowledgment

This research has been partially funded by the Spanish Ministry of Science, Innovation and University through the University Faculty Training (FPU) program (FPU19/00550). Funding for open access charge: CRUE-Universitat Politècnica de València

### Appendix. Blue and green H<sub>2</sub> comparison

As a complementary section to this study, in this part the GHG-100 and NO<sub>x</sub> emissions of the FCReX architecture design spaces considering blue and green H<sub>2</sub> are compared. The pathway defining green H<sub>2</sub> production was exactly the same as that for black H<sub>2</sub> presented in Fig. 5 but changing the source of the electricity used for the electrolysis process with electricity produced from solar energy. As such, the fuel production cycle emissions of green H<sub>2</sub> are significantly smaller compared to those of any other production pathway (0.056 kg CO<sub>2</sub> eq./kWh H<sub>2</sub> and 6.8·10<sup>-5</sup> kg NO<sub>x</sub>/kWh H<sub>2</sub>). Nevertheless, the results in Figs. A.12 and A.13 must be analyzed carefully to identify the scenario they represent. For green H<sub>2</sub>, the source of energy is renewable, while for the electricity in the battery, the source is the electricity mix. Therefore, these results represent and scenario that may lead to a certain bias towards FCV rather than towards BEV since it could be argued that renewable energy could be part of the electricity mix thus decreasing the emissions coming from using the battery. This is the reason why these results were included in the appendix only for completeness and must be analyzed taking into account the particular scenario just described.

It is important to note that green H<sub>2</sub> emissions are not completely zero since some of the processes in the production pathway require the use of non-renewable energy for H<sub>2</sub> treatment and distribution. Nonetheless, the global emissions of the process are still significantly lower than with other H<sub>2</sub> production pathways.

In Fig. A.12 the GHG-100 emissions produced during the fuel cycle and cradle-to-grave process are shown for both blue (left column) and green (right column) H<sub>2</sub> for a 600 km of range FCReX vehicle. This same information is presented for NO<sub>x</sub> in Fig. A.13. In these two figures the trends of increasing or decreasing the emissions are the same, hence a common explanation can be given to explain them. For both blue and green H<sub>2</sub> increasing the battery capacity implies an increase in emissions since the GHG-100 and NO<sub>x</sub> emissions released when producing 1 kWh of H<sub>2</sub> are significantly lower than those for producing 1 kWh of electricity with the current electricity mix. Therefore, emissions decrease with increasing battery capacity since increasing the battery capacity implies a higher usage of electricity and a lower H<sub>2</sub> tank capacity (Fig. 6). The emissions variation with the FC maximum power is that explained along the study: increasing the FC maximum power implies a more efficient use of H<sub>2</sub>, thus requiring less fuel to cover a given distance and thus decreasing emissions.

As explained in Section 5, changing the H<sub>2</sub> production pathway does not only imply a variation on the cradle-to-grave process emissions but also on the relative weight of the fuel production cycle. In the case of blue H<sub>2</sub> the fuel production cycle supposes ~33% of the total emissions while for green H<sub>2</sub> it is ~26%. This is, again, a proof of the fact that as the industry moves towards low emissions propulsion systems and/or fuels, the vehicle manufacturing cycle will become more relevant in the cradle-to-grave emissions.

When comparing how the emissions change in the cradle-to-grave process with blue and green H<sub>2</sub> in both Figs. A.12 and A.13, it is possible to identify how increasing the FC maximum power if green H<sub>2</sub> is considered yields higher emissions. This is justified by the low emissions produced by green H<sub>2</sub> in the fuel production process, whose variation when sizing the components of the FCReX architecture is even smaller than the change in emissions in the vehicle manufacturing cycle. As a consequence, the cradle-to-grave emissions of green H<sub>2</sub> present a similar trend to the emissions in the vehicle manufacturing cycle (Fig. 7, graphs B & E).

Finally, it is important to understand that for green H<sub>2</sub> the GHG-100 and NO<sub>x</sub> emissions in the cradle-to-grave process may change up to 11.8% and 12.5% depending on the sizing choice respectively, in contrast with blue H<sub>2</sub> whose GHG-100 and NO<sub>x</sub> may vary up to 9.1% and 8.8% respectively. This is motivated by the lower absolute value of total emissions for green H<sub>2</sub>, which makes the vehicle manufacturing cycle dominate the cradle-to-grave emissions.

### References

- [1] Fuel Cells & Hydrogen (FCH). Hydrogen roadmap Europe - a sustainable pathway for the European energy transition. first ed.. Publications Office of the European Union; 2019, p. 70. <http://dx.doi.org/10.2843/341510>.
- [2] Wang J, Wang H, Fan Y. Techno-economic challenges of fuel cell commercialization. *Engineering* 2018;4(3):352–60. <http://dx.doi.org/10.1016/j.eng.2018.05.007>.
- [3] García A, Monsalve-Serrano J, José Sanchís E, Fogué-Robles A. Exploration of suitable injector configuration for dual-mode dual-fuel engine with diesel and OMEx as high reactivity fuels. *Fuel* 2020;280(June):118670. <http://dx.doi.org/10.1016/j.fuel.2020.118670>.
- [4] Desantes JM, Molina S, Novella R, Lopez-Juarez M. Comparative global warming impact and NOx emissions of conventional and hydrogen automotive propulsion systems. *Energy Convers Manage* 2020;221(X):113137. <http://dx.doi.org/10.1016/j.enconman.2020.113137>.
- [5] Gandolfi A, Patel A, Vigna MD, Pombeiro M, Pidoux M. Green hydrogen the next transformational driver of the utilities industry. *Tech. rep., Goldman Sachs; 2020*.
- [6] International Energy Agency. The future of hydrogen. In: *The future of hydrogen*. Tech. rep., (June). 2019, <http://dx.doi.org/10.1787/1e0514c4-en>.
- [7] Molina S, Novella R, Pla B, Lopez-Juarez M. Optimization and sizing of a fuel cell range extender vehicle for passenger car applications in driving cycle conditions, vol. 285. (January). Elsevier Ltd; 2021.
- [8] Purnima P, Jayanti S. Optimal sizing of a fuel processor for auxiliary power applications of a fuel cell-powered passenger car. *Int J Hydrogen Energy* 2020;45(48):26005–19. <http://dx.doi.org/10.1016/j.ijhydene.2020.03.127>.
- [9] Purnima P, Jayanti S. Fuel processor-battery-fuel cell hybrid drivetrain for extended range operation of passenger vehicles. *Int J Hydrogen Energy* 2019;44(29):15494–510. <http://dx.doi.org/10.1016/j.ijhydene.2019.04.081>.
- [10] Changizian S, Ahmadi P, Raeesi M, Javani N. Performance optimization of hybrid hydrogen fuel cell-electric vehicles in real driving cycles. *Int J Hydrogen Energy* 2020;45(60):35180–97. <http://dx.doi.org/10.1016/j.ijhydene.2020.01.015>.
- [11] Feroldi D, Carignano M. Sizing for fuel cell/supercapacitor hybrid vehicles based on stochastic driving cycles. *Appl Energy* 2016;183:645–58. <http://dx.doi.org/10.1016/j.apenergy.2016.09.008>.
- [12] Xu L, Ouyang M, Li J, Yang F, Lu L, Hua J. Optimal sizing of plug-in fuel cell electric vehicles using models of vehicle performance and system cost. *Appl Energy* 2013;103:477–87. <http://dx.doi.org/10.1016/j.apenergy.2012.10.010>.
- [13] Xu L, Mueller CD, Li J, Ouyang M, Hu Z. Multi-objective component sizing based on optimal energy management strategy of fuel cell electric vehicles. *Appl Energy* 2015;157:664–74. <http://dx.doi.org/10.1016/j.apenergy.2015.02.017>.
- [14] Wu Z, Wang C, Wolfram P, Zhang Y, Sun X, Hertwich E. Assessing electric vehicle policy with region-specific carbon footprints. *Appl Energy* 2019;256(7491):113923. <http://dx.doi.org/10.1016/j.apenergy.2019.113923>.
- [15] Wu X, Hu X, Yin X, Peng Y, Pickert V. Convex programming improved online power management in a range extended fuel cell electric truck. *J Power Sources* 2020;476(2019):228642. <http://dx.doi.org/10.1016/j.jpowsour.2020.228642>.

- [16] Gaikwad SD, Ghosh PC. Sizing of a fuel cell electric vehicle: A pinch analysis-based approach. *Int J Hydrogen Energy* 2020;45(15):8985–93. <http://dx.doi.org/10.1016/j.ijhydene.2020.01.116>.
- [17] Hu Z, Li J, Xu L, Song Z, Fang C, Ouyang M, et al. Multi-objective energy management optimization and parameter sizing for proton exchange membrane hybrid fuel cell vehicles. *Energy Convers Manage* 2016;129:108–21. <http://dx.doi.org/10.1016/j.enconman.2016.09.082>.
- [18] Fan A, Wang J, He Y, Perčić M, Vladimir N, Yang L. Decarbonising inland ship power system: Alternative solution and assessment method. *Energy* 2021;226(X). <http://dx.doi.org/10.1016/j.energy.2021.120266>.
- [19] Perčić M, Ančić I, Vladimir N. Life-cycle cost assessments of different power system configurations to reduce the carbon footprint in the Croatian short-sea shipping sector. *Renew Sustain Energy Rev* 2020;131(December 2019). <http://dx.doi.org/10.1016/j.rser.2020.110028>.
- [20] Perčić M, Vladimir N, Fan A. Life-cycle cost assessment of alternative marine fuels to reduce the carbon footprint in short-sea shipping: A case study of Croatia. *Appl Energy* 2020;279(June). <http://dx.doi.org/10.1016/j.apenergy.2020.115848>.
- [21] García A, Monsalve-Serrano J, Villalta D, Lago Sari R, Gordillo Zavaleta V, Gaillard P. Potential of e-Fischer Tropsch diesel and oxymethyl-ether (OMeX) as fuels for the dual-mode dual-fuel concept. *Appl Energy* 2019;253(July):113622. <http://dx.doi.org/10.1016/j.apenergy.2019.113622>.
- [22] Fernández-Dacosta C, Shen L, Schakel W, Ramirez A, Kramer GJ. Potential and challenges of low-carbon energy options: Comparative assessment of alternative fuels for the transport sector. *Appl Energy* 2019;236(May 2018):590–606. <http://dx.doi.org/10.1016/j.apenergy.2018.11.055>.
- [23] Bongartz D, Doré L, Eichler K, Grube T, Heuser B, Hombach LE, et al. Comparison of light-duty transportation fuels produced from renewable hydrogen and green carbon dioxide. *Appl Energy* 2018;231(September):757–67. <http://dx.doi.org/10.1016/j.apenergy.2018.09.106>.
- [24] Bareiß K, de la Rua C, Möckl M, Hamacher T. Life cycle assessment of hydrogen from proton exchange membrane water electrolysis in future energy systems. *Appl Energy* 2019;237(July 2018):862–72. <http://dx.doi.org/10.1016/j.apenergy.2019.01.001>.
- [25] Ehrenstein M, Galán-Martín A, Tulus V, Guillén-Gosálbez G. Optimising fuel supply chains within planetary boundaries: A case study of hydrogen for road transport in the UK. *Appl Energy* 2020;276(June):115486. <http://dx.doi.org/10.1016/j.apenergy.2020.115486>.
- [26] Evangelisti S, Tagliaferrri C, Brett DJ, Lettieri P. Life cycle assessment of a polymer electrolyte membrane fuel cell system for passenger vehicles. *J Cleaner Prod* 2017;142:4339–55. <http://dx.doi.org/10.1016/j.jclepro.2016.11.159>.
- [27] Agostini A, Belmonte N, Masala A, Hu J, Rizzi P, Fichtner M, et al. Role of hydrogen tanks in the life cycle assessment of fuel cell-based auxiliary power units. *Appl Energy* 2018;215(June 2017):1–12. <http://dx.doi.org/10.1016/j.apenergy.2018.01.095>.
- [28] Navas-Anguita Z, García-Gusano D, Dufour J, Iribarren D. Prospective techno-economic and environmental assessment of a national hydrogen production mix for road transport. *Appl Energy* 2020;259(August 2019):114121. <http://dx.doi.org/10.1016/j.apenergy.2019.114121>.
- [29] Dimitrova Z, Maréchal F. Environmental design for electric vehicles with an integrated solid oxide fuel cell (SOFC) unit as a range extender. *Renew Energy* 2017;112:124–42. <http://dx.doi.org/10.1016/j.renene.2017.05.031>.
- [30] Corbo P, Migliardini F, Veneri O. Experimental analysis of a 20 kW PEM fuel cell system in dynamic conditions representative of automotive applications. *Energy Convers Manage* 2008;49(10):2688–97. <http://dx.doi.org/10.1016/j.enconman.2008.04.001>.
- [31] Corbo P, Migliardini F, Veneri O. Experimental analysis and management issues of a hydrogen fuel cell system for stationary and mobile application. *Energy Convers Manage* 2007;48(8):2365–74. <http://dx.doi.org/10.1016/j.enconman.2007.03.009>.
- [32] Teng T, Zhang X, Dong H, Xue Q. A comprehensive review of energy management optimization strategies for fuel cell passenger vehicle. *Int J Hydrogen Energy* 2020;45(39). <http://dx.doi.org/10.1016/j.ijhydene.2019.12.202>.
- [33] Hyundai. Hyundai nexo - technical specifications. p. 0–2.
- [34] Sciarretta A, Guzzella L. Control of hybrid electric vehicles. *IEEE Control Syst Mag* 2007;27(2):60–70.
- [35] Onori S, Serrao L, Rizzoni G. Hybrid electric vehicles: energy management strategies. Springer; 2016.
- [36] Luján JM, Guardiola C, Pla B, Reig A. Cost of ownership-efficient hybrid electric vehicle powertrain sizing for multi-scenario driving cycles. *Proc Inst Mech Eng D* 2016;230(3):382–94.
- [37] Serrao L, Onori S, Rizzoni G. ECMS as a realization of Pontryagin's minimum principle for HEV control. In: 2009 American control conference. IEEE; 2009, p. 3964–9.
- [38] Howell D, Cunningham B, Duong T, Faguy P. Overview of the DOE VTO advanced battery R&D program. Tech. rep., U.S. Department Of Energy; 2016, p. 24.
- [39] Ballard. Product data sheet - FCvelocity-MD. 2016.
- [40] Ballard. Product data sheet - FCmove-HD. 2016.
- [41] USDepartment Of Energy. DOE Technical targets for onboard hydrogen storage for light-duty vehicles. 2015.
- [42] IPCC. Climate change 2014. In: Core Writing Team RP, Meyer L, editors. Synthesis report. contribution of working groups I, II and III to the fifth assessment report of the intergovernmental panel on climate change. Tech. rep., Cambridge: Cambridge University Press; 2015, p. 3–22.
- [43] Cheng F, Porter MD, Colosi LM. Is hydrothermal treatment coupled with carbon capture and storage an energy-producing negative emissions technology? *Energy Convers Manage* 2020;203(August 2019):112252. <http://dx.doi.org/10.1016/j.enconman.2019.112252>.
- [44] Choi W, Song HH. Well-to-wheel greenhouse gas emissions of battery electric vehicles in countries dependent on the import of fuels through maritime transportation: A South Korean case study. *Appl Energy* 2018;230(August):135–47. <http://dx.doi.org/10.1016/j.apenergy.2018.08.092>.
- [45] Obnamia JA, Dias GM, MacLean HL, Saville BA. Comparison of U.S. Midwest corn stover ethanol greenhouse gas emissions from GREET and GHGenius. *Appl Energy* 2019;235(October 2018):591–601. <http://dx.doi.org/10.1016/j.apenergy.2018.10.091>.
- [46] Al-Qahtani A, Parkinson B, Hellgardt K, Shah N, Guillen-Gosalbez G. Uncovering the true cost of hydrogen production routes using life cycle monetisation. *Appl Energy* 2021;281:115958. <http://dx.doi.org/10.1016/j.apenergy.2020.115958>.
- [47] European Environmental Agency (EEA). Overview of electricity production and use in Europe - Indicator Assessment. 2018.
- [48] Council of European Energy Regulators (CEER). CEER report on power losses. Tech. rep., 2017.
- [49] Notter DA, Kouravelou K, Karachalios T, Daletou MK, Haberland NT. Life cycle assessment of PEM FC applications: Electric mobility and  $\mu$ -CHP. *Energy Environ Sci* 2015;8(7):1969–85. <http://dx.doi.org/10.1039/c5ee01082a>.
- [50] Keoleian G, Miller S, Kleine RD, Fang A, Mosley J. Life cycle material data update for GREET model - report no. CSS12-12. Tech. rep., 2012, p. 214.
- [51] Sherwood SC, Dixit V, Salomez C. The global warming potential of near-surface emitted water vapour. *Environ Res Lett* 2018;13(10):104006. <http://dx.doi.org/10.1088/1748-9326/aae018>.
- [52] Bradley S, Ducrocq J, Gallarda J, Mineur B, Ott W, Ritter A, et al. Best available techniques for the co-production of hydrogen, carbon monoxide & their mixtures by steam reforming. Tech. rep., Brussels: EUROPEAN INDUSTRIAL GASES ASSOCIATION AISBL; 2013.
- [53] Thomas M, Ellingsen LA-W, Hung CR. Research for TRAN Committee - Resource and climate aspects of lithium-ion traction batteries and battery electric vehicles. Brussels: European Parliament, Policy Department for Structural and Cohesion Policies; 2018, <http://dx.doi.org/10.2861/944056>.